ISWS CONTRACT REPORT 2019-10

Frequency Distributions of Heavy Precipitation in Illinois: Spatio-Temporal Analysis

Momcilo Markus, James Angel, Kexuan Wang,
Brian Kerschner, and Shailendra Singh

December 2019

ILLINOIS
Illinois State Water Survey
PRAIRIE RESEARCH INSTITUTE

Frequency Distributions of Heavy Precipitation in Illinois: Spatio-Temporal Analyses

Momcilo Markus, James Angel, Kexuan Wang, Brian Kerschner,
and Shailendra Singh

Illinois State Water Survey

Prairie Research Institute

University of Illinois

Prepared for the

Illinois Department of Commerce and Economic Opportunity

December 2019

Acknowledgments

This material is based on work supported by the Illinois Department of Commerce and Economic Opportunity under Grant No. 08-355061 and funded by the U.S. Department of Housing and Urban Development's Community Development Block Grants Award No. B-08-DI-17-0001. Any opinions, findings, and conclusions or recommendations expressed in this publication are those of the authors and do not necessarily reflect the views of the Illinois Department of Commerce and Economic Opportunity, the U.S. Department of Housing and Urban Development, the Illinois State Water Survey, or the University of Illinois.

We would like to acknowledge the contributions of Sally McConkey as a project advisor and reviewer and David Kristovich, who also reviewed the final version of the report, both from ISWS. Greg Byard (ISWS) and Wes Cattoor (Illinois Department of Natural Resources) also provided several important review comments. Tom Over from the U.S. Geological Survey, Annie Peiyong Qu from the Department of Statistics, and Francina Dominguez and Ryan Sriver from the Department of Atmospheric Sciences, University of Illinois, provided additional insights and suggestions in the early stages of the project. Lisa Sheppard from ISWS edited the text.

Contents

Introduction

This document is a companion report to "Frequency Distributions of Heavy Precipitation in Illinois: Updated Bulletin 70" by Angel and Markus, published in March 2019. As stated in the Angel and Markus report, "Additional research results on precipitation relationships will be shared in a second report to be published in 2019. That report will revisit the distribution of precipitation within the storm, also known as Huff curves, along with the relationship between point and areal precipitation patterns out to 400 square miles." Accordingly, this report shows results of the distribution of precipitation within a storm, presented in Section 1, and relations between point and areal precipitation amounts (areal reduction factor), shown in Section 2. Modified Huff curves were adopted based on new rich datasets. This study also recommended the use of the existing areal reduction factors, as the new analyses resulted in large uncertainties.

In addition, in Sections 3–5, this report also addresses several key questions and comments received from various users after the Angel and Markus report was published. Section 3 describes a methodology to determine the representative year of the heuristic formula for temporal trend adjustment used in the Angel and Markus report. It was determined that the trend adjustment approximately represents the time period around the ending year of the record, in this case 2017. Section 4 compares the results based on the heuristic formula used in this study with other methods for temporal trend adjustment. This analysis supports the selection of the adopted trend adjustment formula, as it was shown to be more robust than other approaches. Section 5 expands the range of the original frequency tables by adding storm durations and recurrence intervals not published in the Angel and Markus report. The new tables include 5-minute through 10-day (240 hours) storm durations and 2-month through 500-year recurrence intervals.

Data used in this report include daily NOAA datasets, shown in Appendix 1, National Center for Environmental Information (NCEI) hourly precipitation data (HPD), shown in Appendix 2, and Cook County Precipitation Network (CCPN) and Imperial Valley Precipitation Network (IVPN) data. CCPN and IVPN station descriptions can be found in Bauer and Westcott (2017) and Westcott et al. (2009), respectively.

1. Adjustment of the Huff curves

Introduction

Knowledge concerning the time distributions of rainfall in storms has proven to be important for numerous engineering and hydrological problems requiring estimates of runoff or peak flow rates. Illinois state agencies adopted the Huff curves (Huff, 1990) as a companion to the design rainfall study Bulletin 70 (Huff and Angel, 1989a), which has been the design rainfall standard in Illinois since the late 1980s (IDOT, 2011). As noted in ISWS Circular 173 (Huff, 1990), "This document provides the best available information on the time-distribution characteristics of heavy rainstorms at a point and on small basins encompassing areas of up to 400 square miles in Illinois and the Midwest. It is recommended for use in conjunction with Illinois State Water Survey Bulletin 70 (Huff and Angel, 1989a) and Circular 172 (Huff and Angel, 1989b) for runoff computations related to the design and operation of runoff control structures." The analyses of frequency distributions of heavy precipitation (Angel and Markus, 2019) provided an update to rainfall depths. This study provides an update to the companion rainfall distributions, a.k.a. Huff distributions, using currently available data. Huff's method separates the available rainfall data into four distinct groupings based on the quartile in which the maximum precipitation intensity occurred (Huff, 1967; Huff, 1990). Bonta and Roa (1987) and Huff (1990) investigated the advantages and recommended usage of each quartile grouping. The final Huff curves are dimensionless and probabilistic and have the flexibility to represent a wide range of rainfall patterns.

Data

The objective of this study was to compare the time distributions derived in Huff (1990) to recent quality-controlled, hourly precipitation data from the existing datasets. Cook County Precipitation Network (CCPN) (1989–2016), Imperial Valley Precipitation Network (IVPN) and National Center for Environmental Information (NCEI) hourly precipitation data (HPD) for Illinois and the collar counties (1948–2013) were considered. However, after further analysis, it was determined that the HPD dataset was not suitable for this study. It had large data gaps and discontinuity across stations, combined with less than ideal spatial resolution, which made areal precipitation across multiple gages unreliable.

For this study, hourly, quality-controlled precipitation data from the CCPN (Bauer and Westcott, 2017) and from the IVPN (Westcott et al., 2009) were used. The CCPN consists of 25 recording raingages with approximately uniform spacing covering an area of about 600 square miles of Cook County in an urban environment (Figure 1.1). This network was deemed particularly appropriate, given the population density and economic importance of this region to the state of Illinois. The IVPN network (Figure 1.2) is a 20-site weighing-bucket raingage array in a rural environment operated by the Illinois State Water Survey (ISWS) for the Imperial Valley

Water Authority since 1992. The purpose of this network, located in Mason and Tazewell Counties in Illinois, is to help determine the rate of groundwater draw-down. Using CCPN and IVPN provides a consistent comparison with the original study (Huff, 1990) in which the author also combined urban and rural datasets. By using these different datasets, a range of different geographic locations and land uses in the state is better represented, as in Huff (1990).

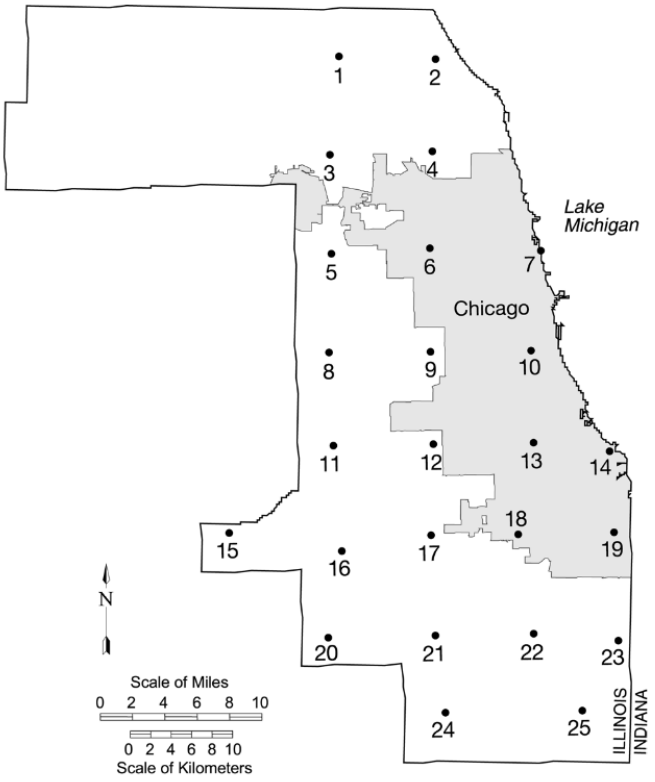

Figure 1.1. Locations of recording precipitation gages in the CCPN

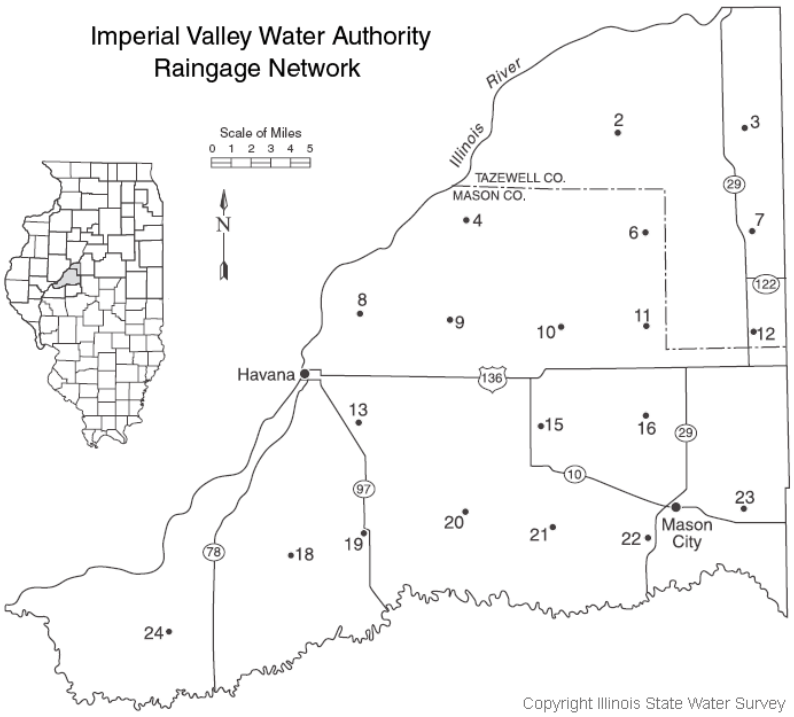

Figure 1.2. Locations of recording precipitation gages in the IVPN

Methodology

A storm event for this study is defined as a period of precipitation lasting between 3 and 48 hours, with a minimum-duration dry period separating the preceding rainfall by at least 6 hours. Methods and variations of identification of individual storm events have been researched and discussed in previous studies (Restrepo and Eagleson, 1981; Bonta and Roa, 1987). Storm events in this study were derived using similar methods to the original work done by Huff (Huff, 1967; Huff, 1990). As in the original research, the curves were calculated separately for three ranges of areas: 0–10, 10–50, and 50–400 square miles. In this report, the distributions (curves) for areas 0–10 square miles are also referred to as point distributions. As in the original studies, only storms with a cumulative rainfall amount of 0.50 inches or greater were considered for point distributions. For areal distributions, storms with a mean areal cumulative rainfall of 0.50 inches or greater and/or storms containing one or more gages recording 1.00 inch or greater were considered.

Huff curves were developed using the data.table and ggplot libraries within the CRAN/R programming language. Bonta (2004) provided a base methodology for the development and use of Huff curves, which were coded in the R language (R Core Team, 2017).

For all the storms selected based on the adopted criteria, the hourly precipitation data that contained grouped individual storm events were used to determine the total duration and depth of each storm and to calculate the cumulative duration and depth at each hourly breakpoint. Each observed storm was then standardized into a dimensionless form, with both time and precipitation amount now ranging between 0 and 100 percent. All storms were then divided into four quartiles. Rainfall distributions can be grouped according to the first, second, third, or fourth quartile, depending on whether the greatest percentage of the total storm rainfall occurred in the first, second, third, or fourth quarter of the storm (Huff, 1990).

For point estimates (areas between 0 and 10 mi^2), all first-quartile storms at each station with a cumulative rainfall amount of 0.50 inches or more were first standardized and then their median was averaged for all stations in the two selected datasets. This average is the final modified Huff curve for point estimates for the first quartile. The method was the same for the other quartiles.

For areal estimates for smaller areas (10–50 mi^2), the areas were divided into subareas with a size ranging between 10 and 50 square miles. Similarly, for areal estimates for larger areas (50–400 mi^2), the areas were divided into subareas with a size ranging between 50 and 400 square miles. For both small and large areas, the procedure was similar to that for point estimates (0–10 mi^2). All first-quartile storms with a mean areal cumulative rainfall of 0.50 inches or greater and/or storms containing one or more gages recording 1.00 inch or greater were first standardized and then averaged for all subareas in the two selected datasets. These averages for small and large areas represented the final modified Huff curves for the first quartile. The method is the same for calculating the modified Huff curves for other quartiles.

Probabilities from the dimensionless mass curves can be tabulated with different increments. In Huff (1967, 1990), 5 percent increments along the storm duration axis were used. Bonta (2004) used 2 percent increments. For the purpose of hydrological modeling, breakpoints for this study were chosen at intervals of 1/24, which allow data to be easily entered in 12- and 24-hour watershed models.

Huff curves represent the median percentages of storms with the median percentages of time for each quartile. Naturally, the observed storms are variable and generally differ from the median. Some of the observed standardized storms for certain quartiles and areas are close to the median, but some differ significantly from it. To provide a measure of variability of the final curves, percentages chosen were 10 percent, 50 percent (median), and 90 percent, as in Huff (1967), showing the central 80 percent of all observed storms. Figure 1.3 shows an illustration of this process for a single location at CCPN Gage 1, irrespective of when the heaviest rainfall occurred.

Shorter storm durations are most often associated with first- and second-quartile storms, while longer duration storms are often associated with third- and fourth-quartile storms (Huff, 1990). For illustration, an example set of curves representing the quartile

distribution from a point location was calculated at Gage 1 in the CCPN (Figure 1.4). The four plots show the distribution for each of the grouped storms having the heaviest precipitation in the first, second, third, and fourth quartiles, respectively. The final curves were, however, determined as average curves for all sites at the CCPN and IVPN.

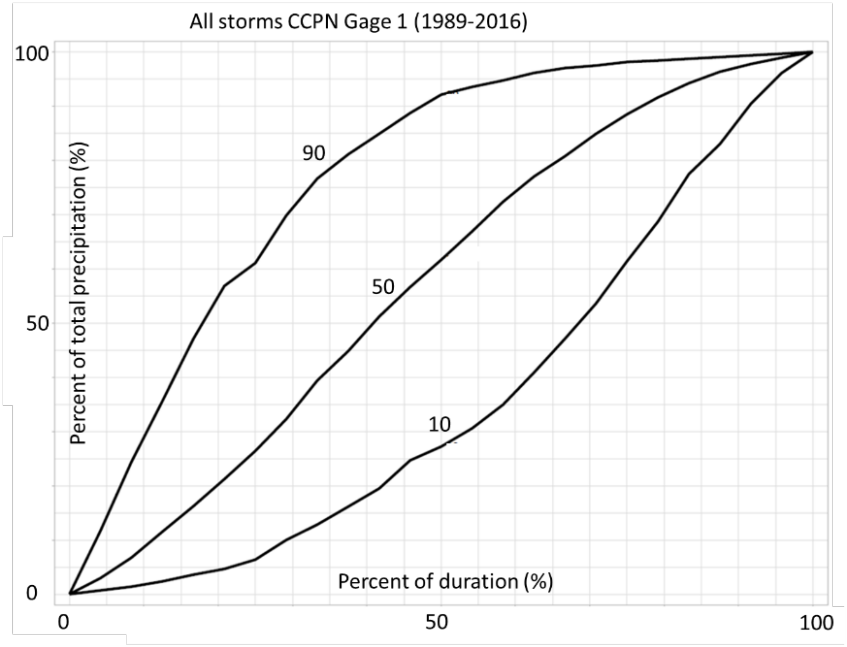

Figure 1.3. Example of a single-site (CCPN 1, 1989–2016) Huff curve using all available storm events

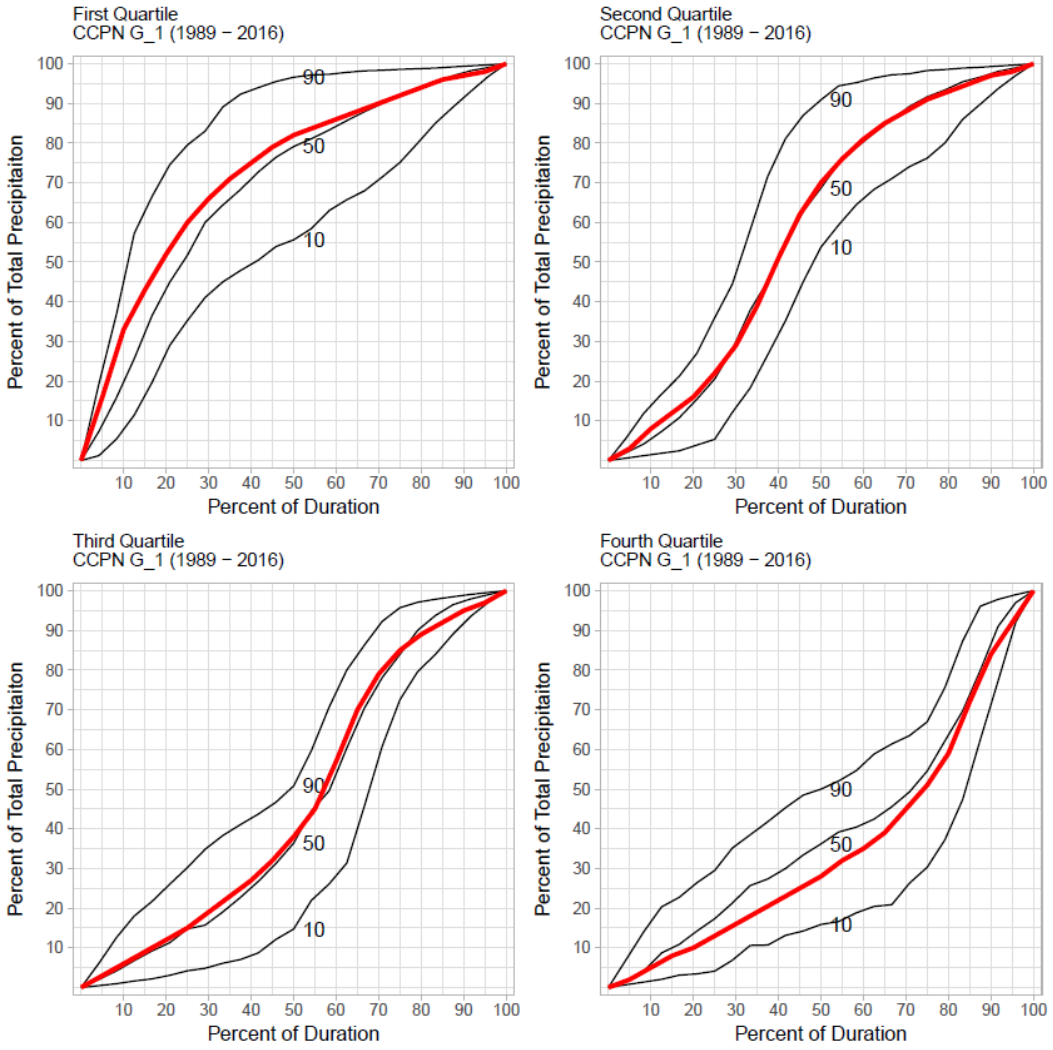

Figure 1.4. Examples of single-site quartile curves for CCPN Gage 1 (1989–2016) with a comparison to the median point time distributions (thick red line) from Huff, 1990, Table 4

Results

In this study, quartile curves for areas 0 to 10 square miles (point curves), areas 10 to 50 square miles, and areas 50 to 400 square miles were generated using the combined data observed at 25 CCPN and 20 IVPN gages. Point curves determined in this study were compared to those from Table 3 in Huff (1990); the curves for areas between 10 and 50 square miles were compared to the curves from Table 4 in Huff (1990); and curves for areas between 50 and 400 square miles were compared to the area median distribution curve from Table 1 in Huff (1990). These comparisons in this study are presented as tables and figures. Tables 1.1–1.3 represent

the new time distribution of rainfall in heavy storms for a point (0–10 square miles), small areas (10–50 square miles), and large areas (50–400 square miles), respectively. The values in these tables are shown in percentages of total rainfall for each quartile. Corresponding Huff curves with comparisons to the results obtained in this study are shown in Figures 1.5–1.7. The new updated curves are reasonably similar to the original Huff curves, except for the fourth quartile, for areas 10–50 and 50–400 square miles, and for the first quartile for areas 0–10 square miles.

Table 1.1. Median Time Distribution of Heavy Storm Rainfall, Using the Mean of All Point Time Distributions (0 to 10 square miles) from Gages in the CCPN and IVPN. Units are a percentage of the total accumulated precipitation within the storm.

Portion of the Storm	First Quartile	Second Quartile	Third Quartile	Fourth Quartile
0/24	0.00	0.00	0.00	0.00
1/24	8.36	2.29	2.05	2.31
2/24	17.73	4.82	4.31	4.79
3/24	28.11	7.78	6.67	7.12
4/24	38.33	11.33	9.12	9.78
5/24	47.45	15.79	11.71	12.53
6/24	55.50	21.39	14.36	15.23
7/24	62.25	28.41	16.91	17.91
8/24	67.22	36.44	19.64	20.33
9/24	70.82	45.29	22.78	22.83
10/24	74.17	54.35	26.33	25.41
11/24	76.97	62.38	30.93	28.35
12/24	79.81	69.76	36.35	31.25
13/24	82.55	75.48	43.92	33.90
14/24	85.18	80.38	52.11	36.33
15/24	87.40	84.70	61.02	38.61
16/24	89.47	87.81	69.89	41.24
17/24	91.17	90.22	78.19	45.08
18/24	92.70	92.17	84.92	51.29
19/24	94.03	93.81	89.74	59.31
20/24	95.36	95.29	93.11	69.19
21/24	96.56	96.57	95.34	80.05
22/24	97.74	97.74	97.06	89.71
23/24	98.85	98.84	98.56	96.04
24/24	100.00	100.00	100.00	100.00

Table 1.2. Median Time Distribution of Heavy Storm Rainfall on Medium-size Areas (10 to 50 square miles) in the CCPN and IVPN. Units are a percentage of the total accumulated precipitation within the storm.

Portion of the Storm	First Quartile	Second Quartile	Third Quartile	Fourth Quartile
0/24	0.00	0.00	0.00	0.00
1/24	6.41	1.48	1.33	1.48
2/24	15.69	3.57	3.02	3.34
3/24	27.45	6.39	5.13	5.72
4/24	38.91	10.02	7.53	8.56
5/24	49.34	14.71	10.01	11.69
6/24	58.55	20.89	12.65	14.19
7/24	65.88	28.91	15.24	17.19
8/24	71.10	37.55	18.17	19.69
9/24	74.92	46.86	21.46	22.27
10/24	78.30	56.25	25.36	24.81
11/24	81.16	64.84	29.90	27.46
12/24	83.75	72.90	35.60	30.33
13/24	86.20	79.07	43.42	32.42
14/24	88.64	83.97	52.18	34.28
15/24	90.81	87.58	61.88	36.89
16/24	92.58	90.67	71.81	39.73
17/24	93.99	92.76	80.43	43.85
18/24	95.19	94.59	87.25	49.87
19/24	96.35	95.97	92.01	58.93
20/24	97.27	97.10	95.04	69.85
21/24	98.03	97.99	96.90	82.36
22/24	98.74	98.72	98.22	92.59
23/24	99.37	99.39	99.21	97.96
24/24	100.00	100.00	100.00	100.00

Table 1.3. Median Time Distribution of Heavy Storm Rainfall on Large Areas (50 to 400 square miles) in the CCPN and IVPN. Units are the percentage of total accumulated precipitation within the storm.

Portion of the Storm	First Quartile	Second Quartile	Third Quartile	Fourth Quartile
0/24	0.00	0.00	0.00	0.00
1/24	4.59	0.88	0.72	0.90
2/24	13.49	2.38	1.85	2.29
3/24	25.94	4.93	3.47	4.36
4/24	39.17	8.52	5.57	7.10
5/24	51.04	13.19	8.28	9.93
6/24	60.79	19.59	10.96	12.84
7/24	69.26	27.46	13.79	15.46
8/24	74.80	37.17	16.35	17.83
9/24	78.74	47.77	19.66	20.12
10/24	82.20	58.18	23.46	23.12
11/24	85.13	67.64	28.07	25.76
12/24	87.38	75.86	34.06	28.26
13/24	89.58	82.04	42.30	30.99
14/24	91.45	86.92	52.02	33.68
15/24	93.35	90.33	62.76	36.12
16/24	94.80	93.09	72.80	39.07
17/24	95.99	94.82	82.27	42.93
18/24	96.94	96.25	89.19	48.98
19/24	97.70	97.34	93.60	59.22
20/24	98.35	98.21	96.33	71.66
21/24	98.86	98.83	97.97	85.18
22/24	99.28	99.30	98.98	94.64
23/24	99.66	99.67	99.58	98.77
24/24	100.00	100.00	100.00	100.00

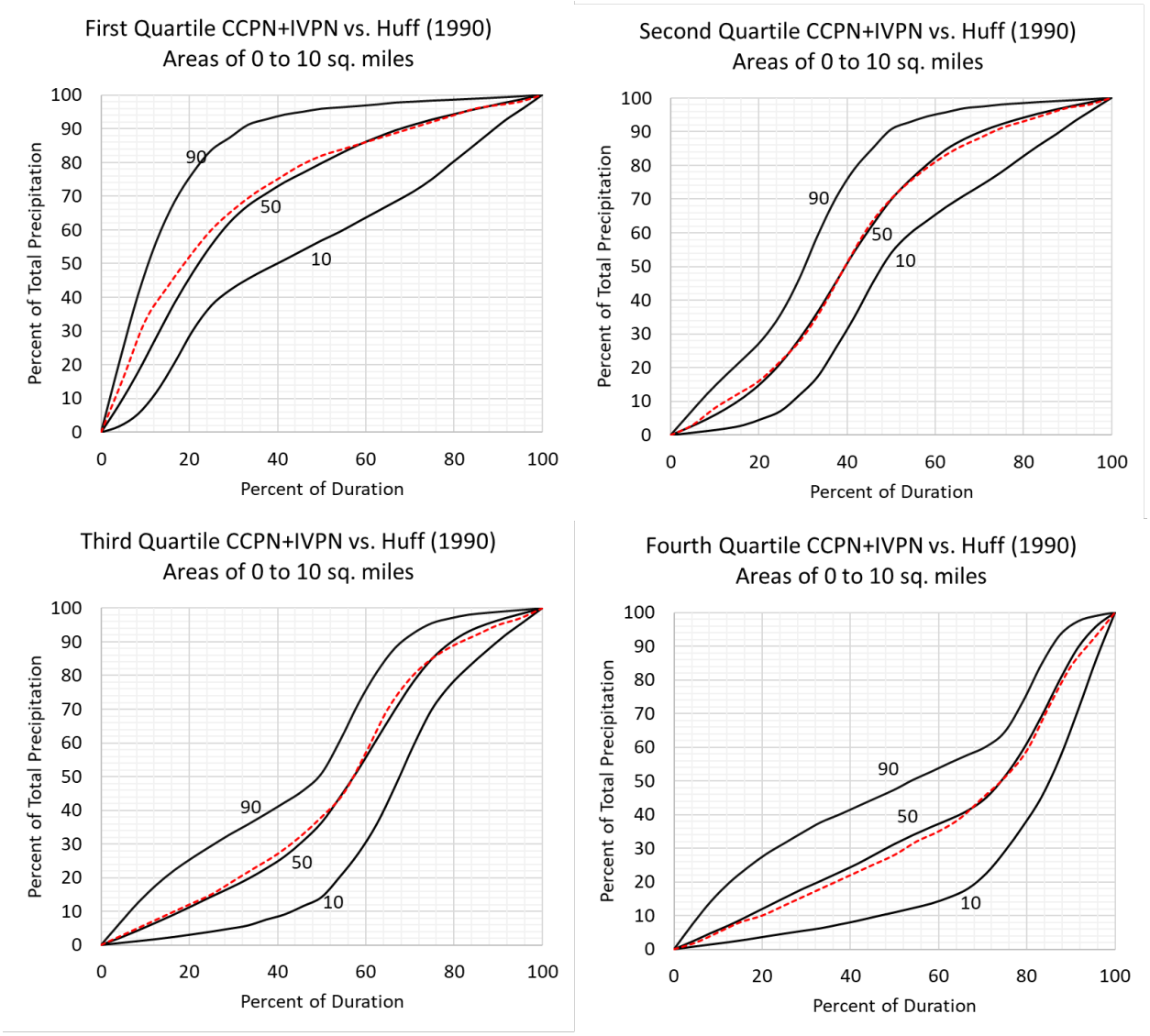

Figure 1.5. Curves for point (0 to 10 square miles) time distributions from all gages within the CCPN and IVPN compared to the median time distribution from Huff (1990), (red dashed line)

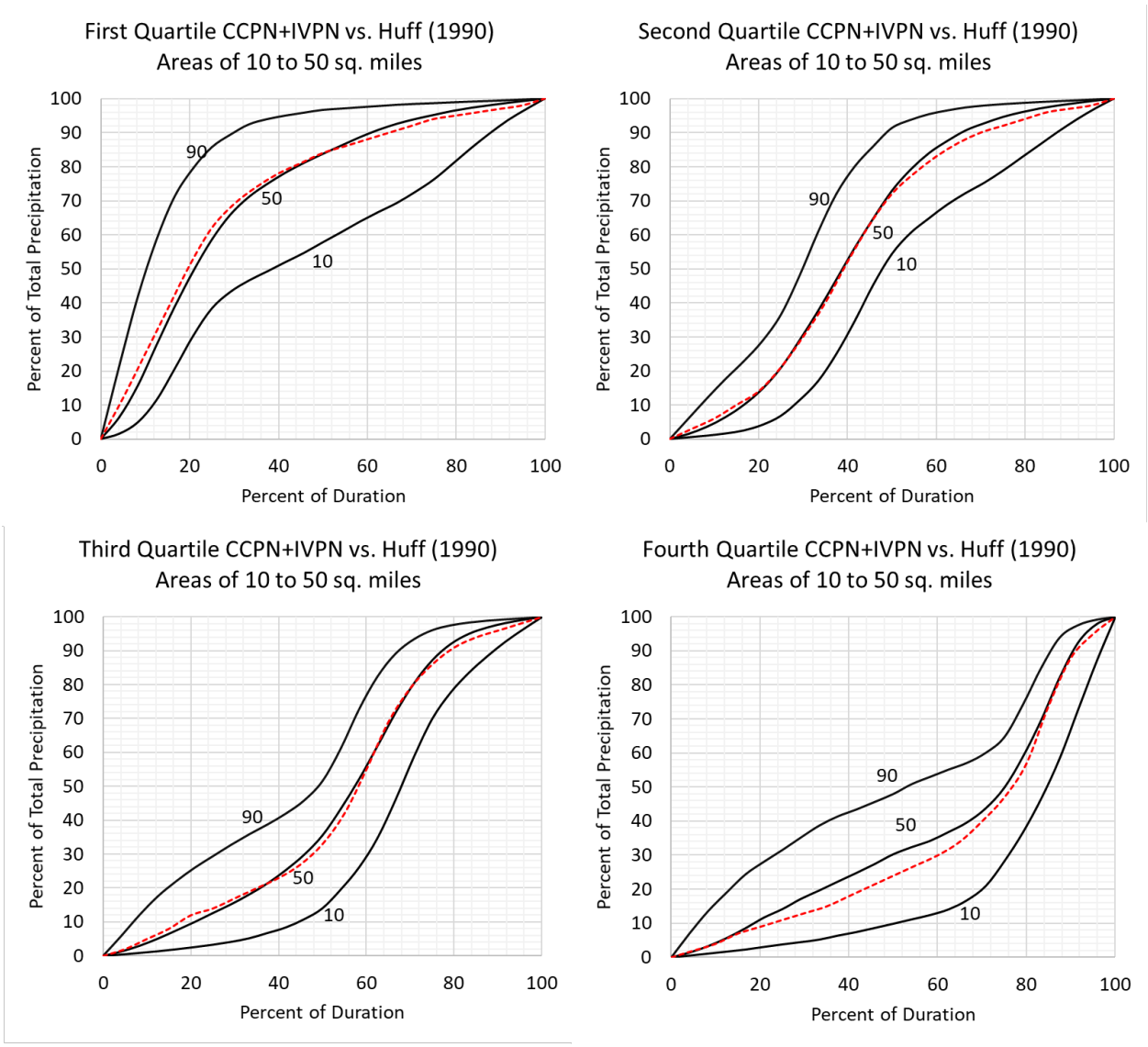

Figure 1.6. Curves for areal (10 to 50 square miles) time distributions from all gages within the CCPN and IVPN compared to the median time distribution from Huff (1990), (red dashed line)

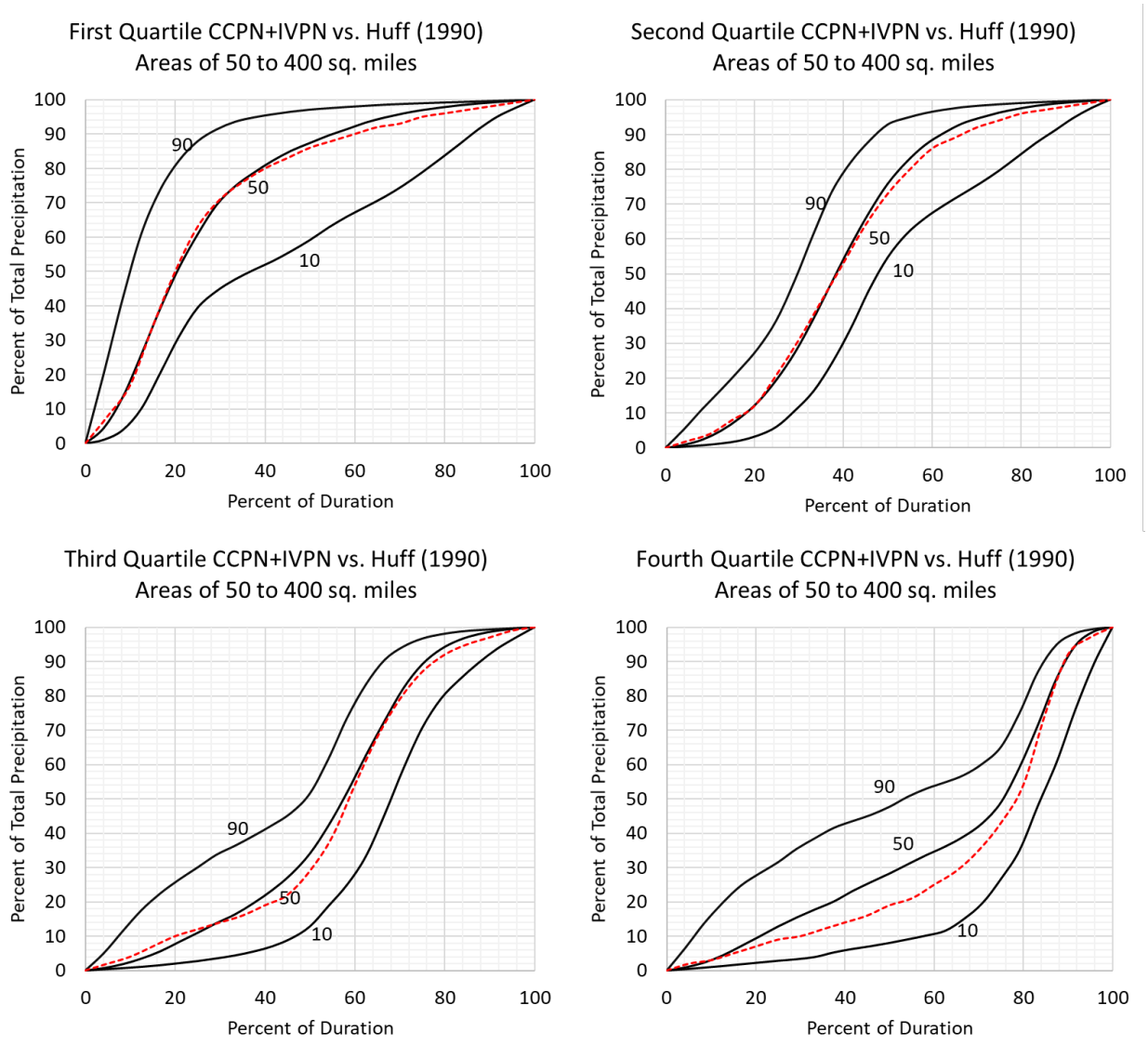

Figure 1.7. Curves for areal (50 to 400 square miles) time distributions from all gages within the CCPN and IVPN compared to the median time distribution from Huff (1990), (red dashed line)

Discussion and recommendations

The CCPN and IVPN have been selected as the key precipitation networks for this task. These extensive precipitation monitoring networks have sufficient record lengths to evaluate if and how much the temporal storm distributions from the original Huff curves (Huff, 1990) have changed. The original precipitation network data used to determine the original Huff curves were lost over time as storage media changed. Gages in the other available source HPD were not dense enough to adequately determine areal distributions (10–50 and 50–400 square miles).

A comparison between the original Huff (1990) curves and those updated in this study revealed that most of the differences occurred in the first quartile for the smallest areas (0 to 10 square miles) and in the fourth quartile, particularly for the largest areas (50–400 square miles). The new updated storm time distributions (Tables 1.1–1.3 and Figures 1.5–1.7) are recommended to be used in place of the older Huff (1990) curves.

References

Angel, J. and M. Markus. 2019. *Frequency Distributions of Heavy Precipitation in Illinois: Updated Bulletin 70*. Illinois State Water Survey Contract Report 2019-05, Champaign, IL.

Bonta, J. V. 2004. Development and utility of Huff curves for disaggregating precipitation amounts. *Applied Engineering in Agriculture* 20(5):641–653.

Bonta, J. V. and A. R. Roa. 1987. Factors affecting development of Huff curves. *Transaction of the ASAE* 31(1):102–106.

Bauer, E. and N. Westcott. 2017. *Continued Operation of a 25-Raingage Network for Collection, Reduction, and Analysis of Precipitation Data for Lake Michigan Diversion Accounting: Water Year 2016*. Illinois State Water Survey Contract Report 2017-03, Champaign, IL.

Huff, F. A. 1967. Time distribution of rainfall in heavy storms. *Water Resources Research* 3(4):1007–1019.

Huff, F. A. 1990. *Time Distribution of Heavy Rainstorms in Illinois*. Illinois State Water Survey Circular 173, Champaign, IL.

Huff, F. A. and J. R. Angel. 1989a. *Frequency Distributions and Hydroclimatic Characteristics of Heavy Rainstorms in Illinois*. Illinois State Water Survey Bulletin 70, Champaign, IL.

Huff, F. A., and J. R. Angel. 1989b. *Frequency Distributions of Heavy Rainstorms in Illinois*. Illinois State Water Survey Circular No. 172, Champaign, IL.

Illinois Department of Transportation. 2011. *IDOT Drainage Manual*. Illinois Department of Transportation, Bureau of Bridges and Structures, Springfield, IL.

R Core Team. 2017. *R: A Language and Environment for Statistical Computing*. R Foundation for Statistical Computing, Vienna, Austria. https://www.R-project.org/.

Restrepo, P. J. and P. S. Eagleson. 1982. Identification of independent rainstorms. *Journal of Hydrology* 55(1982).

Westcott, N. E., K. L. Rennels, and S. D. Wilson. 2009. *Operation of Rain Gauge and Groundwater Monitoring Networks for the Imperial Valley Water Authority Year Fifteen: September 2006-August 2007*. Illinois State Water Survey Contract Report 2009-05, Champaign, IL.

2. Areal reduction factors

Introduction

Numerous hydrological and meteorological applications require estimates of spatial and temporal variability of rainfall over a large area. The intensity of point rainfall is only applicable for relatively small areas (e.g., 2 mi^2) but for larger areas should be converted to average areal depths (Srikanthan, 1995). Areal reduction factors (ARFs) are the most widely used method to estimate area-equivalent rainfall using point precipitation data. A typical ARF, presented in Technical Paper 29 (TP-29) (U.S. Weather Bureau, 1957, 1958, 1959, 1960) is estimated by dividing the average areal rainfall of the annual maximum point rainfall by the annual point rainfall for a specific area and duration.

In this report two areal reduction methods have been applied to precipitation data obtained from two dense precipitation networks, Cook County Precipitation Network (CCPN) (Bauer and Westcott, 2017), shown in Figure 1.1, and Imperial Valley Precipitation Network (IVPN) (Westcott et al., 2009) located in central Illinois (Figure 1.2), using the statistical program CRAN/R (R Core Team, 2017). The two methods for estimating areal reduction factors used in this report are the fixed-area method, such as that used in TP-29 (U.S. Weather Bureau, 1957, 1958), and the storm-centered method described by Bell (1976).

Methods

The U.S. Weather Bureau TP-29 method remains one of the most widely used methods for calculating ARFs in the United States (U.S. Weather Bureau, 1957, 1958, 1959, 1960). This method is classified as an empirical, fixed-area method and does not consider the return period and shape of the area in ARFs estimation. In this method, the area of a watershed containing *n* number of gages is equal to that of *n* circles, each having a diameter equal to the average station spacing. Thus, this method produces reasonable areas for equally spaced precipitation stations. For each duration, the ARF is calculated by evaluating the ratio of the mean area annual maximum series to that of the mean of the maximum point precipitation for all gages in the given area. This method is generally accepted for areal averages of approximately 400 square miles or less (U.S. Weather Bureau, 1959, 1960).

Storm-centered ARFs are calculated for individual rainfall events by dividing the maximum areal rainfall within the storm zone for a given area and duration by the maximum point rainfall within the same storm and duration (Bell, 1976). The purpose of this study was to compare the fixed-area and the storm-centered methods with the results published in Bulletin 70 (Huff and Angel, 1989) (Table 35, p. 97). The results are described in “Results” and “Conclusions” in this section.

Bulletin 70 used rainfall data from two dense raingage networks located in east central Illinois (Huff, 1990) to determine the relationship between point and areal mean rainfall frequencies for areas ranging from 10 to 400 square miles. For the first network, a 10-year rainfall data record from an urban network of 11 recording raingages located in Urbana-Champaign, Illinois, was used to calculate ARFs for 10 square miles. For the second network, a 12-year rainfall data record from a network of 49 raingages on 400 square miles in east central Illinois was used to estimate ARFs for sampling areas of 50, 100, 200, and 400 square miles. The areal mean was then calculated using the arithmetic average of all gages in each sampling area (10–400 square miles). Point rainfall was calculated as the value of the central gage in each sampling area. For each storm period (30 minutes to 48 hours), the study was restricted to storms in which the central gage recorded rainfall that equaled or exceeded the amount expected to occur on average once in two years.

Results

For comparison with the ARF curves published in Bulletin 70, the CCPN and IVPN networks were used to develop ARF curves based on the fixed-area method and the storm-centered method. The networks used by Huff were not continued, thus no additional data were available for comparison. The results are shown in Figures 2.1–2.4.

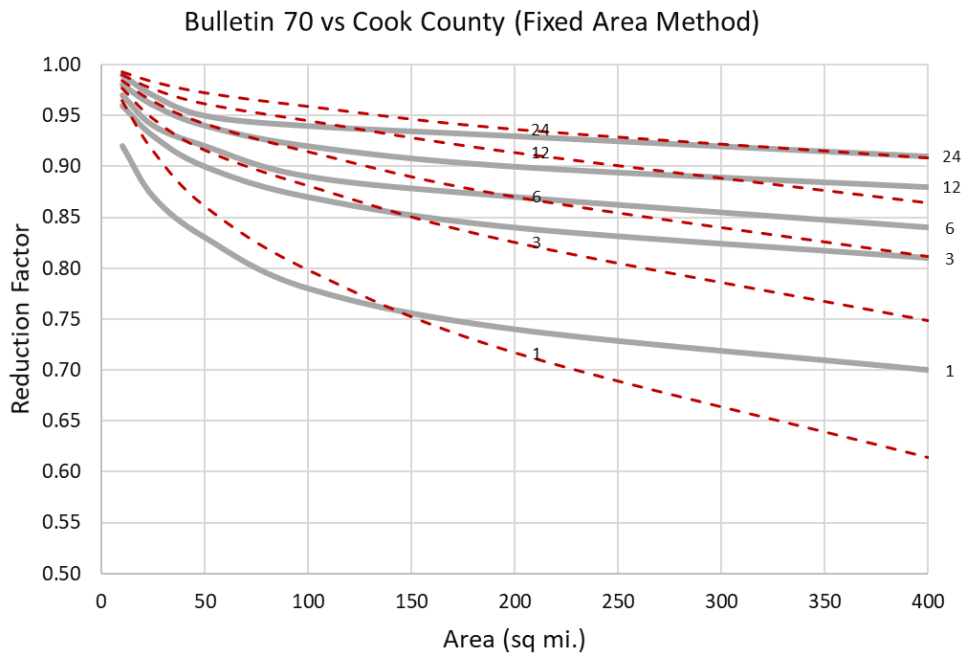

Figure 2.1. ARF curves based on Bulletin 70 (solid lines) and the fixed-area method applied to the CCPN data (red dashed lines). Storm durations of 1 to 24 hours are shown.

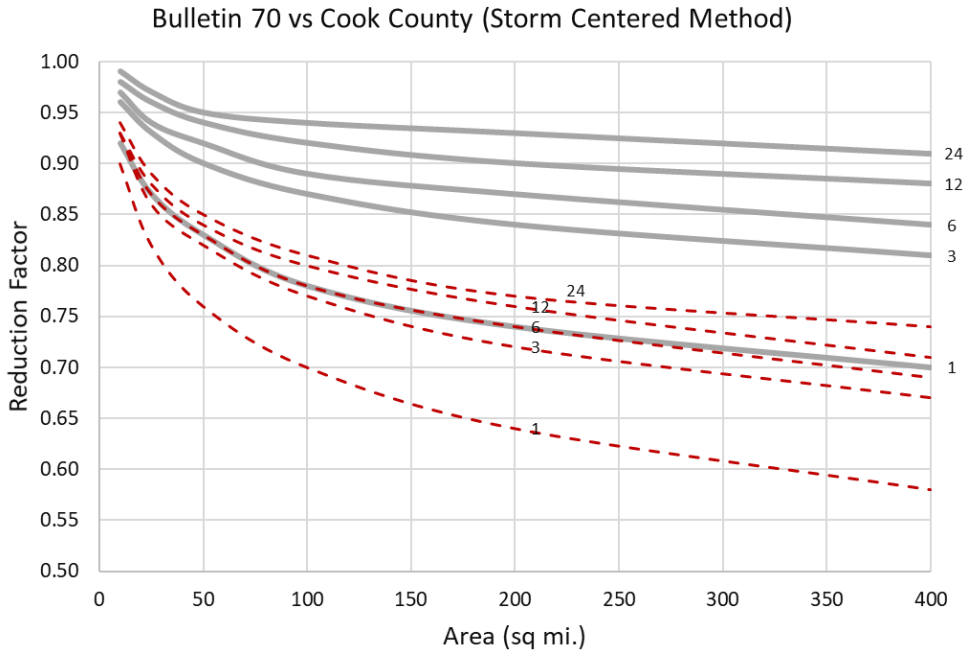

Figure 2.2. ARF curves based on Bulletin 70 (solid lines) and the storm-centered method applied to the CCPN data (red dashed lines). Storm durations of 1 to 24 hours are shown.

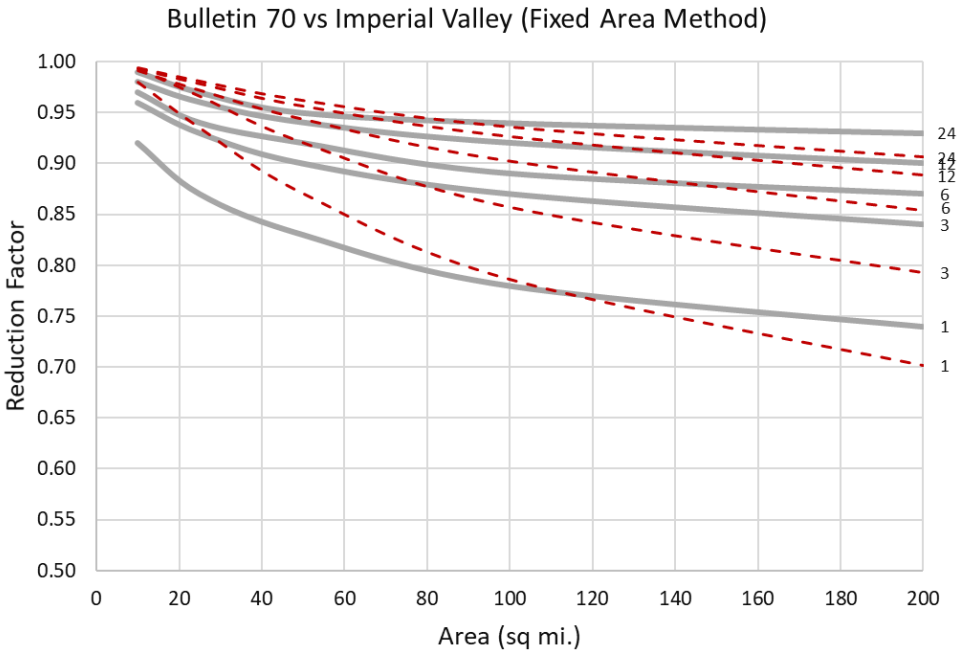

Figure 2.3. ARF curves based on Bulletin 70 (solid lines) and the fixed-area method applied to the IVPN data (red dashed lines). Storm durations of 1 to 24 hours are shown.

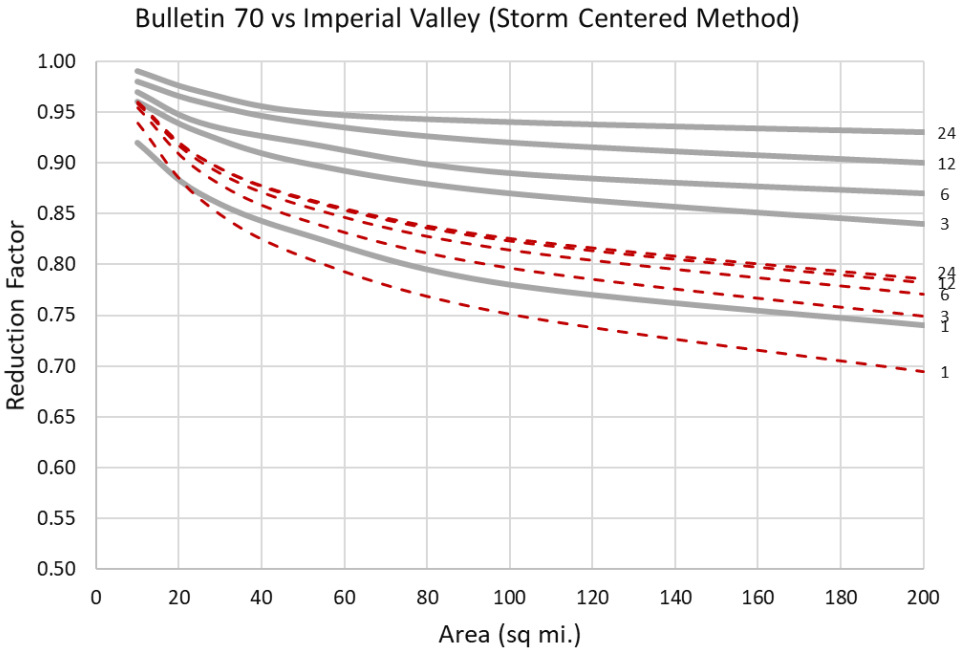

Figure 2.4. ARF curves based on Bulletin 70 (solid lines) and the storm-centered method applied to the IVPN data (red dashed lines). Storm durations of 1 to 24 hours are shown.

The comparisons (Figures 2.1–2.4) indicate that the storm-centered, method-based curves are typically lower than the curves given in Bulletin 70, meaning that the areal reduction factors produce lower estimates for areal rainfall. Conversely, the fixed-area method generally produces higher estimates than the Bulletin 70 curves, resulting in a smaller reduction than both Bulletin 70 and the storm-centered method. It is important to note that these differences are particularly significant for more frequently used smaller areas (e.g., areas less than 50 square miles). The significantly different estimates of ARF curves based on the two methods confirmed the findings of Pavlovic et al. (2016) that there are "significant uncertainties in the ARF estimates, regardless of the method used. Even when calculated from the same dataset and for the same geographic area, the ARF estimates from the selected methods differ."

Recommendations

The results produced in this study were highly variable depending on the ARF estimation method used. This variability hinders the ability to reach a strong and unequivocal conclusion. To explain and potentially reduce the large uncertainty in the results of this study, a more comprehensive study with additional considerations, methods, and datasets would be required. This study did not produce results consistent enough to suggest modifications for the currently used ARF curves. Therefore, at this time, it is recommended to use the existing ARFs published in Bulletin 70 (Table 35, p. 97). For convenience, this table has been reproduced and included in this report (Table 2.1).

Table 2.1. Relations Between Areal Mean and Point Rainfall Frequency Distributions (adopted from Huff and Angel, 1989)

Storm period (hours)	Ratio of areal to point rainfall for given area					
	10	25	50	100	200	400
0.5	0.88	0.80	0.74	0.68	0.62	0.56
1.0	0.92	0.87	0.83	0.78	0.74	0.70
2.0	0.95	0.91	0.88	0.84	0.81	0.78
3.0	0.96	0.93	0.90	0.87	0.84	0.81
6.0	0.97	0.94	0.92	0.89	0.87	0.84
12.0	0.98	0.96	0.94	0.92	0.90	0.88
24.0	0.99	0.97	0.95	0.94	0.93	0.91
48.0	0.99	0.98	0.97	0.96	0.95	0.94

References

Bauer, E. and N. Westcott. 2017. *Continued Operation of a 25-Raingage Network for Collection, Reduction, and Analysis of Precipitation Data for Lake Michigan Diversion Accounting: Water Year 2016*. Illinois State Water Survey Contract Report 2017-03, Champaign, IL.

Bell, F. 1976. *The Areal Reduction Factor in Rainfall Frequency Estimation*. Institute of Hydrology. IH Report No. 35, Wallingford, U.K.

Huff, F. A. and J. R. Angel. 1989. *Frequency Distributions and Hydroclimatic Characteristics of Heavy Rainstorms in Illinois.* Illinois State Water Survey Bulletin 70, Champaign, IL.

Pavlovic, S., S. Perica, M. St. Laurent, and A. Mejía. 2016. Intercomparison of selected fixed-area areal reduction factor methods. *Journal of Hydrology* 537(38):419–430. https://doi.org/10.1016/j.jhydrol.2016.03.027.

R Core Team. 2017. *R: A Language and Environment for Statistical Computing*. R Foundation for Statistical Computing, Vienna, Austria. https://www.R-project.org/.

Srikanthan, R. 1995. *A Review of the Methods for Estimating Areal Reduction Factors for Design Rainfalls*. CRC for Catchment Hydrology. Department of Civil Engineering, Monash University.

U.S. Weather Bureau. 1957. *Rainfall Intensity Frequency Regime*. Technical Paper No. 29, Part 1, Ohio Valley. U.S. Department of Commerce, Washington, D.C., 44 pp.

U.S. Weather Bureau. 1958. *Rainfall Intensity Frequency Regime*. Technical Paper No. 29, Part 2, Southeastern United States; Part 3, Middle Atlantic Region. U.S. Department of Commerce, Washington, D.C.

U.S. Weather Bureau. 1959. *Rainfall Intensity Frequency Regime*. Technical Paper No. 29, Part 4, Northeastern United States, U.S. Department of Commerce, Washington, D.C., 35 pp.

U.S. Weather Bureau. 1960. *Rainfall Intensity Frequency Regime*. Technical Paper No. 29, Part 5, Great Lakes Region, U.S. Department of Commerce, Washington, D.C., 31 pp.

Westcott et al. 2009. Continued Operation of a 25-Raingage Network for Collection, Reduction, and Analysis of Precipitation Data for Lake Michigan Diversion Accounting: Water Year 2008. Illinois State Water Survey Contract Report 2009-02, Champaign, IL.

3. Monte Carlo experiment: representative year

Introduction

Several studies, including the recent National Climate Assessment (Easterling et al., 2017), have shown that in many regions of the United States, including the Midwest, the risk of increased heavy precipitation has become greater. Moreover, climate modeling-based scientific studies indicate that this trend will continue in the future. This finding is applicable to Illinois, as numerous studies and publications, e.g., Huff and Changnon (1987) and Markus et al. (2007), indicate that the assumption of stationarity (constant statistical properties over time) is not valid for heavy precipitation in this state.

Two main approaches are commonly used in studying the nonstationary (changing) frequency of heavy precipitation. One approach assumes two or more quasi-stationary time periods of the annual maximum series and treats each as stationary (Markus et al., 2018). Then, frequencies are calculated and compared for each time period. The other approach expresses frequency distribution parameters as a function of time (Katz, 2013; Cheng et al., 2014), producing the frequency estimates that also change with time.

The Bulletin 70 type of adjustment (Huff and Angel, 1989) was adopted in this study as one of the earliest methods to account for non-stationarity in heavy precipitation. This adjustment is calculated first by dividing the entire observation period into two halves for which precipitation frequency is calculated separately. The symbols RFA_0, RFA_1, and RFA_2 denote the frequency quantiles for the entire period, the first half, and the second half, respectively. The nonstationary adjustment factor F_2 is defined as

$$F_2 = \frac{RFA_2}{RFA_1}. \qquad (3.1)$$

The final frequency quantile RFA after nonstationary adjustment is

$$RFA = F_2 \cdot RFA_0 = RFA_0 \frac{RFA_2}{RFA_1}. \qquad (3.2)$$

A weakness of this method, however, is that it does not specify the year that it represents. To determine the year the adjustment factor represents, a new experiment was designed based on a nonstationary generalized extreme value (GEV) model introduced by Serago and Vogel (2018) and the Monte Carlo simulation method. The new experiment is described in the following paragraph.

Description of the experiment

The steps of the experiment are presented in Figure 3.1. For each site, the experiment starts with the observed annual maximum series (AMS) and fits the Serago-Vogel (Serago and Vogel, 2018) nonstationary model assuming the GEV distribution. As a result of this model, each year is represented by a different frequency distribution and thus in different frequency estimates. Serago and Vogel (2018) proposed a method of frequency analysis under a nonstationary assumption using the GEV distribution. The traditional GEV distribution has three parameters: location, shape, and scale. Instead of fixed parameters for the whole time period, in the nonstationary GEV model, location, and scale parameters can vary with time, while the shape parameter is kept constant. The quantiles for each year are expressed by Equation (3.3),

$$\hat{x}_{p|w} = \hat{\xi}_{x|w} + \frac{\hat{\alpha}_{x|w}}{\hat{\kappa}_{x|w}}\left(1 - \left[-\ln(p)\right]^{\hat{\kappa}_{x|w}}\right). \quad (3.3)$$

In this equation, $\hat{x}_{p|w}$ is the nonstationary quantile for nonexceedance probability *p* for year *w*. Symbols $\hat{\xi}_{x|w}$, $\hat{\alpha}_{x|w}$, and $\hat{\kappa}_{x|w}$ denote nonstationary location, scale, and shape parameters, respectively, for year *w*. To illustrate this experiment, the historical record of station Aurora in the NE section from 1895 to 2017 for a 100-year return period for p=0.99 is used. An example is shown in Figure 3.2.

In the next step, these determined distribution parameters are used to generate 1,000 synthetic AMS time series sampled from the same distribution as the observed data. For each of those time series, the Bulletin 70 type of trend adjustment factor (F_2) was calculated and applied to the original observed dataset.

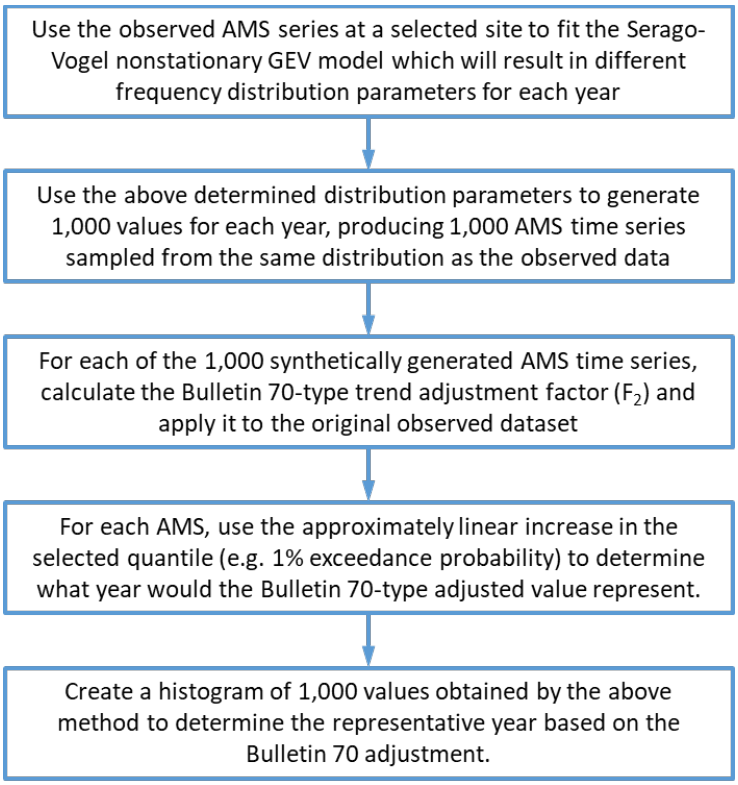

Figure 3.1. Flow chart of the steps in the experiment designed to provide an estimate of the representative year for the Bulletin 70 temporal trend adjustment

A schematic in Figure 3.3 illustrates the frequency estimates prior to and after trend adjustment. The representative year for each synthetically generated sample is then determined as the year of intersection between the quantile line (e.g., 1% exceedance probability) and the horizontal line equal to the trend-adjusted Bulletin 70 estimate. This illustrative example determined that the representative year is 2040. The final step in this approach is to create a histogram of 1,000 values obtained by the Monte Carlo experiment to determine the distribution of representative years based on the Bulletin 70 adjustment.

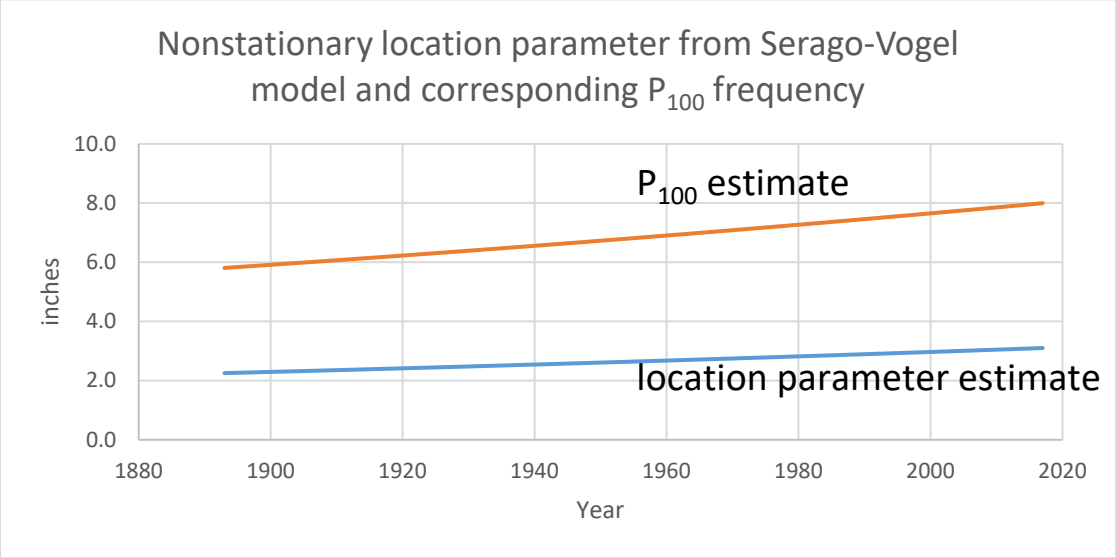

Figure 3.2. Time-dependent location parameter and 100-year (P_{100}) quantile estimate for 24-hour storm duration at Aurora (NE region), 1895–2017

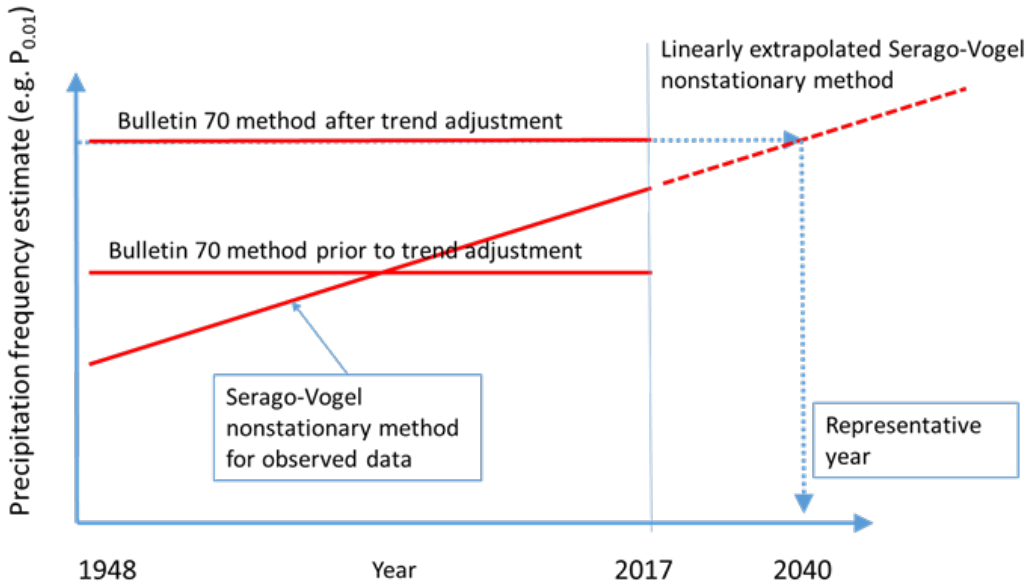

Figure 3.3. Illustration of the method for determining the representative year for the adopted Bulletin 70 type temporal trend adjustment

Data

Several stations with significant trends in the annual maximum series (AMS) and long-term records, including Aurora (USC00110338), Marengo (USC00115326), and Chicago O'Hare International Airport (USW00094846) in the NE region and Carbondale Sewage Plant (USC00111265) in the S region were selected.

Results

A key assumption for this experiment is that the AMS time series can be described by the Serago-Vogel model and that only two parameters are variable (location and scale) but the shape parameter is constant. In addition, it is assumed that the change in the frequency is linear. Accordingly, the meaning of these results should be interpreted in light of the assumptions and limitations of the Monte Carlo method. Nonetheless, despite the uncertainties caused by these assumptions, the results were deemed sufficient for the scope of this study. Further justification could be provided using a suite of similar Monte Carlo-based methods along with other emerging methods to account for precipitation nonstationarity, such as Cheng et al. (2014).

The histograms presented in Figures 3.4–3.10 show distributions of the representative years for the Bulletin 70-type trend adjustment. The distribution is highly variable and depends on the random selection of the synthetic AMS time series, but it is centered approximately on the end year of the observed record. The results are reasonably consistent for shorter (Figures 3.5 and 3.7) and longer time periods (Figures 3.4, 3.6, 3.8, 3.9, and 3.10), indicating that, on average, the Bulletin 70 adjustment factor adopted in this study represents the end year of the observed dataset.

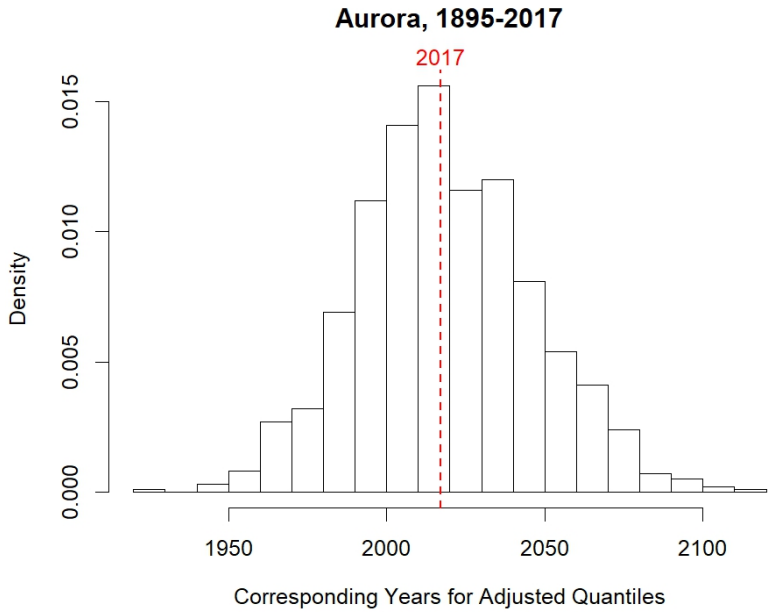

Figure 3.4. Distribution of representative years of Bulletin 70 based on the Monte Carlo experiment for Aurora 1895–2017, indicating the observed dataset end year (2017)

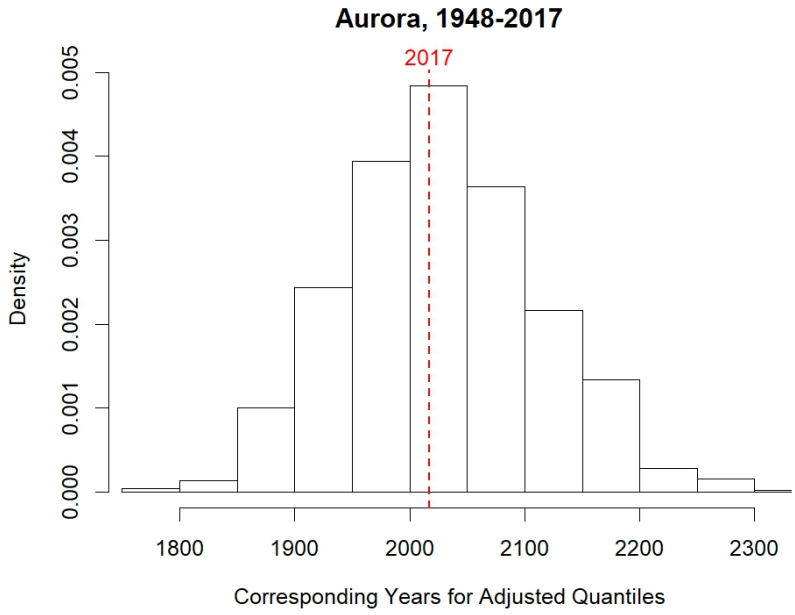

Figure 3.5. Distribution of representative years of Bulletin 70 based on the Monte Carlo experiment for Aurora 1948–2017, indicating the observed dataset end year (2017)

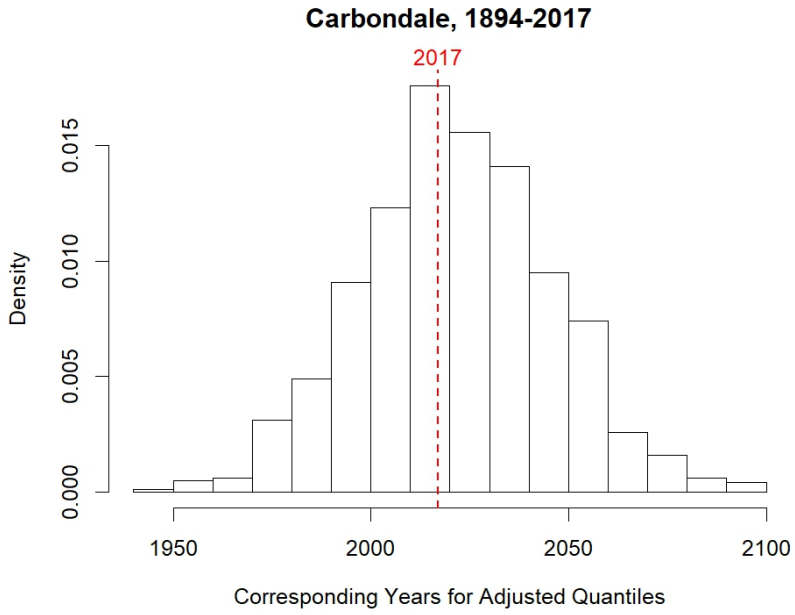

Figure 3.6. Distribution of representative years of Bulletin 70 based on the Monte Carlo experiment for Carbondale 1894–2017, indicating the observed dataset end year (2017)

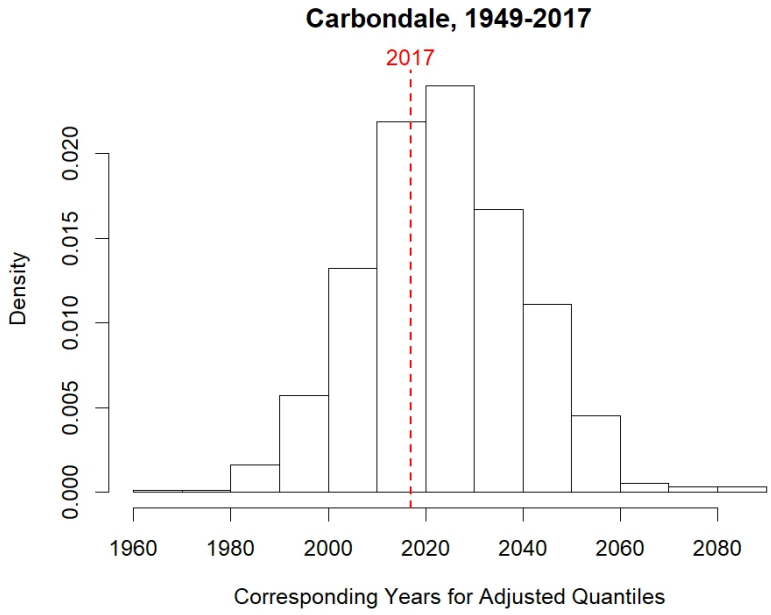

Figure 3.7. Distribution of representative years of Bulletin 70 based on the Monte Carlo experiment for Carbondale 1949–2017, indicating the observed dataset end year (2017)

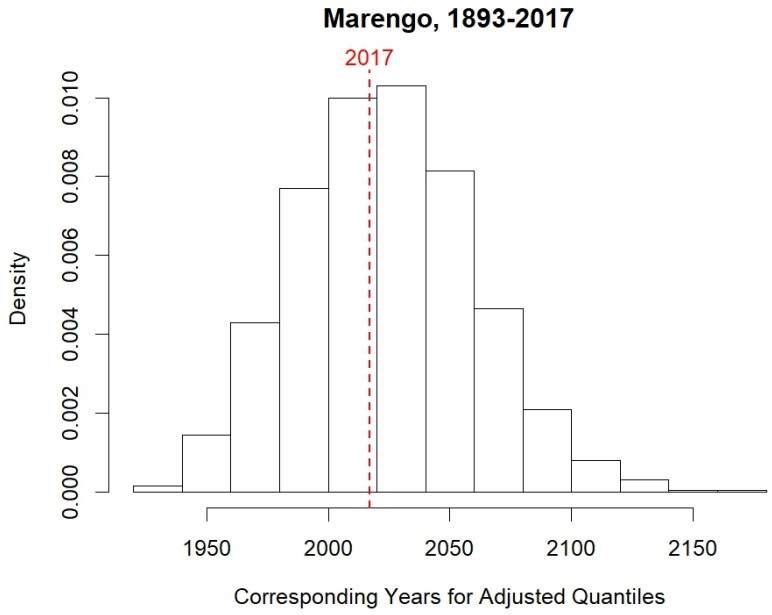

Figure 3.8. Distribution of representative years of Bulletin 70 based on the Monte Carlo experiment for Marengo 1893–2017, indicating the observed dataset end year (2017)

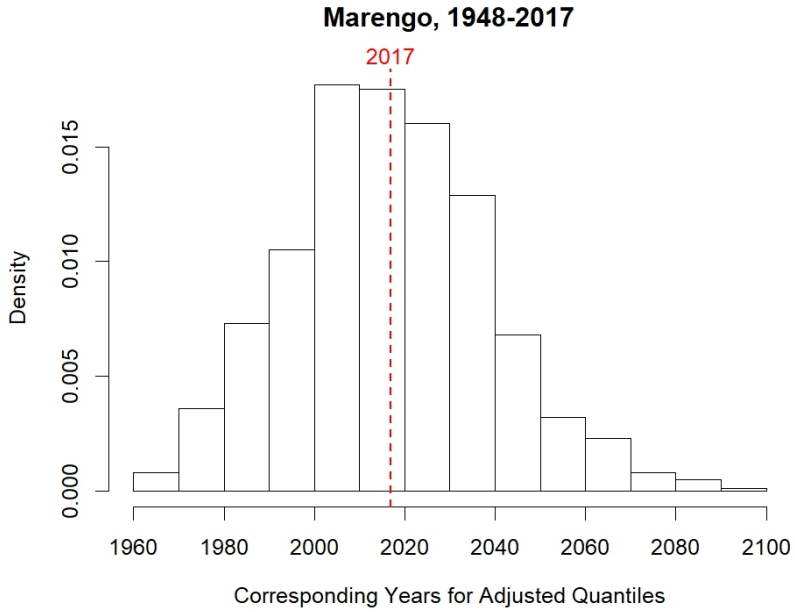

Figure 3.9. Distribution of representative years of Bulletin 70 based on the Monte Carlo experiment for Marengo 1948–2017, indicating the observed dataset end year (2017)

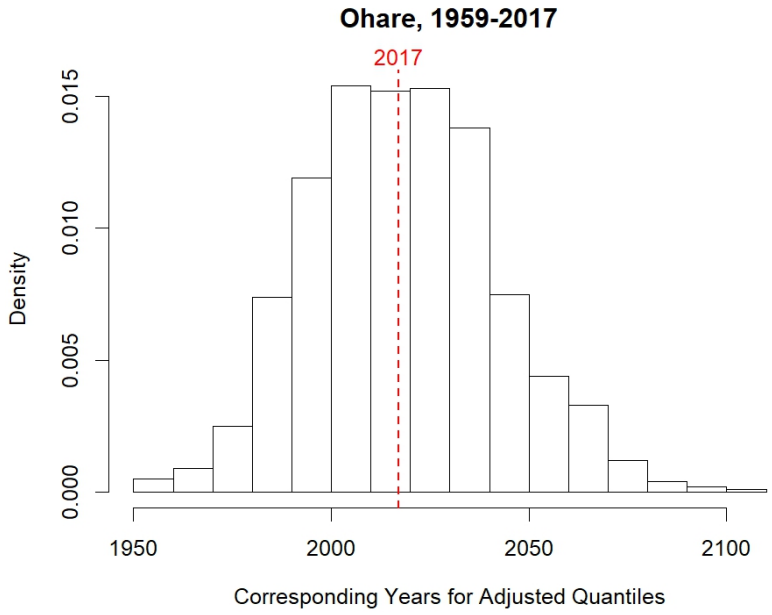

Figure 3.10. Distribution of representative years of Bulletin 70 based on the Monte Carlo experiment for O'Hare 1959–2017, indicating the observed dataset end year (2017)

References

Cheng, L., A. AghaKouchak, E. Gilleland, and R. W. Katz. 2014. Non-stationary extreme value analysis in a changing climate. *Climatic Change* 127:353-369.

Easterling, D. R., K. E. Kunkel, J. R. Arnold, T. Knutson, A. N. LeGrande, L. R. Leung, R. S. Vose, D. E. Waliser, and M. F. Wehner. 2017. Precipitation change in the United States. In: *Climate Science Special Report*: *Fourth National Climate Assessment, Volume I.* DOI:10.7930/J0H993CC.

Fahey, K. A. Hibbard, D. J. Dokken, B. C. Stewart, and T. K. Maycock, eds. *Precipitation Change in the United States*. U.S. Global Change Research Program, Washington, D.C., pp. 207–230, DOI: 10.7930/J0H993CC.

Huff, F. A., and J. R. Angel. 1989. *Frequency Distributions and Hydroclimatic Characteristics of Heavy Rainstorms in Illinois.* Illinois State Water Survey Bulletin 70, Champaign, IL.

Huff, F. A. and S. A. Changnon. 1987. Temporal changes in design rainfall frequencies in Illinois. *Climatic Change* 10:195. https://doi.org/10.1007/BF00140255.

Katz, R. W. 2013. Statistical methods for nonstationary extremes. In *Extremes in a Changing Climate: Detection, Analysis and Uncertainty*. Eds. A. Kouchak, D. Easterling, K. Hsu, S. Schubert, S. Sorooshian. Springer: Dordrecht, The Netherlands, pp. 15–37.

Markus, M., J. R. Angel, L. Yang, and M. Hejazi. 2007. Changing estimates of design precipitation in northeastern Illinois: Comparison between different sources and sensitivity analysis. *Journal of Hydrology* 344(3–4):210–222.

Markus, M., J. Angel, G. Byard, C. Zhang, S. McConkey, X. Cai, L. D. Notaro, and M. Ashfaq. 2018. Communicating the impacts of projected climate change on heavy rainfall using a weighted ensemble approach. *Journal of Hydrologic Engineering* 23(4):04018004.

Serago, J., and R. M. Vogel. 2018. Parsimonious nonstationary flood frequency analysis. *Advances in Water Resources* 112:1–16.

4. Comparison between nonstationary frequency estimation methods and the adopted trend adjustment factor

Introduction

This section describes attempts to provide additional insights into the applicability of the Bulletin 70-based (Huff and Angel, 1989) temporal trend adjustment factor through a comparison with other methods designed to account for nonstationarity in heavy precipitation (Cheng et al., 2014; Serago-Vogel, 2018). Numerous applications demonstrated that all trend adjustment methods, including that of Bulletin 70, are generally sensitive to site-specific data and thus can be highly variable within a region. A way to reduce this sensitivity of site-specific data to outliers and to provide more reasonable estimates of temporal trend adjustment factors is to provide regional statistics and estimates of these factors. However, most of the published methods for non-stationary frequency analysis are developed for a single site. For this reason, and to provide consistent comparisons, the methods in this study were compared using only their site-specific versions. For comparison, the figures in this section also show the results of a regional approach based on Bulletin 70.

The Bulletin 70 method has been described in the previous section of this narrative (Section 3, Equations 3.1–3.2). Both Cheng et al. (2014) and Serago-Vogel (2018) developed methods producing non-stationary frequency estimates, which are based on the assumption that in a nonstationary environment, frequency estimates change gradually with time. The general extreme value (GEV) distribution was adopted for frequency analysis of heavy precipitation. The location, scale, and shape parameters of this distribution were generally assumed to vary with time. However, in some applications, only one parameter (location) or two parameters (location and scale) are assumed to vary, and the other parameters are assumed to be constant. In our applications, the Serago-Vogel model had variable location and scale parameters, and the Cheng et al. model was tested in two forms: one having only the location parameter variable, and the other with all three parameters (location, scale, and shape) variable with time.

In this chapter, the five methods are referred to in the following manner. The “Huff and Angel (1989) region” method refers to the adjustment of the precipitation frequency estimates using a regional average of the change over time. The “Huff and Angel (1989) station” refers to the adjustment of the precipitation estimates using the observed change over time at each particular station. The “Serago and Vogel (2018)” method refers to the method described in more detail in Chapter 3. The “Cheng et al. (2014) 1” method refers to their method with only the location parameter allowed to vary. The “Cheng et al. (2014) 2” method refers to their method with all three parameters allowed to vary.

Results

Thirteen stations from northeastern Illinois were selected based on their data completeness to illustrate these methods. The results for each method are presented in Tables 4.1–4.6. and Figures 4.1–4.13. Table 4.1 shows the unadjusted frequency estimates for all stations in the northeastern Illinois climate section. Table 4.2 shows adjusted frequency estimates, for which the Huff and Angel (1989) region method was used. As stated earlier, for a consistent comparison with other site-specific methods, the Huff and Angel (1989) station method results are shown in Table 4.3. Finally, Tables 4.4, 4.5, and 4.6. show the corresponding results for the Serago and Vogel (2018) method with varying location and scale parameters, the Cheng et al. (2014) 1 method with a varying location parameter, and the Cheng et al. (2014) 2 method with all three parameters (location, scale, and shape parameters) changing with time, respectively.

Table 4.1. Stationary Frequency Estimates for Northeastern Illinois for 1948–2017

Station Name	Recurrence Interval						
	2-yr	5-yr	10-yr	25-yr	50-yr	100-yr	500-yr
AURORA IL	3.60	4.57	5.38	6.53	7.54	8.64	11.58
BARRINGTON 3 SW IL	3.09	3.92	4.61	5.61	6.47	7.41	9.93
CHICAGO BOTANICAL GARDEN	3.22	4.08	4.80	5.84	6.74	7.71	10.34
CHICAGO MIDWAY AIRPORT 3 SW	3.36	4.26	5.01	6.09	7.03	8.05	10.79
CHICAGO OHARE INT. AIRPORT	3.21	4.07	4.79	5.82	6.72	7.69	10.31
DEKALB	3.19	4.05	4.76	5.79	6.68	7.65	10.26
ELGIN	3.11	3.94	4.64	5.64	6.50	7.45	9.98
JOLIET BRANDON RD DM	3.19	4.04	4.76	5.78	6.68	7.64	10.25
MARSEILLES LOCK	3.11	3.95	4.65	5.65	6.52	7.46	10.01
MORRIS 1 NW	3.20	4.06	4.77	5.80	6.70	7.67	10.28
OTTAWA 5 SW	2.87	3.64	4.28	5.20	6.00	6.87	9.21
PARK FOREST	3.15	4.00	4.71	5.72	6.60	7.56	10.14
PEOTONE	3.57	4.53	5.33	6.47	7.47	8.56	11.47

Table 4.2. Region-Based Nonstationary Frequency Estimates for Northeastern Illinois Based on the Huff and Angel (1989) Region Method. In the previous section it was shown that the Bulletin 70-type trend adjustment represents the end year of the record, in this case 2017.

Station Name	Recurrence Interval						
	2-yr	5-yr	10-yr	25-yr	50-yr	100-yr	500-yr
AURORA IL	3.74	4.74	5.61	6.88	8.03	9.32	12.94
BARRINGTON 3 SW IL	3.21	4.07	4.81	5.91	6.89	8.00	11.10
CHICAGO BOTANICAL GARDEN	3.34	4.23	5.01	6.15	7.17	8.32	11.55
CHICAGO MIDWAY AIRPORT 3 SW	3.49	4.42	5.22	6.42	7.49	8.68	12.06
CHICAGO OHARE INT. AIRPORT	3.33	4.22	4.99	6.13	7.15	8.30	11.52
DEKALB	3.32	4.20	4.97	6.10	7.12	8.26	11.46
ELGIN	3.23	4.09	4.83	5.94	6.93	8.04	11.16
JOLIET BRANDON RD DM	3.31	4.20	4.96	6.09	7.11	8.25	11.45
MARSEILLES LOCK	3.24	4.10	4.84	5.95	6.94	8.05	11.18
MORRIS 1 NW	3.32	4.21	4.98	6.11	7.13	8.27	11.48
OTTAWA 5 SW	2.98	3.77	4.46	5.48	6.39	7.41	10.29
PARK FOREST	3.28	4.15	4.91	6.03	7.03	8.16	11.32
PEOTONE	3.71	4.70	5.55	6.82	7.96	9.23	12.81

Table 4.3. Frequency Estimates for Northeastern Illinois based on the Huff and Angel (1989) Station Method. In the previous section it was shown that the Bulletin 70-type trend adjustment represents the end year of the record, in this case 2017. The Chicago Botanical Garden is not presented in this table. It had no observed data in the first half, making it impossible to apply the Bulletin 70-type adjustment (Huff and Angel, 1989).

Station Name	Recurrence Interval						
	2-yr	5-yr	10-yr	25-yr	50-yr	100-yr	500-yr
AURORA IL	3.08	4.13	5.45	8.27	11.87	17.40	44.66
BARRINGTON 3 SW IL	3.56	4.64	5.48	6.59	7.48	8.39	10.56
CHICAGO BOTANICAL GARDEN	n/a	n/a	n/a	n/a	n/a	n/a	n/a
CHICAGO MIDWAY AIRPORT 3 SW	3.96	4.84	5.36	5.86	6.14	6.33	6.50
CHICAGO OHARE INT. AIRPORT	3.65	5.20	6.63	8.89	11.05	13.59	21.43
DEKALB	3.13	4.24	5.29	6.97	8.62	10.60	16.92
ELGIN	3.30	4.16	4.86	5.86	6.70	7.60	9.96
JOLIET BRANDON RD DM	2.92	3.79	4.85	7.03	9.74	13.78	32.79
MARSEILLES LOCK	3.35	4.08	4.63	5.32	5.86	6.39	7.56
MORRIS 1 NW	3.83	4.74	5.47	6.47	7.32	8.20	10.44
OTTAWA 5 SW	2.66	3.15	3.57	4.20	4.77	5.41	7.23
PARK FOREST	3.32	3.89	4.34	4.96	5.47	6.00	7.31
PEOTONE	3.64	4.24	4.67	5.19	5.57	5.94	6.69

Table 4.4. Frequency Estimates for Northeastern Illinois for 2017 Based on the Serago and Vogel (2018) Method

Station Name	Recurrence Interval						
	2-yr	5-yr	10-yr	25-yr	50-yr	100-yr	500-yr
AURORA IL	3.95	5.45	6.52	7.96	9.09	10.28	13.27
BARRINGTON 3 SW IL	3.36	4.44	5.17	6.12	6.84	7.57	9.32
CHICAGO BOTANICAL GARDEN	3.04	4.05	4.71	5.53	6.12	6.70	8.01
CHICAGO MIDWAY AIRPORT 3 SW	3.68	4.82	5.58	6.53	7.23	7.92	9.51
CHICAGO OHARE INT. AIRPORT	3.51	4.73	5.57	6.66	7.49	8.33	10.36
DEKALB	3.46	4.53	5.27	6.23	6.96	7.71	9.51
ELGIN	2.96	3.85	4.41	5.11	5.61	6.10	7.18
JOLIET BRANDON RD DM	3.49	4.71	5.54	6.62	7.44	8.28	10.28
MARSEILLES LOCK	2.94	3.92	4.57	5.37	5.96	6.54	7.85
MORRIS 1 NW	3.01	4.09	4.79	5.67	6.31	6.94	8.37
OTTAWA 5 SW	2.72	3.56	4.10	4.78	5.28	5.77	6.87
PARK FOREST	3.44	4.47	5.15	6.00	6.63	7.25	8.69
PEOTONE	3.89	5.18	6.06	7.20	8.07	8.95	11.06

Table 4.5. Frequency Estimates for Northeastern Illinois for 2017 Based on the Cheng et al. (2014) 1 Method, Where Only the Location Parameter Varies

Station Name	Recurrence Interval						
	2-yr	5-yr	10-yr	25-yr	50-yr	100-yr	500-yr
AURORA IL	3.16	4.24	5.28	7.08	8.84	11.01	18.45
BARRINGTON 3 SW IL	2.89	3.61	4.14	4.83	5.35	5.85	6.99
CHICAGO BOTANICAL GARDEN	3.15	3.80	4.26	4.83	5.24	5.64	6.49
CHICAGO MIDWAY AIRPORT 3 SW	3.25	3.98	4.50	5.16	5.63	6.09	7.08
CHICAGO OHARE INT. AIRPORT	2.80	3.65	4.39	5.51	6.49	7.59	10.75
DEKALB	2.77	3.60	4.31	5.36	6.26	7.26	10.05
ELGIN	2.84	3.46	3.95	4.61	5.13	5.66	6.97
JOLIET BRANDON RD DM	3.11	3.89	4.60	5.76	6.84	8.11	12.12
MARSEILLES LOCK	2.89	3.58	4.15	4.95	5.61	6.30	8.12
MORRIS 1 NW	3.16	3.86	4.39	5.12	5.68	6.25	7.63
OTTAWA 5 SW	2.59	3.23	3.80	4.68	5.46	6.34	8.97
PARK FOREST	2.93	3.72	4.48	5.78	7.03	8.56	13.71
PEOTONE	3.54	4.42	5.20	6.40	7.47	8.67	12.22

Table 4.6. Frequency Estimates for Northeastern Illinois for 2017 Based on the Cheng et al. (2014) 2 Method, Where All Three Parameters Vary

Station Name	Recurrence Interval						
	2-yr	5-yr	10-yr	25-yr	50-yr	100-yr	500-yr
AURORA IL	2.94	3.87	4.79	6.41	8.01	10.03	17.10
BARRINGTON 3 SW IL	3.01	3.88	4.57	5.50	6.22	6.96	8.77
CHICAGO BOTANICAL GARDEN	3.32	3.64	3.76	3.83	3.86	3.88	3.90
CHICAGO MIDWAY AIRPORT 3 SW	3.66	4.35	4.73	5.10	5.31	5.47	5.71
CHICAGO OHARE INT. AIRPORT	3.32	4.81	6.25	8.71	11.10	14.06	24.12
DEKALB	2.73	3.67	4.59	6.15	7.66	9.52	15.81
ELGIN	2.99	3.71	4.26	5.02	5.61	6.21	7.69
JOLIET BRANDON RD DM	3.01	3.73	4.42	5.59	6.72	8.11	12.75
MARSEILLES LOCK	3.00	3.68	4.19	4.86	5.36	5.85	7.00
MORRIS 1 NW	3.24	4.05	4.70	5.59	6.30	7.03	8.85
OTTAWA 5 SW	2.45	2.94	3.35	3.95	4.46	5.00	6.48
PARK FOREST	2.72	3.36	3.98	5.04	6.08	7.36	11.74
PEOTONE	3.16	3.73	4.22	4.95	5.58	6.28	8.27

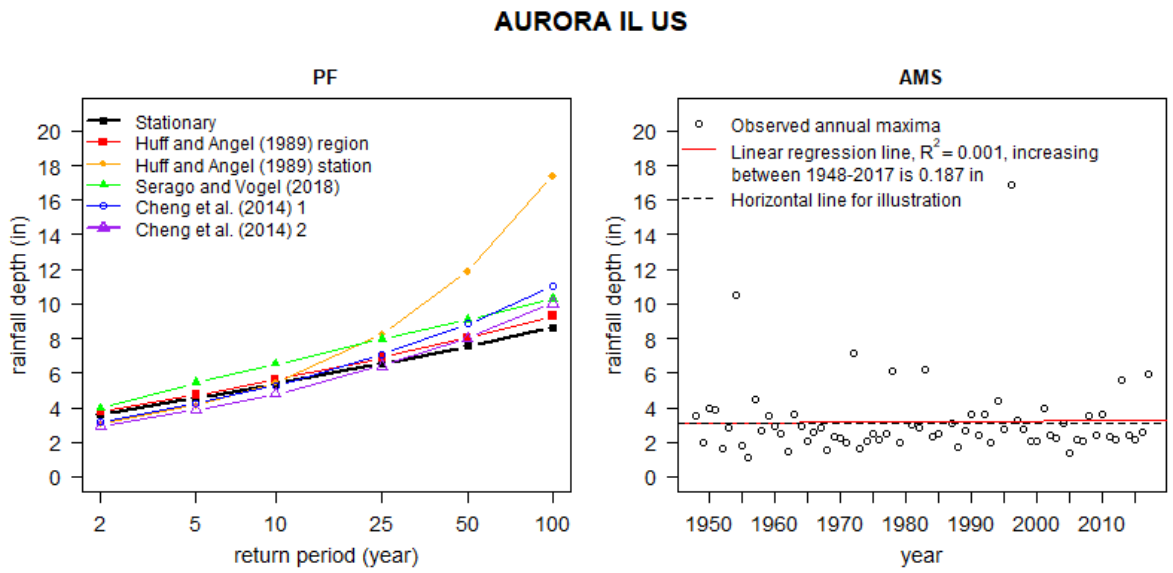

Fig. 4.1. Frequency estimates based on the methods described in this study (left) and observed AMS time series for Aurora (right). The rainfall estimates with no adjustments (i.e., stationary) is used as a benchmark for comparison. While this station showed a slightly increasing trend in the AMS, most of the methods yield lower values at the return periods of 2 to 10 years. Beyond 10 years, they yield higher values than the stationary line. The Huff and Angel (1989) station method yielded much higher amounts at the longer return periods, probably due to the record 16.94-inch rainfall in July 1999, with other methods being less sensitive to this value.

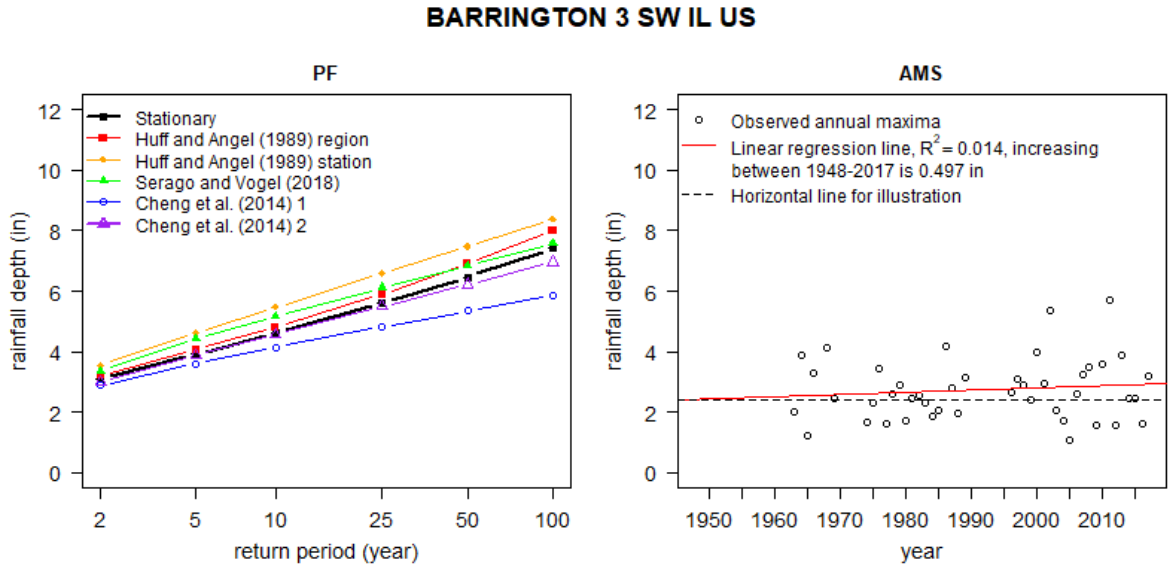

Fig. 4.2. Frequency estimates based on the methods described in this study (left) and observed AMS time series for Barrington 3 SW (right). While this station showed an increasing trend in the AMS, the Cheng et al. (2014) 1 method yielded consistently lower values than the stationary line, an unexpected result. The Huff and Angel methods and the Serago and Vogel (2018) method yielded values consistently higher than the stationary line.

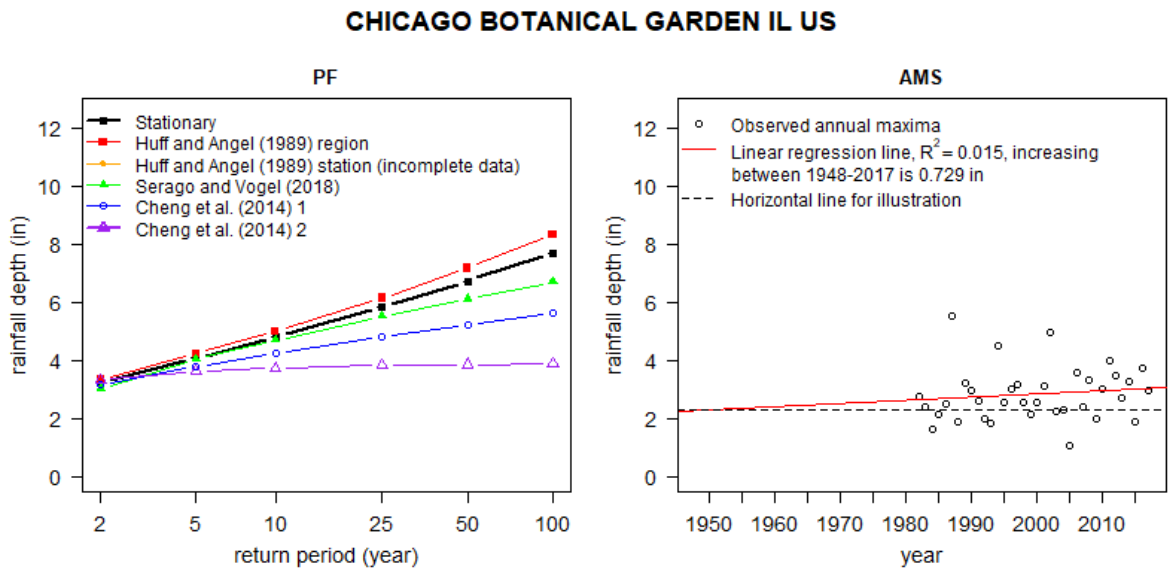

Fig. 4.3. Frequency estimates based on the methods described in this study (left) and observed AMS time series for Chicago Botanical Garden (right). While this station showed an increasing trend in the AMS, the Serago and Vogel (2018) and both Cheng et al. (2014) methods yielded amounts below the stationary curve. The Cheng et al. (2014) 2 method yielded especially unrealistic results with little difference between the 2-year and 100-year values. The Huff and Angel (1989) station method was not presented due to the absence of data in the first half of the record at this gage.

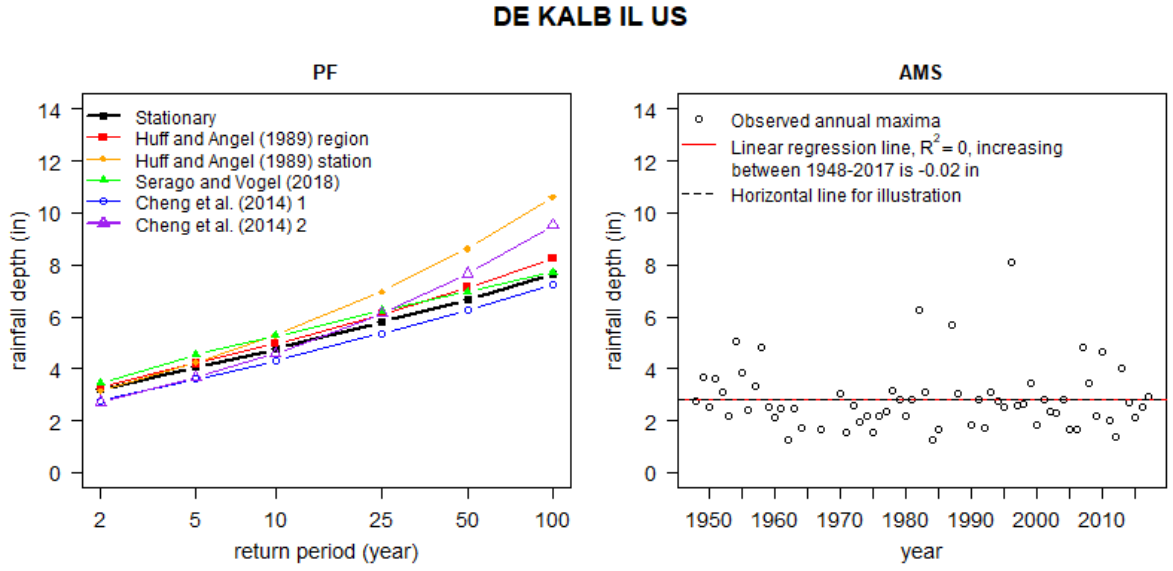

Fig. 4.4. Frequency estimates based on the methods described in this study (left) and observed AMS time series for DeKalb (right). While this station showed no trend in the AMS, there were three storms in the second half of the record that were near to above 6 inches. The Cheng et al. (2014) 1 method stayed below the stationary curve, while the Cheng et al. (2014) 2 method did yield values higher than the benchmark at the longer return periods. The Huff and Angel (1989) station method yielded the largest increase, probably due to the three large storms in the second half of the record.

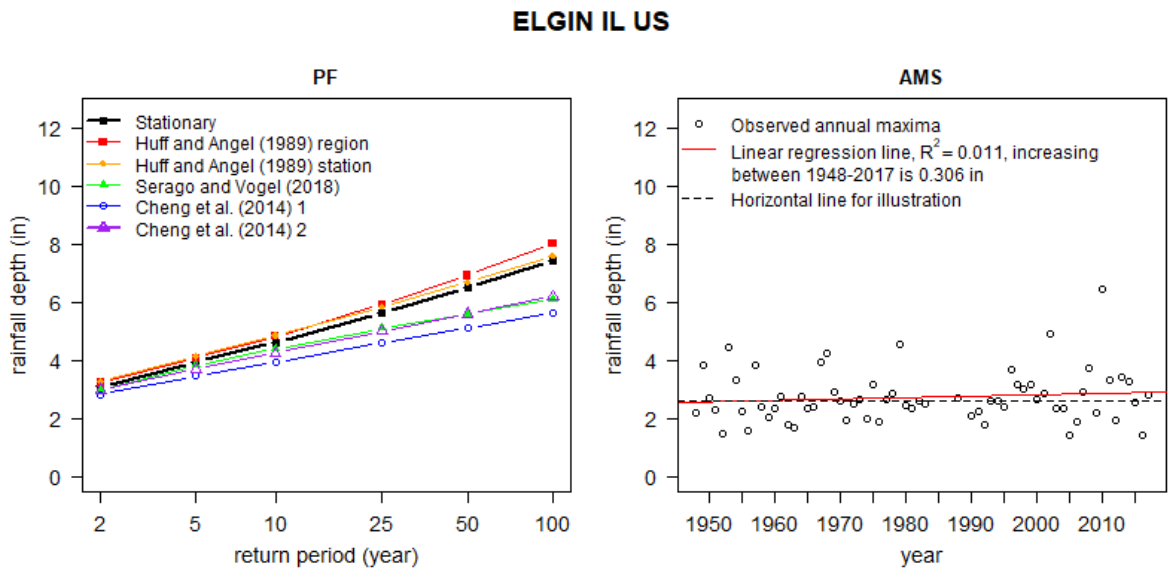

Fig. 4.5. Frequency estimates based on the methods described in this study (left) and observed AMS time series for Elgin (right). While this station showed a slightly increasing trend in the AMS, three of the methods yielded results below the stationary curve and the two Huff and Angel methods yielded results slightly above the curve.

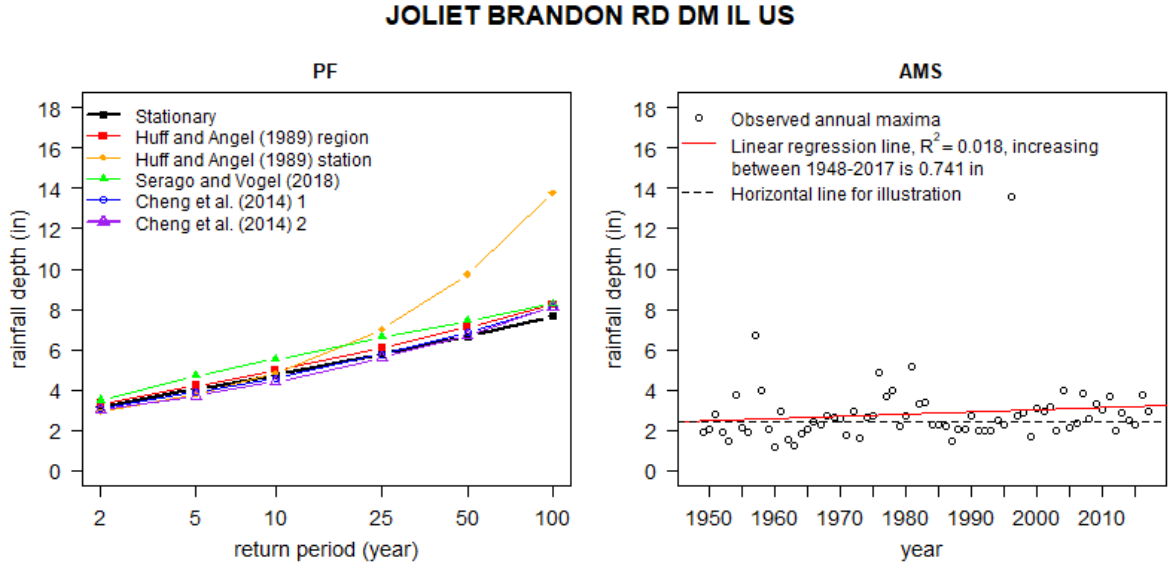

Fig. 4.6. Frequency estimates based on the methods described in this study (left) and observed AMS time series for Joliet Brandon (right). While this station showed an increasing trend in the AMS, all but one of the methods yielded values relatively close to the stationary curve, particularly for the 100-year return period. The Huff and Angel (1989) station method yielded much higher values at the longer return periods, probably influenced by the one 14-inch event in 1996.

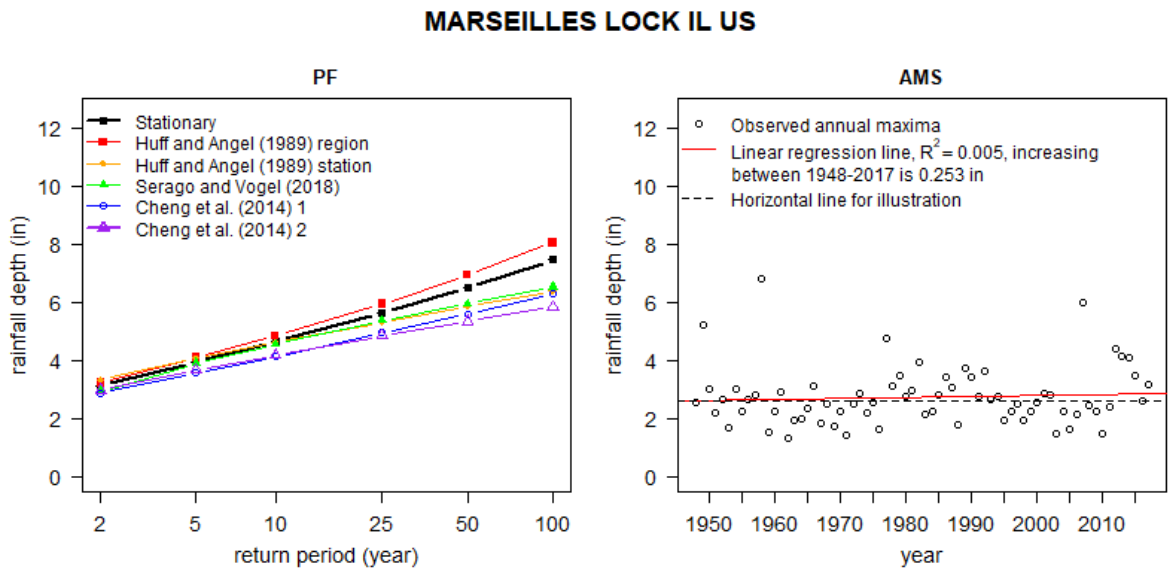

Fig. 4.7. Frequency estimates based on the methods described in this study (left) and observed AMS time series for Marseilles (right). While this station showed a slightly increasing trend in the AMS, all but the Huff and Angel (1989) method yielded values below the stationary curve.

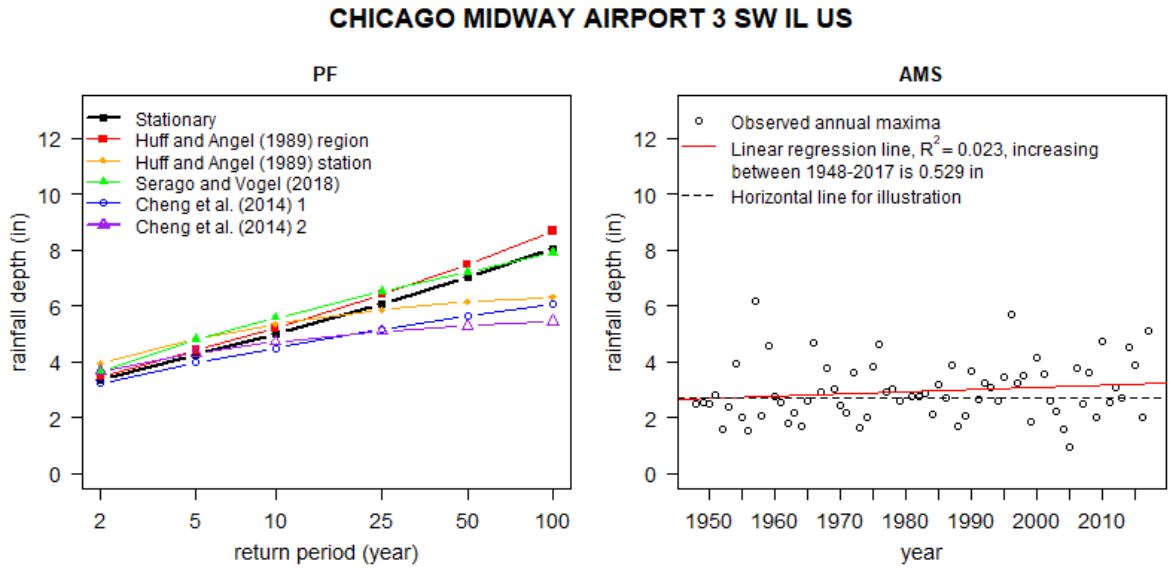

Fig. 4.8. Frequency estimates based on the methods described in this study (left) and observed AMS time series for Chicago Midway Airport 3 SW (right). While this station showed an increasing trend in the AMS, three of the methods yielded results below the stationary curve, especially at the longer return periods. The Serago and Vogel (2018) method yielded values slightly above the station curve until the 100-year return period. The Huff and Angel (1989) region method yielded values slightly above the station curve for return periods at 5 years and above.

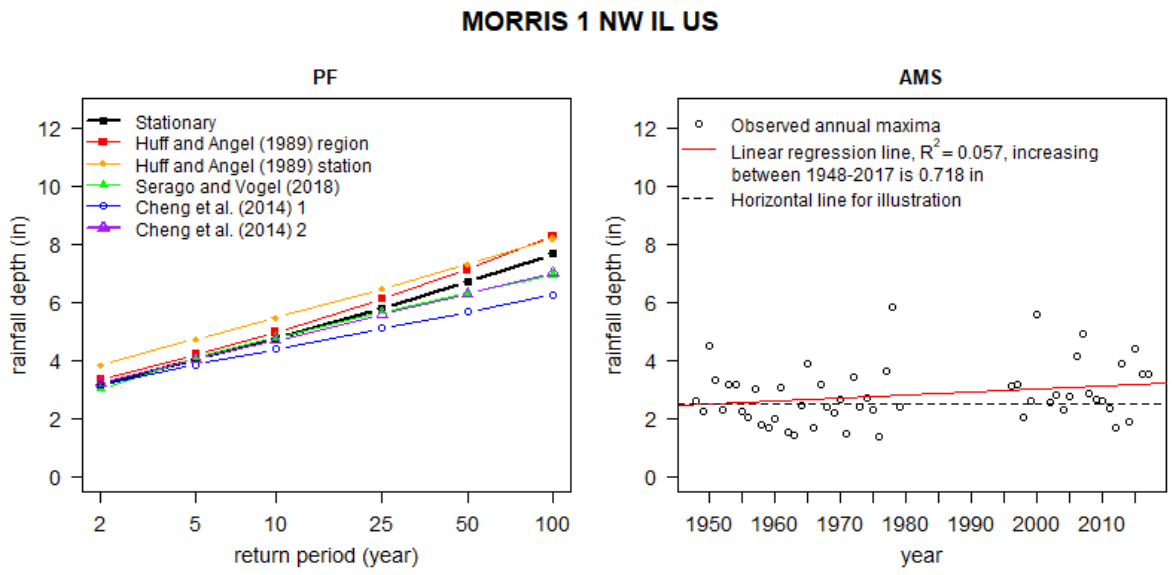

Fig. 4.9. Frequency estimates based on the methods described in this study (left) and observed AMS time series for Chicago Morris 1 NW (right). While this station showed an increasing trend in the AMS, three methods yielded values below the stationary curve. The two Huff and Angel methods yielded values above the stationary curve.

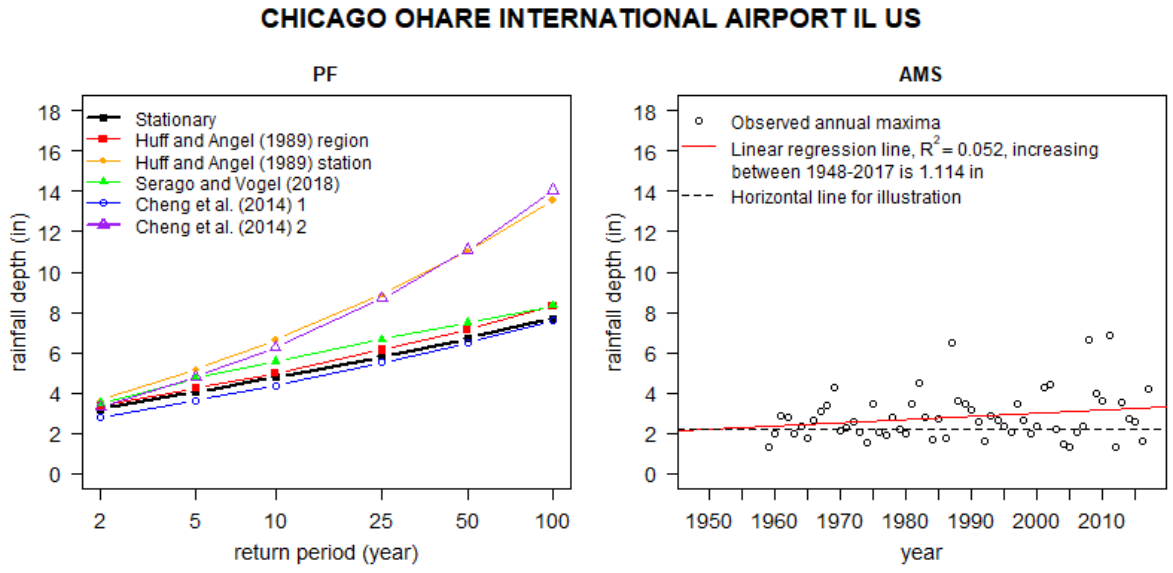

Fig. 4.10. Frequency estimates based on the methods described in this study (left) and observed AMS time series for Chicago O'Hare International Airport (right). This station showed an increasing trend in the AMS, and all methods except the Cheng et al. (2014) 1 method yielded values above the stationary curve. The two methods that yielded the highest estimates were the Cheng et al. (2014) 2 and Huff and Angel (1989) station methods.

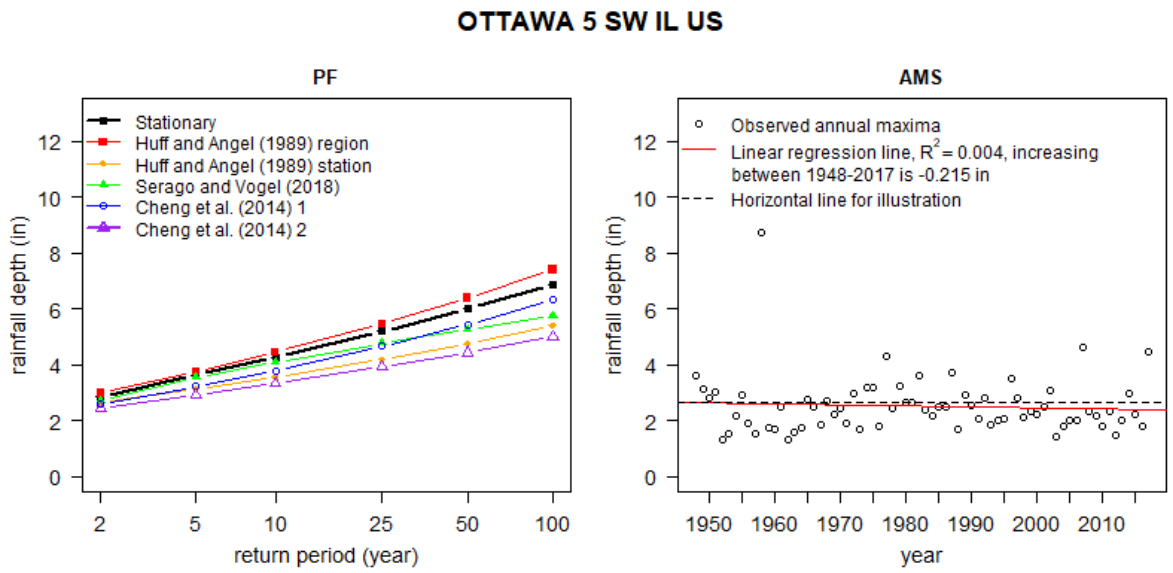

Fig. 4.11. Frequency estimates based on the methods described in this study (left) and observed AMS time series for Ottawa 5 SW (right). This station showed a slightly decreasing trend in the AMS. All methods yielded values below the stationary curves, as expected; however, the Huff and Angel (1989) region method yielded values slightly above the stationary curve.

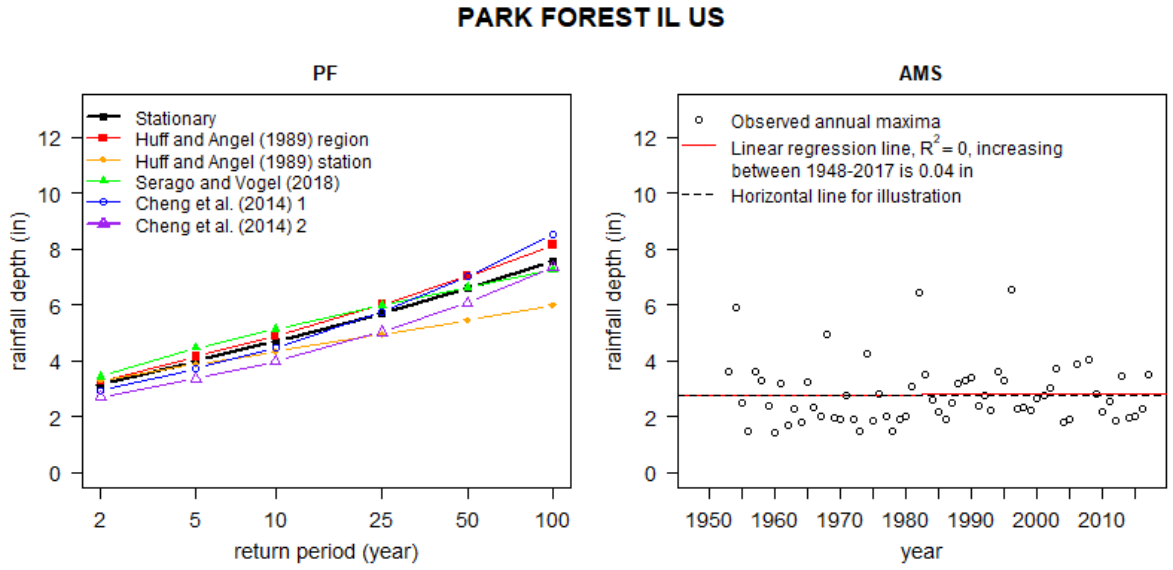

Fig. 4.12. Frequency estimates based on the methods described in this study (left) and observed AMS time series for Park Forest (right). This station showed no trend in the AMS. Most of the methods were close to the stationary curve, with exceptions including the Huff and Angel (1989) station method, which yielded considerably lower values at the longer return periods; Cheng et al. (2014) 1 method, which produced the highest 100-year estimate; and Cheng et al. (2014) 2 method, which resulted in the lowest estimates for shorter return periods.

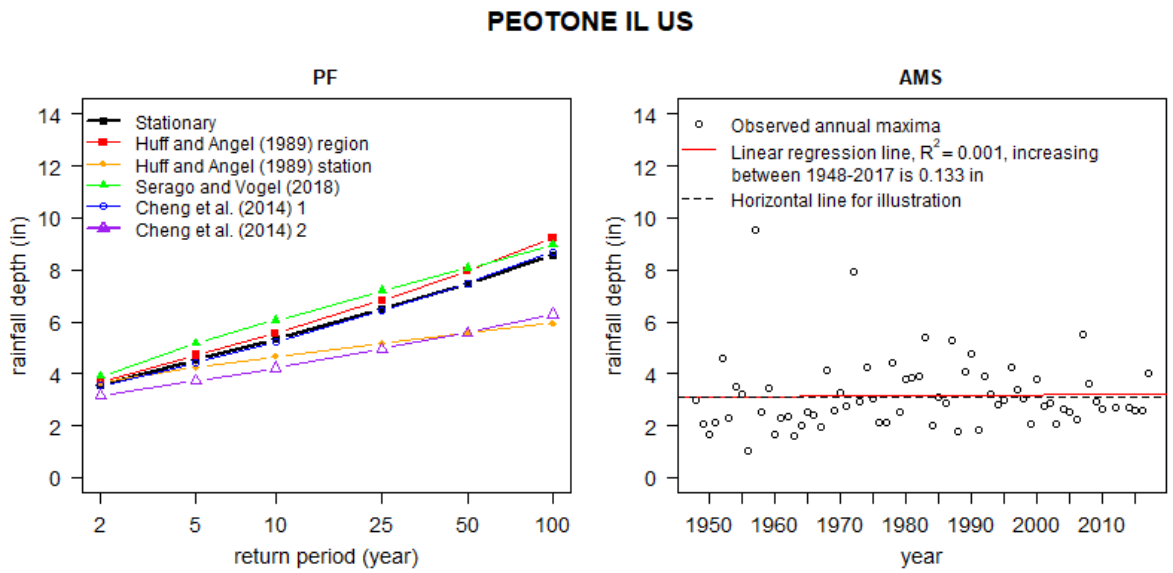

Fig. 4.13. Frequency estimates based on the methods described in this study (left) and observed AMS time series for Peotone (right). While the station showed no trend in the AMS, the Cheng et al. (2014) 2 and the Huff and Angel (1989) station method yielded values much below the stationary curve. This could be explained possibly by the decrease in variability in AMS. The other methods were close to the stationary curve.

Conclusions

Five non-stationary methods were applied to sites in the northeast area of Illinois, including four station-based and one region-based method. The station-based methods included the Angel and Huff (1989) method, the Serago and Vogel (2018) method, and the Cheng et al. (2014) methods 1 and 2. The Cheng et al. (2014) 1 method was applied with a variable location parameter and the Cheng et al. (2014) 2 method was applied with variable location, scale, and shape parameters. The Angel and Huff (1989) method was the one region-based method.

The information presented in Figures 4.1–4.13 indicated that each method has advantages and limitations. In general, all the station-based methods were less consistent than the regional approach. For example, the Huff and Angel (1989) station method appeared to be sensitive to larger observations in the second half of the period of record at Aurora, Joliet, and O'Hare. The Serago-Vogel method failed to capture the increasing trends in AMS at Elgin and Park Forest as its estimates were smaller than those based on the Huff and Angel (1989) station frequency analysis. Similarly, both Cheng at al. methods failed to detect the increase in AMS peaks at Barrington, Elgin, and Morris.

The results presented herein indicate that the region-specific Bulletin 70 type of adjustment, adopted for this study, is the most consistent among the five methods for trend adjustment.

References

Cheng, L., A. AghaKouchak, E. Gilleland, and R. W. Katz. 2014. Non-stationary extreme value analysis in a changing climate. *Climatic Change* 127:353-369.

Huff, F.A., and J.R. Angel. 1989. *Frequency Distributions and Hydroclimatic Characteristics of Heavy Rainstorms in Illinois.* Illinois State Water Survey, Bulletin 70, Champaign, IL.

Serago, J., and R.M. Vogel. 2018. Parsimonious nonstationary flood frequency analysis. *Advances in Water Resources* 112:1–16.

5. Frequencies for sub-hourly durations and for sub-2-year recurrence intervals

Introduction

The precipitation frequency estimates for ranges of durations shorter than 1 hour and return periods of less than 2 years were not a part of the original contract agreement and thus were not included in the report "Frequency Distributions of Heavy Precipitation in Illinois: Updated Bulletin 70" (Angel and Markus, 2019). However, due to numerous user inquiries and for completeness, additional results were included in this report. Specifically, the frequency estimates for 5-, 10-, 15-, and 30-minute durations were added. The frequency estimates for 2-, 3-, 4-, 6-, and 9-month, as well as 1-year recurrence intervals were also included. The following ratios, the same as those in the original Bulletin 70, were used to produce additional results. Table 5.1 was derived from Table 11 in Bulletin 70, showing the ratios used to calculate sub-hourly frequency estimates based on the hourly estimates. Table 5.2 shows the ratios used to calculate the frequency estimates for recurrence intervals of less than 2 years. This table was derived from Table 12 in Bulletin 70.

Table 5.1. Ratios Used to Calculate Sub-hourly Frequency Estimates Based on the Known Hourly Estimates, x-minute/1-hour

5-minute/1-hour	10-minute/1-hour	15-minute/1-hour	30-minute/1-hour
0.255	0.468	0.574	0.787

Table 5.2. Factors Used to Calculate Frequency Estimates for Recurrence Intervals Less than 2 Years Based on the Known Estimates for the 2-Year Recurrence Interval

2 months to 2 years	3 months to 2 years	4 months to 2 years	6 months to 2 years	9 months to 2 years	1 year to 2 years
0.470	0.538	0.590	0.672	0.762	0.830

Results

The complete results, including those in the report "Frequency Distributions of Heavy Precipitation in Illinois: Updated Bulletin 70" (Angel and Markus, 2019) and the additional ones, including frequency estimates for 5-, 10-, 15-, and 30-minute durations, as well as the estimates for 2-, 3-, 4-, 6-, and 9-month and 1-year recurrence intervals, are presented in Tables 5.3–5.12 and in Figures 5.1–5.10. For easier use, the tables in this report present results in a different format compared to Angel and Markus (2019) and the original Bulletin 70 (Huff and Angel, 1989). In the new format, each table presents a climate section.

Table 5.3. Rainfall (inches) for Given Recurrence Interval for Section 1 (Northwest)

Storm Duration	2-month	3-month	4-month	6-month	9-month	1-year	2-year	5-year	10-year	25-year	50-year	100-year	500-year
5 minutes	0.19	0.22	0.24	0.27	0.31	0.33	0.40	0.51	0.60	0.74	0.86	0.99	1.30
10 minutes	0.33	0.38	0.41	0.47	0.53	0.58	0.70	0.89	1.06	1.30	1.51	1.73	2.28
15 minutes	0.42	0.49	0.53	0.61	0.69	0.75	0.90	1.14	1.36	1.67	1.94	2.23	2.93
30 minutes	0.58	0.66	0.73	0.83	0.94	1.03	1.24	1.56	1.86	2.30	2.66	3.05	4.01
1 hour	0.74	0.84	0.93	1.05	1.20	1.30	1.57	1.98	2.36	2.92	3.38	3.88	5.09
2 hours	0.91	1.04	1.14	1.30	1.48	1.61	1.94	2.45	2.92	3.60	4.17	4.78	6.29
3 hours	1.00	1.15	1.26	1.44	1.63	1.77	2.14	2.70	3.22	3.97	4.61	5.28	6.94
6 hours	1.18	1.35	1.48	1.68	1.91	2.08	2.51	3.17	3.77	4.65	5.40	6.19	8.13
12 hours	1.37	1.56	1.71	1.95	2.21	2.41	2.91	3.67	4.38	5.40	6.26	7.18	9.43
18 hours	1.48	1.69	1.85	2.11	2.39	2.61	3.14	3.97	4.73	5.83	6.77	7.75	10.19
24 hours	1.57	1.80	1.97	2.24	2.55	2.77	3.34	4.22	5.03	6.20	7.20	8.25	10.84
48 hours	1.70	1.94	2.13	2.43	2.75	3.00	3.61	4.59	5.43	6.72	7.73	8.83	11.53
72 hours	1.83	2.10	2.30	2.62	2.97	3.23	3.90	4.95	5.87	7.21	8.30	9.45	12.30
120 hours	2.05	2.34	2.57	2.92	3.32	3.61	4.35	5.51	6.46	7.88	8.96	10.20	13.33
240 hours	2.57	2.95	3.23	3.68	4.17	4.55	5.48	6.86	7.98	9.55	10.84	12.14	15.65

Table 5.4. Rainfall (inches) for Given Recurrence Interval for Section 2 (Northeast)

Storm Duration	2-month	3-month	4-month	6-month	9-month	1-year	2-year	5-year	10-year	25-year	50-year	100-year	500-year
5 minutes	0.19	0.22	0.24	0.27	0.31	0.33	0.40	0.52	0.62	0.77	0.90	1.03	1.35
10 minutes	0.33	0.38	0.41	0.47	0.53	0.58	0.70	0.90	1.08	1.35	1.58	1.80	2.36
15 minutes	0.42	0.49	0.53	0.61	0.69	0.75	0.90	1.16	1.39	1.74	2.03	2.32	3.04
30 minutes	0.58	0.66	0.73	0.83	0.94	1.03	1.24	1.59	1.91	2.39	2.78	3.17	4.16
1 hour	0.74	0.84	0.93	1.05	1.20	1.30	1.57	2.02	2.42	3.03	3.53	4.03	5.28
2 hours	0.91	1.04	1.14	1.30	1.48	1.61	1.94	2.49	2.99	3.74	4.35	4.97	6.52
3 hours	1.00	1.15	1.26	1.44	1.63	1.77	2.14	2.75	3.30	4.13	4.80	5.49	7.20
6 hours	1.18	1.35	1.48	1.68	1.91	2.08	2.51	3.23	3.86	4.84	5.63	6.43	8.43
12 hours	1.37	1.56	1.71	1.95	2.21	2.41	2.91	3.74	4.48	5.61	6.53	7.46	9.78
18 hours	1.48	1.69	1.85	2.11	2.39	2.61	3.14	4.04	4.84	6.06	7.05	8.06	10.57
24 hours	1.57	1.80	1.97	2.24	2.55	2.77	3.34	4.30	5.15	6.45	7.50	8.57	11.24
48 hours	1.72	1.97	2.16	2.46	2.79	3.04	3.66	4.71	5.62	6.99	8.13	9.28	12.10
72 hours	1.87	2.14	2.34	2.67	3.03	3.30	3.97	5.08	6.05	7.49	8.64	9.85	12.81
120 hours	2.08	2.38	2.61	2.97	3.37	3.67	4.42	5.63	6.68	8.16	9.39	10.66	13.81
240 hours	2.63	3.01	3.30	3.76	4.27	4.65	5.60	7.09	8.25	9.90	11.26	12.65	16.00

Table 5.5. Rainfall (inches) for Given Recurrence Interval for Section 3 (West)

Storm Duration	2-month	3-month	4-month	6-month	9-month	1-year	2-year	5-year	10-year	25-year	50-year	100-year	500-year
5 minutes	0.20	0.22	0.25	0.28	0.32	0.35	0.42	0.53	0.63	0.77	0.87	0.97	1.19
10 minutes	0.34	0.39	0.43	0.49	0.56	0.61	0.73	0.93	1.10	1.34	1.52	1.69	2.08
15 minutes	0.44	0.51	0.55	0.63	0.72	0.78	0.94	1.20	1.41	1.72	1.96	2.18	2.68
30 minutes	0.61	0.69	0.76	0.87	0.98	1.07	1.29	1.65	1.94	2.36	2.68	2.98	3.67
1 hour	0.77	0.88	0.97	1.10	1.25	1.36	1.64	2.09	2.46	3.00	3.41	3.79	4.66
2 hours	0.95	1.09	1.19	1.36	1.54	1.68	2.02	2.58	3.04	3.70	4.21	4.67	5.75
3 hours	1.05	1.20	1.31	1.50	1.70	1.85	2.23	2.85	3.35	4.08	4.64	5.16	6.34
6 hours	1.23	1.40	1.54	1.75	1.99	2.17	2.61	3.34	3.93	4.79	5.44	6.05	7.43
12 hours	1.42	1.63	1.79	2.03	2.31	2.51	3.03	3.87	4.56	5.55	6.31	7.01	8.62
18 hours	1.54	1.76	1.93	2.20	2.49	2.72	3.27	4.18	4.93	6.00	6.82	7.58	9.32
24 hours	1.64	1.87	2.05	2.34	2.65	2.89	3.48	4.45	5.24	6.38	7.25	8.06	9.91
48 hours	1.77	2.03	2.22	2.53	2.87	3.12	3.76	4.76	5.62	6.81	7.72	8.60	10.58
72 hours	1.93	2.21	2.43	2.76	3.13	3.41	4.11	5.18	6.08	7.34	8.31	9.18	11.27
120 hours	2.12	2.43	2.66	3.03	3.44	3.75	4.51	5.66	6.62	7.94	8.93	9.83	11.99
240 hours	2.64	3.03	3.32	3.78	4.28	4.67	5.62	7.00	8.10	9.60	10.65	11.64	13.99

Table 5.6. Rainfall (inches) for Given Recurrence Interval for Section 4 (Central)

Storm Duration	2-month	3-month	4-month	6-month	9-month	1-year	2-year	5-year	10-year	25-year	50-year	100-year	500-year
5 minutes	0.19	0.21	0.24	0.27	0.30	0.33	0.40	0.52	0.61	0.74	0.85	0.94	1.14
10 minutes	0.33	0.38	0.41	0.47	0.53	0.58	0.70	0.90	1.07	1.30	1.48	1.65	2.00
15 minutes	0.42	0.48	0.53	0.60	0.68	0.74	0.90	1.16	1.38	1.67	1.90	2.12	2.57
30 minutes	0.58	0.66	0.72	0.83	0.94	1.02	1.23	1.59	1.89	2.29	2.61	2.90	3.53
1 hour	0.73	0.84	0.92	1.05	1.19	1.30	1.56	2.02	2.40	2.91	3.31	3.69	4.48
2 hours	0.91	1.04	1.14	1.29	1.47	1.60	1.93	2.49	2.96	3.60	4.09	4.55	5.53
3 hours	1.00	1.14	1.25	1.43	1.62	1.76	2.12	2.75	3.26	3.97	4.51	5.02	6.10
6 hours	1.17	1.34	1.47	1.67	1.90	2.07	2.49	3.23	3.83	4.65	5.29	5.89	7.15
12 hours	1.36	1.55	1.70	1.94	2.20	2.40	2.89	3.74	4.44	5.39	6.13	6.83	8.29
18 hours	1.47	1.68	1.84	2.10	2.38	2.59	3.12	4.04	4.79	5.83	6.63	7.38	8.96
24 hours	1.56	1.79	1.96	2.23	2.53	2.76	3.32	4.30	5.10	6.20	7.05	7.85	9.53
48 hours	1.69	1.93	2.12	2.41	2.73	2.98	3.59	4.61	5.47	6.65	7.55	8.40	10.21
72 hours	1.82	2.09	2.29	2.60	2.95	3.22	3.88	4.96	5.90	7.17	8.09	8.98	10.81
120 hours	2.01	2.30	2.52	2.87	3.26	3.55	4.27	5.42	6.42	7.75	8.72	9.60	11.54
240 hours	2.57	2.94	3.22	3.67	4.16	4.54	5.46	6.87	8.04	9.53	10.55	11.50	13.65

Table 5.7. Rainfall (inches) for Given Recurrence Interval for Section 5 (East)

Storm Duration	2-month	3-month	4-month	6-month	9-month	1-year	2-year	5-year	10-year	25-year	50-year	100-year	500-year
5 minutes	0.18	0.20	0.22	0.25	0.29	0.31	0.37	0.48	0.57	0.69	0.79	0.89	1.12
10 minutes	0.31	0.35	0.39	0.44	0.50	0.54	0.66	0.83	0.99	1.21	1.39	1.56	1.96
15 minutes	0.40	0.45	0.50	0.57	0.64	0.70	0.84	1.07	1.27	1.56	1.79	2.01	2.52
30 minutes	0.54	0.62	0.68	0.78	0.88	0.96	1.15	1.47	1.74	2.14	2.45	2.75	3.45
1 hour	0.69	0.79	0.87	0.99	1.12	1.22	1.47	1.87	2.21	2.72	3.11	3.49	4.38
2 hours	0.85	0.97	1.07	1.22	1.38	1.50	1.81	2.30	2.73	3.35	3.84	4.31	5.41
3 hours	0.94	1.07	1.18	1.34	1.52	1.66	2.00	2.54	3.01	3.70	4.24	4.76	5.97
6 hours	1.10	1.26	1.38	1.57	1.78	1.94	2.34	2.98	3.53	4.34	4.97	5.57	6.99
12 hours	1.28	1.46	1.60	1.82	2.07	2.25	2.71	3.45	4.10	5.03	5.76	6.46	8.11
18 hours	1.38	1.58	1.73	1.97	2.23	2.43	2.93	3.73	4.43	5.43	6.22	6.98	8.76
24 hours	1.47	1.68	1.84	2.10	2.38	2.59	3.12	3.97	4.71	5.78	6.62	7.43	9.32
48 hours	1.66	1.90	2.09	2.38	2.69	2.93	3.54	4.49	5.32	6.48	7.38	8.27	10.26
72 hours	1.82	2.09	2.29	2.60	2.95	3.22	3.88	4.90	5.78	7.04	8.01	8.93	11.00
120 hours	2.04	2.34	2.56	2.92	3.31	3.60	4.34	5.43	6.41	7.73	8.79	9.80	11.93
240 hours	2.59	2.96	3.25	3.70	4.19	4.57	5.50	6.84	7.90	9.35	10.45	11.55	13.96

Table 5.8. Rainfall (inches) for Given Recurrence Interval for Section 6 (West Southwest)

Storm Duration	2-month	3-month	4-month	6-month	9-month	1-year	2-year	5-year	10-year	25-year	50-year	100-year	500-year
5 minutes	0.18	0.21	0.23	0.26	0.30	0.32	0.39	0.49	0.57	0.69	0.79	0.88	1.08
10 minutes	0.32	0.36	0.40	0.46	0.52	0.56	0.68	0.85	1.00	1.22	1.38	1.54	1.90
15 minutes	0.41	0.47	0.51	0.59	0.66	0.72	0.87	1.10	1.29	1.56	1.77	1.97	2.44
30 minutes	0.56	0.64	0.71	0.80	0.91	0.99	1.20	1.51	1.76	2.14	2.43	2.71	3.34
1 hour	0.71	0.82	0.90	1.02	1.16	1.26	1.52	1.91	2.24	2.72	3.08	3.44	4.25
2 hours	0.88	1.01	1.11	1.26	1.43	1.55	1.87	2.36	2.76	3.36	3.80	4.24	5.24
3 hours	0.97	1.11	1.22	1.39	1.58	1.72	2.07	2.60	3.05	3.71	4.20	4.68	5.79
6 hours	1.14	1.30	1.43	1.63	1.85	2.01	2.42	3.05	3.57	4.34	4.92	5.48	6.78
12 hours	1.32	1.51	1.66	1.89	2.14	2.33	2.81	3.54	4.14	5.04	5.71	6.36	7.86
18 hours	1.43	1.63	1.79	2.04	2.31	2.52	3.04	3.83	4.47	5.44	6.17	6.87	8.50
24 hours	1.52	1.74	1.91	2.17	2.46	2.68	3.23	4.07	4.76	5.79	6.56	7.31	9.04
48 hours	1.72	1.97	2.16	2.46	2.79	3.04	3.66	4.61	5.38	6.48	7.33	8.11	9.93
72 hours	1.88	2.15	2.36	2.69	3.05	3.32	4.00	5.00	5.83	7.01	7.91	8.73	10.61
120 hours	2.11	2.41	2.65	3.02	3.42	3.72	4.49	5.60	6.49	7.77	8.69	9.57	11.53
240 hours	2.82	3.23	3.54	4.03	4.57	4.98	6.00	7.38	8.47	9.95	10.99	11.95	14.08

Table 5.9. Rainfall (inches) for Given Recurrence Interval for Section 7 (East Southeast)

Storm Duration	2-month	3-month	4-month	6-month	9-month	1-year	2-year	5-year	10-year	25-year	50-year	100-year	500-year
5 minutes	0.20	0.23	0.25	0.28	0.32	0.35	0.42	0.52	0.60	0.72	0.81	0.89	1.06
10 minutes	0.34	0.39	0.43	0.49	0.56	0.61	0.73	0.91	1.05	1.26	1.41	1.55	1.86
15 minutes	0.44	0.51	0.56	0.63	0.72	0.78	0.94	1.17	1.35	1.61	1.81	2.00	2.39
30 minutes	0.61	0.69	0.76	0.87	0.98	1.07	1.29	1.60	1.85	2.21	2.48	2.74	3.27
1 hour	0.77	0.88	0.97	1.10	1.25	1.36	1.64	2.04	2.35	2.81	3.15	3.48	4.15
2 hours	0.95	1.09	1.19	1.36	1.54	1.68	2.02	2.51	2.90	3.47	3.89	4.29	5.13
3 hours	1.05	1.20	1.32	1.50	1.70	1.85	2.23	2.77	3.20	3.83	4.29	4.74	5.66
6 hours	1.23	1.41	1.54	1.76	1.99	2.17	2.62	3.25	3.75	4.49	5.03	5.55	6.63
12 hours	1.43	1.63	1.79	2.04	2.31	2.52	3.04	3.77	4.35	5.20	5.84	6.44	7.69
18 hours	1.54	1.76	1.94	2.20	2.50	2.72	3.28	4.07	4.70	5.62	6.31	6.96	8.31
24 hours	1.64	1.88	2.06	2.35	2.66	2.90	3.49	4.33	5.00	5.98	6.71	7.40	8.84
48 hours	1.84	2.11	2.31	2.64	2.99	3.26	3.92	4.85	5.61	6.67	7.46	8.21	9.76
72 hours	2.05	2.34	2.57	2.93	3.32	3.61	4.35	5.37	6.19	7.34	8.19	8.97	10.57
120 hours	2.35	2.69	2.95	3.36	3.81	4.15	5.00	6.11	7.01	8.23	9.11	9.95	11.71
240 hours	3.09	3.53	3.87	4.41	5.00	5.45	6.57	7.86	8.90	10.20	11.20	12.06	13.95

Table 5.10. Rainfall (inches) for Given Recurrence Interval for Section 8 (Southwest)

Storm Duration	2-month	3-month	4-month	6-month	9-month	1-year	2-year	5-year	10-year	25-year	50-year	100-year	500-year
5 minutes	0.21	0.24	0.26	0.30	0.34	0.37	0.44	0.55	0.63	0.76	0.86	0.96	1.21
10 minutes	0.36	0.42	0.46	0.52	0.59	0.64	0.78	0.96	1.11	1.32	1.50	1.67	2.11
15 minutes	0.47	0.54	0.59	0.67	0.76	0.83	1.00	1.23	1.42	1.70	1.93	2.15	2.72
30 minutes	0.64	0.73	0.81	0.92	1.04	1.13	1.37	1.69	1.95	2.33	2.64	2.95	3.72
1 hour	0.82	0.93	1.02	1.17	1.32	1.44	1.73	2.14	2.48	2.96	3.36	3.74	4.73
2 hours	1.01	1.15	1.26	1.44	1.63	1.78	2.14	2.64	3.06	3.65	4.14	4.62	5.83
3 hours	1.11	1.27	1.39	1.59	1.80	1.96	2.36	2.92	3.37	4.03	4.57	5.09	6.44
6 hours	1.30	1.49	1.63	1.86	2.11	2.30	2.77	3.42	3.95	4.73	5.36	5.97	7.54
12 hours	1.51	1.73	1.89	2.16	2.45	2.66	3.21	3.97	4.58	5.48	6.21	6.93	8.75
18 hours	1.63	1.87	2.05	2.33	2.64	2.88	3.47	4.29	4.95	5.92	6.71	7.48	9.45
24 hours	1.73	1.99	2.18	2.48	2.81	3.06	3.69	4.56	5.27	6.30	7.14	7.96	10.06
48 hours	2.01	2.31	2.53	2.88	3.27	3.56	4.28	5.29	6.10	7.25	8.15	9.08	11.40
72 hours	2.23	2.55	2.80	3.19	3.61	3.94	4.74	5.82	6.71	7.96	8.89	9.86	12.32
120 hours	2.50	2.86	3.14	3.57	4.05	4.41	5.31	6.51	7.47	8.79	9.81	10.84	13.45
240 hours	3.17	3.63	3.98	4.54	5.14	5.60	6.75	8.18	9.30	10.80	11.95	13.10	15.95

Table 5.11. Rainfall (inches) for Given Recurrence Interval for Section 9 (Southeast)

Storm Duration	2-month	3-month	4-month	6-month	9-month	1-year	2-year	5-year	10-year	25-year	50-year	100-year	500-year
5 minutes	0.23	0.26	0.29	0.33	0.37	0.41	0.49	0.59	0.67	0.77	0.85	0.92	1.08
10 minutes	0.40	0.46	0.50	0.57	0.65	0.71	0.85	1.03	1.17	1.35	1.48	1.61	1.89
15 minutes	0.52	0.59	0.65	0.74	0.84	0.91	1.10	1.32	1.50	1.73	1.91	2.07	2.43
30 minutes	0.71	0.81	0.89	1.01	1.15	1.25	1.51	1.81	2.05	2.38	2.61	2.84	3.33
1 hour	0.90	1.03	1.13	1.29	1.46	1.59	1.91	2.30	2.61	3.02	3.32	3.61	4.23
2 hours	1.11	1.27	1.39	1.59	1.80	1.96	2.36	2.84	3.22	3.72	4.09	4.46	5.21
3 hours	1.22	1.40	1.54	1.75	1.98	2.16	2.60	3.13	3.55	4.11	4.52	4.92	5.75
6 hours	1.43	1.64	1.80	2.05	2.33	2.53	3.05	3.67	4.16	4.82	5.30	5.76	6.74
12 hours	1.66	1.91	2.09	2.38	2.70	2.94	3.54	4.25	4.83	5.59	6.14	6.69	7.82
18 hours	1.80	2.06	2.26	2.57	2.92	3.18	3.83	4.60	5.22	6.03	6.64	7.22	8.45
24 hours	1.91	2.19	2.40	2.74	3.10	3.38	4.07	4.89	5.55	6.42	7.06	7.68	8.99
48 hours	2.18	2.50	2.74	3.12	3.53	3.85	4.64	5.54	6.27	7.24	7.94	8.58	10.06
72 hours	2.41	2.76	3.03	3.45	3.91	4.26	5.13	6.09	6.86	7.87	8.63	9.34	10.93
120 hours	2.69	3.08	3.38	3.85	4.37	4.76	5.73	6.78	7.60	8.64	9.47	10.20	11.97
240 hours	3.32	3.80	4.17	4.75	5.38	5.86	7.06	8.30	9.22	10.37	11.21	11.96	13.75

Table 5.12. Rainfall (inches) for Given Recurrence Interval for Section 10 (South)

Storm Duration	2-month	3-month	4-month	6-month	9-month	1-year	2-year	5-year	10-year	25-year	50-year	100-year	500-year
5 minutes	0.20	0.23	0.26	0.29	0.33	0.36	0.44	0.54	0.63	0.77	0.87	0.99	1.27
10 minutes	0.36	0.41	0.45	0.51	0.58	0.63	0.76	0.95	1.11	1.34	1.53	1.73	2.22
15 minutes	0.46	0.53	0.58	0.66	0.75	0.81	0.98	1.22	1.42	1.72	1.97	2.22	2.85
30 minutes	0.63	0.72	0.79	0.90	1.02	1.11	1.34	1.67	1.95	2.36	2.70	3.04	3.91
1 hour	0.80	0.92	1.01	1.15	1.30	1.42	1.71	2.12	2.48	3.00	3.43	3.87	4.97
2 hours	0.99	1.13	1.24	1.41	1.60	1.75	2.10	2.62	3.06	3.70	4.23	4.77	6.13
3 hours	1.09	1.25	1.37	1.56	1.77	1.93	2.32	2.89	3.38	4.09	4.66	5.26	6.76
6 hours	1.28	1.46	1.61	1.83	2.07	2.26	2.72	3.39	3.96	4.79	5.47	6.17	7.92
12 hours	1.48	1.70	1.86	2.12	2.41	2.62	3.16	3.93	4.59	5.55	6.34	7.16	9.19
18 hours	1.60	1.84	2.01	2.29	2.60	2.83	3.41	4.25	4.96	6.00	6.85	7.73	9.93
24 hours	1.71	1.95	2.14	2.44	2.77	3.01	3.63	4.52	5.28	6.38	7.29	8.23	10.57
48 hours	1.91	2.18	2.39	2.73	3.09	3.37	4.06	5.02	5.86	7.04	8.01	9.02	11.56
72 hours	2.13	2.44	2.68	3.05	3.46	3.77	4.54	5.61	6.50	7.78	8.79	9.86	12.55
120 hours	2.44	2.79	3.06	3.48	3.95	4.30	5.18	6.30	7.29	8.69	9.78	10.91	13.84
240 hours	2.99	3.42	3.75	4.27	4.84	5.27	6.36	7.65	8.76	10.40	11.66	12.96	16.20

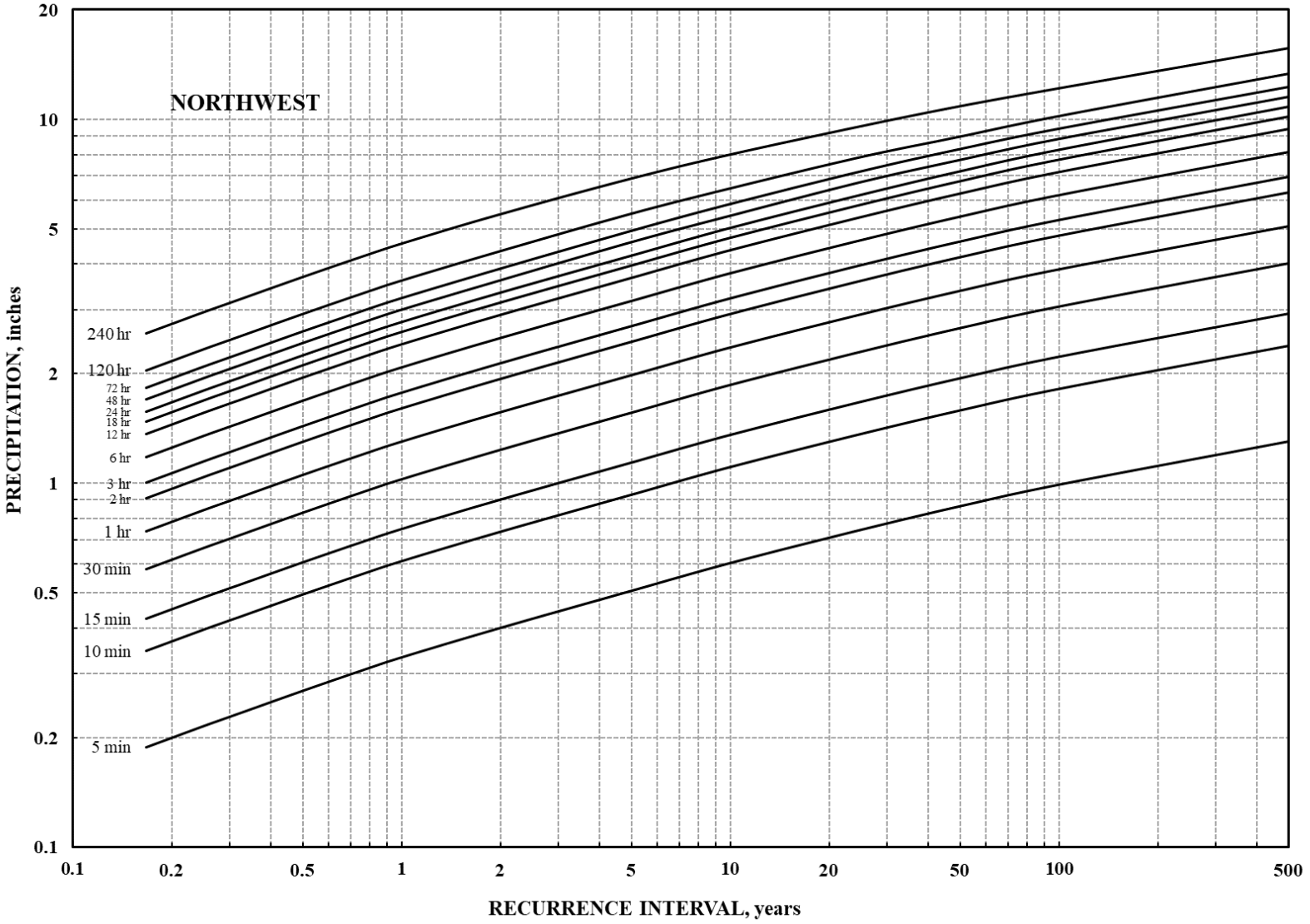

Figure 5.1. Precipitation frequency estimates for Section 1 (Northwest)

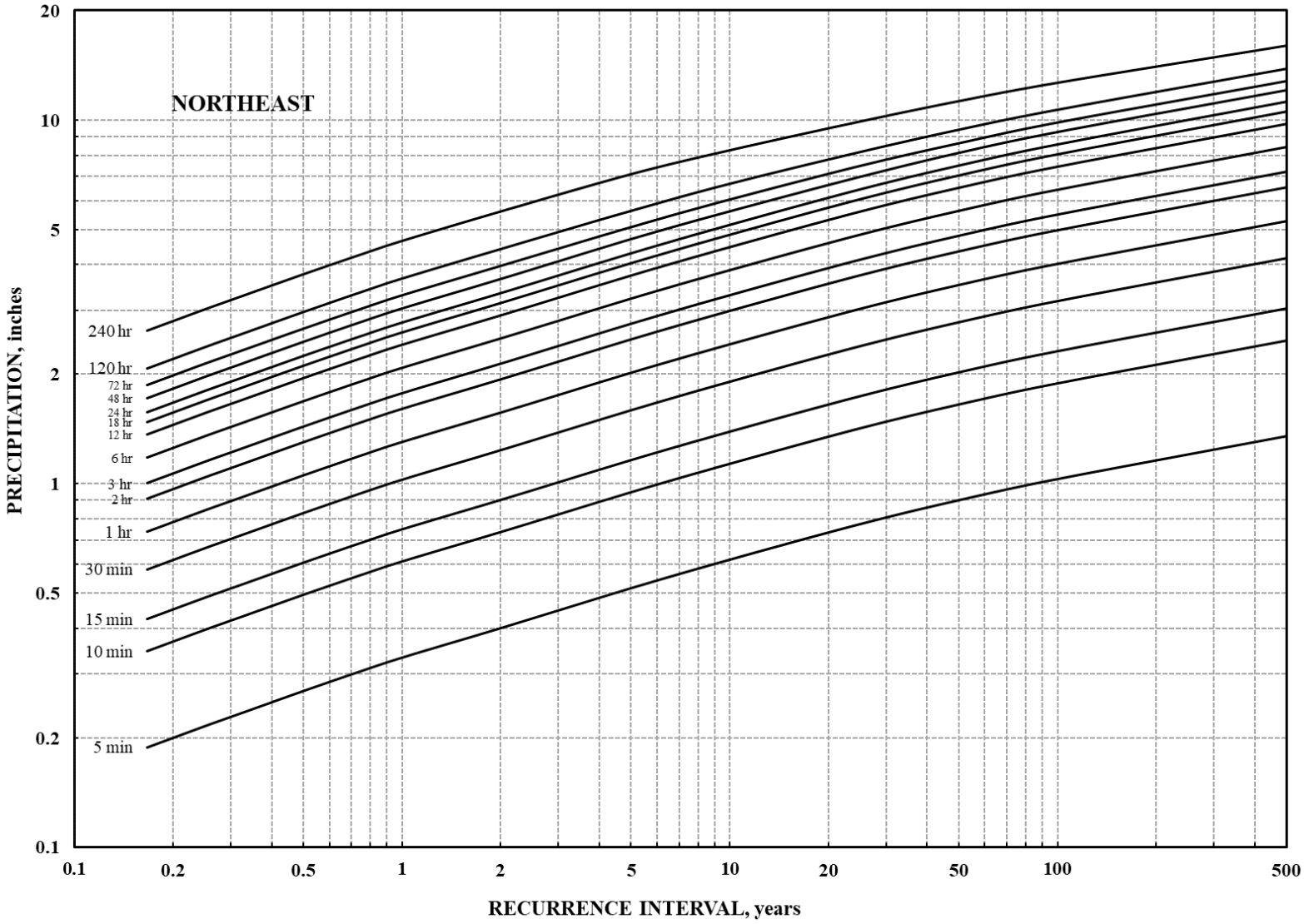

Figure 5.2. Precipitation frequency estimates for Section 2 (Northeast)

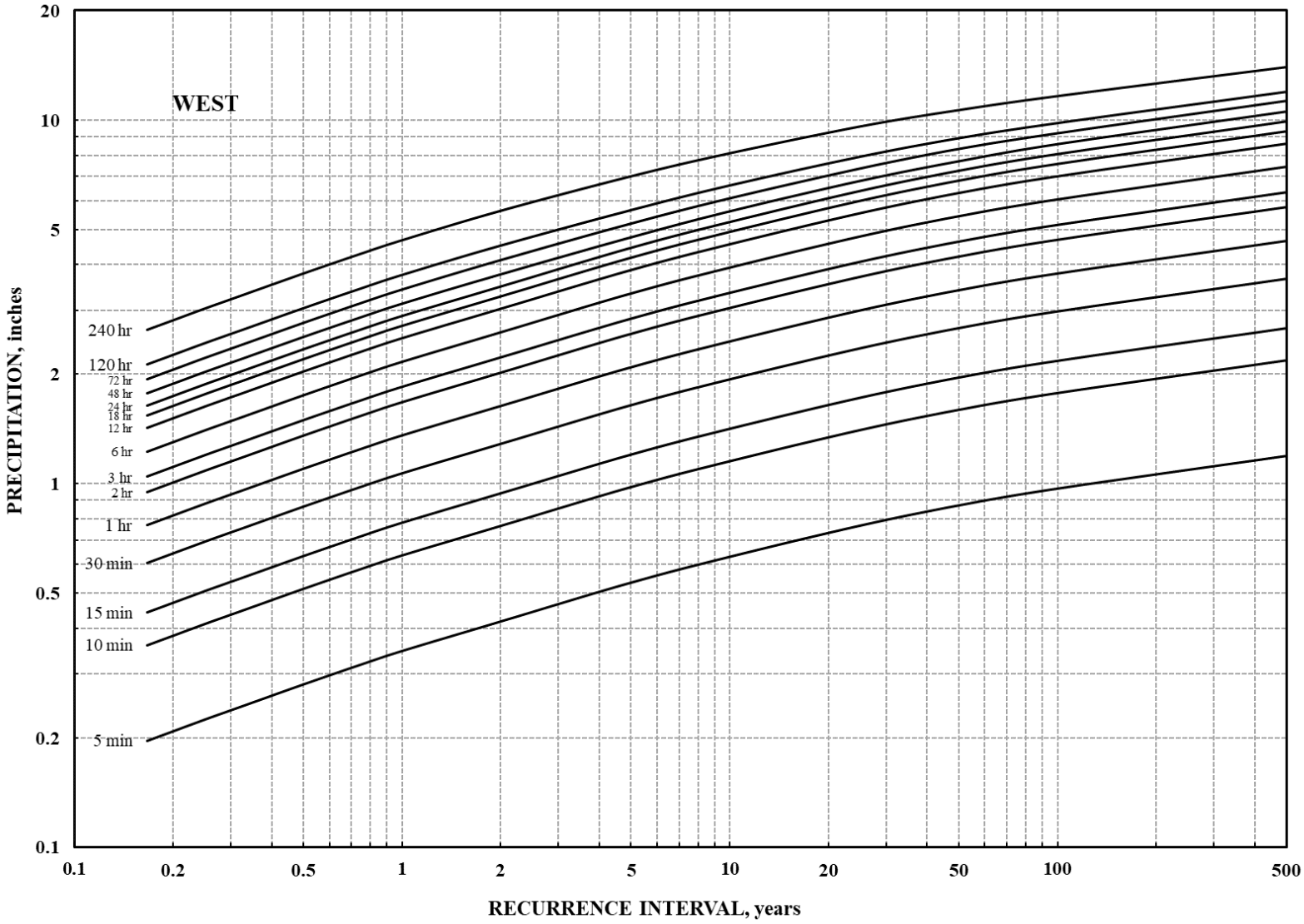

Figure 5.3. Precipitation frequency estimates for Section 3 (West)

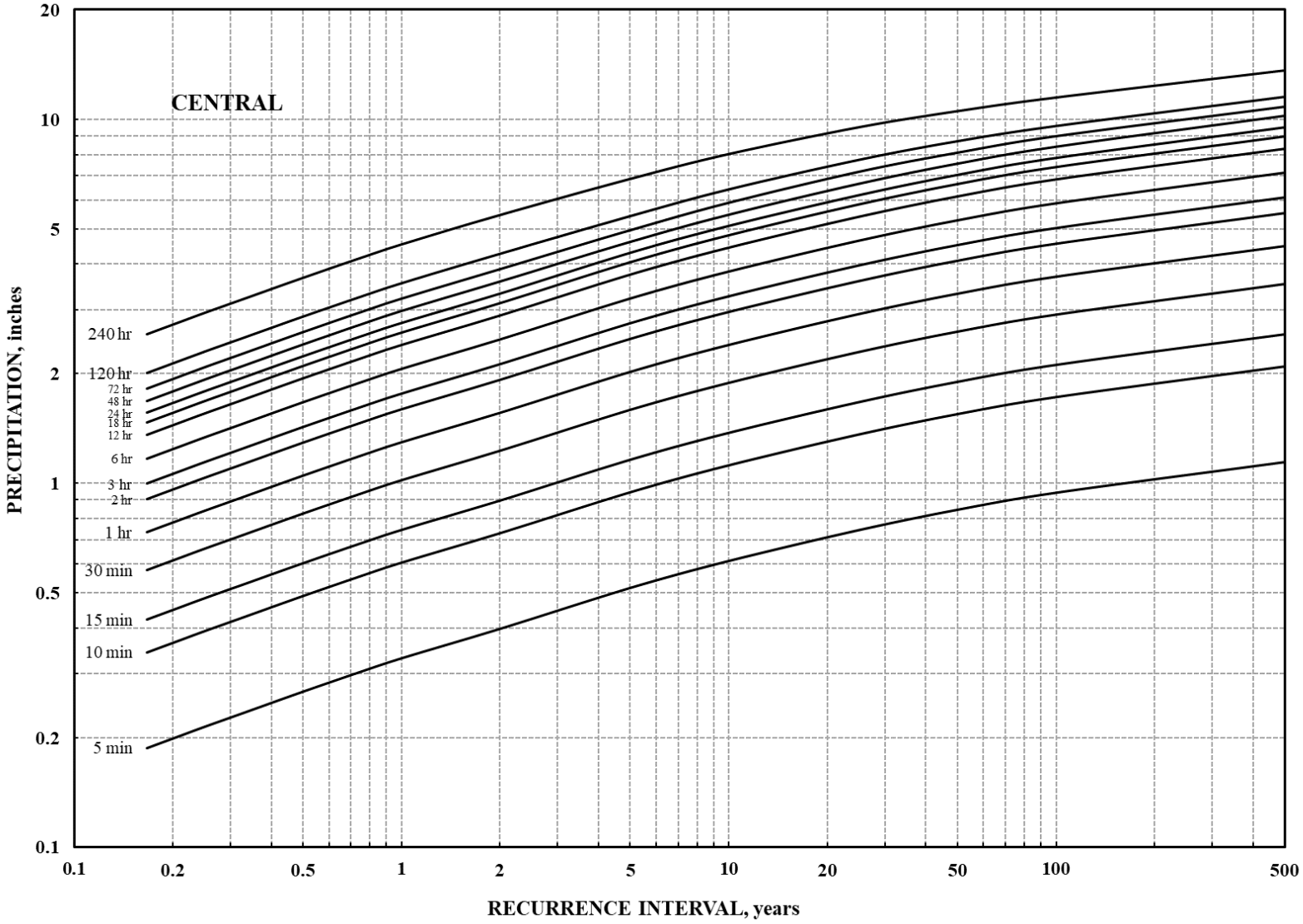

Figure 5.4. Precipitation frequency estimates for Section 4 (Central)

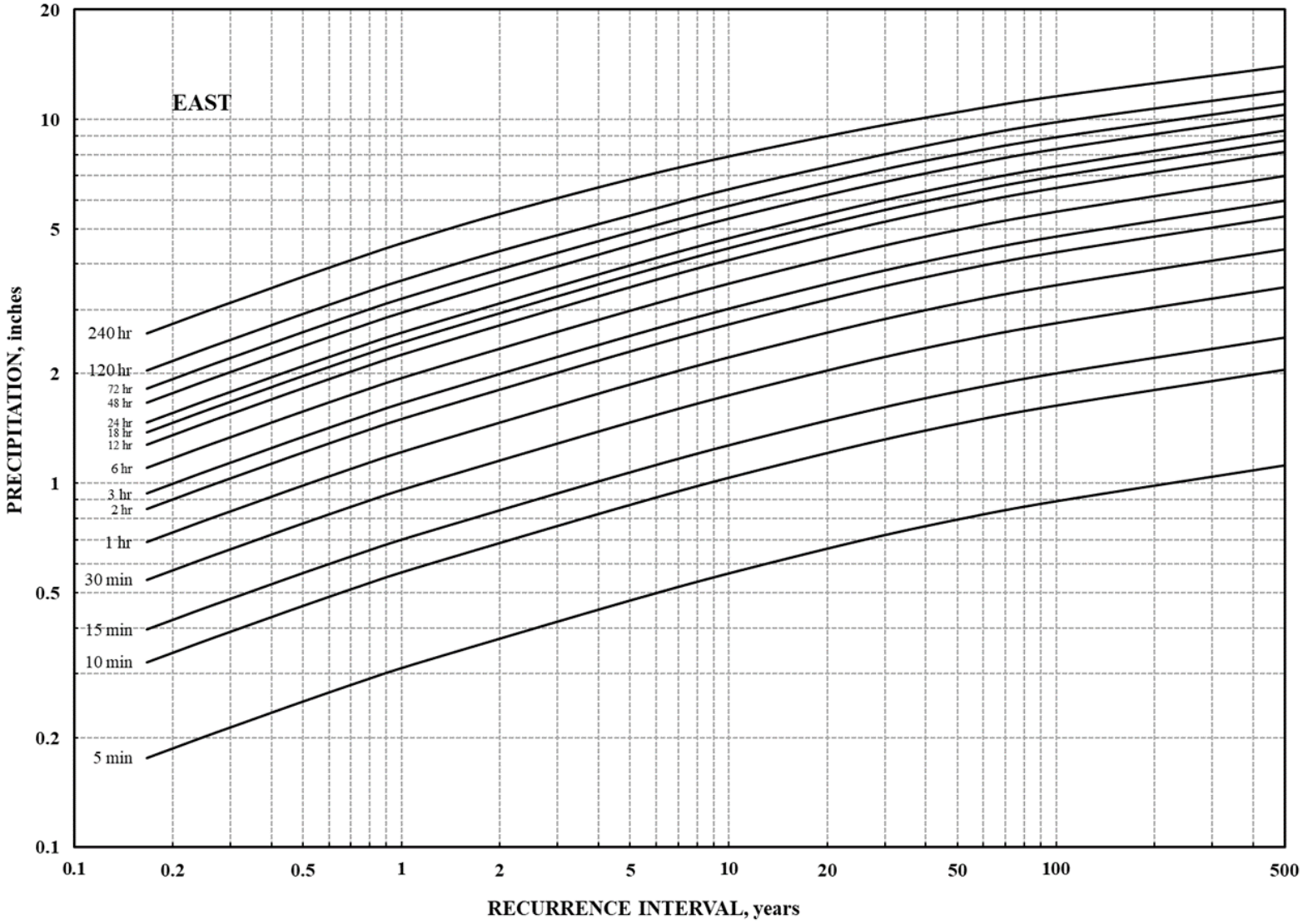

Figure 5.5. Precipitation frequency estimates for Section 5 (East)

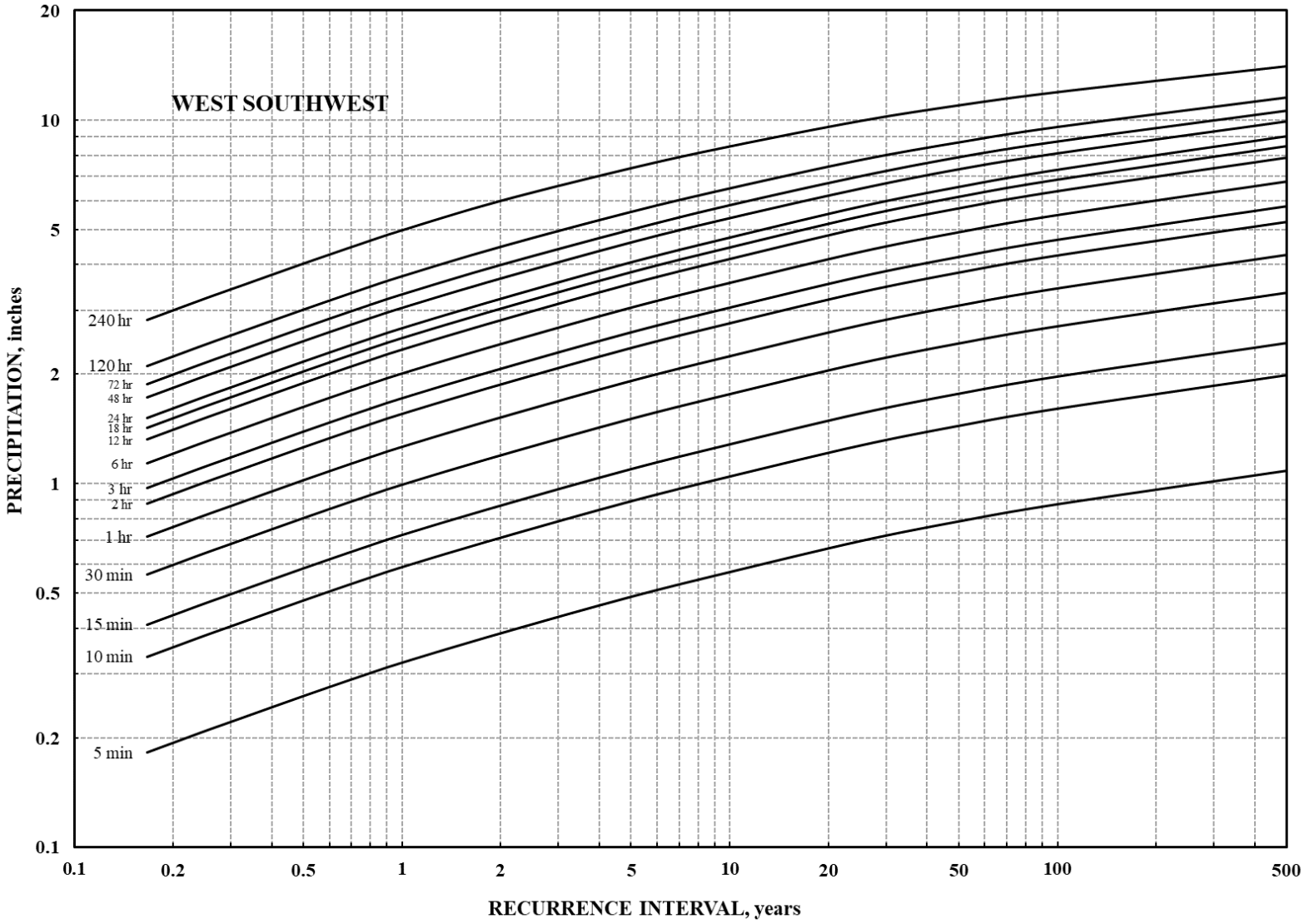

Figure 5.6. Precipitation frequency estimates for Section 6 (West Southwest)

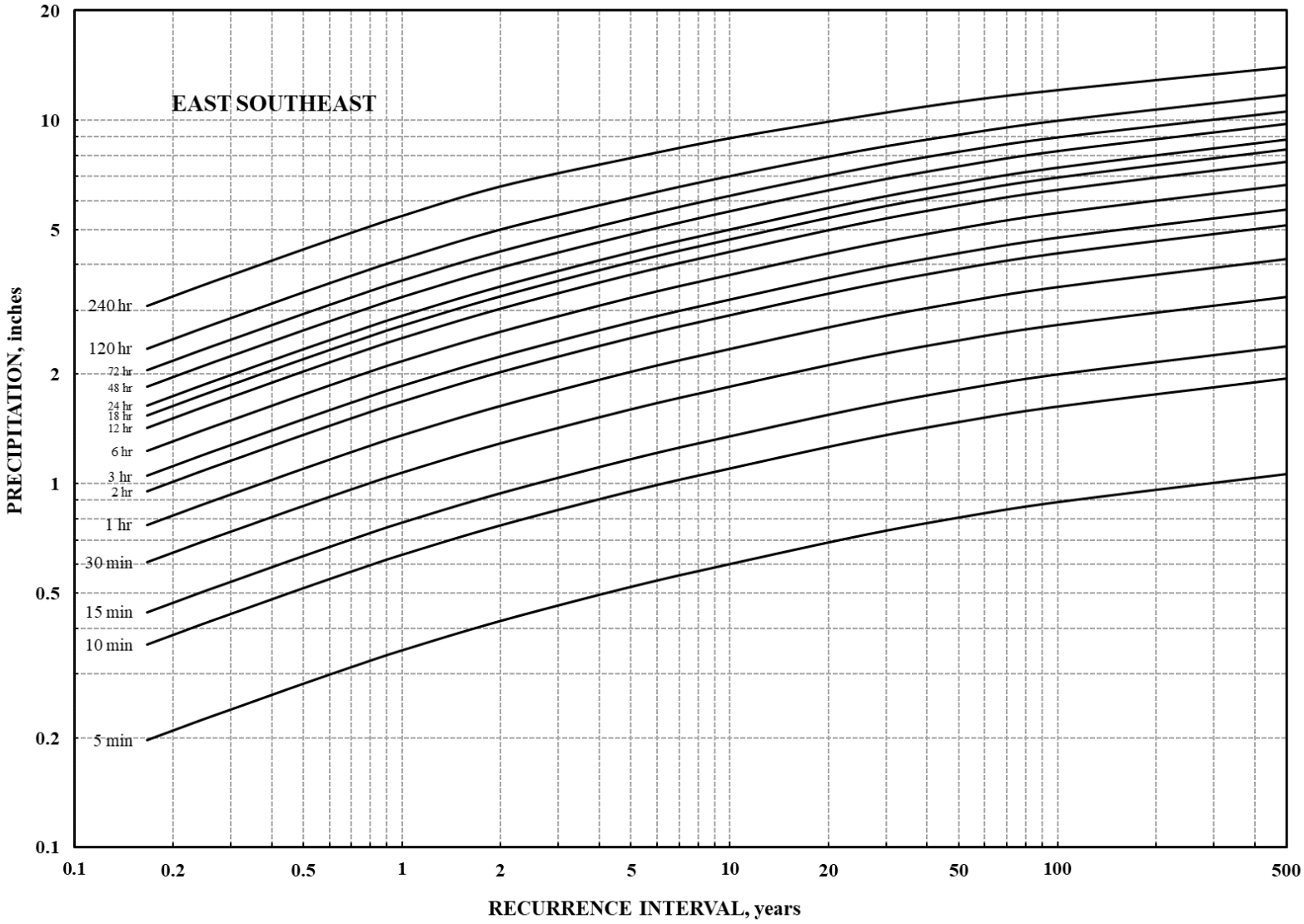

Figure 5.7. Precipitation frequency estimates for Section 7 (East Southeast)

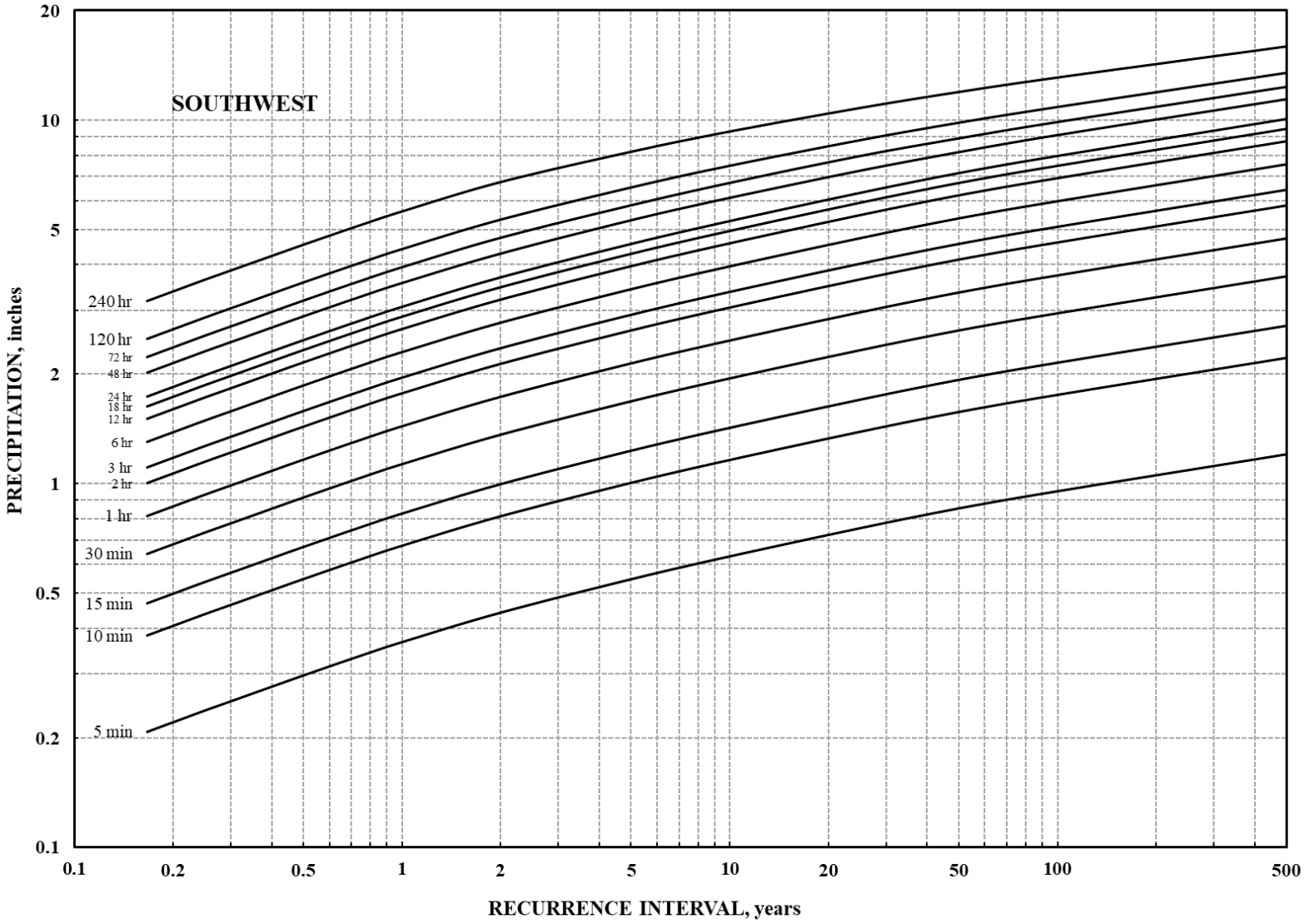

Figure 5.8. Precipitation frequency estimates for Section 8 (Southwest)

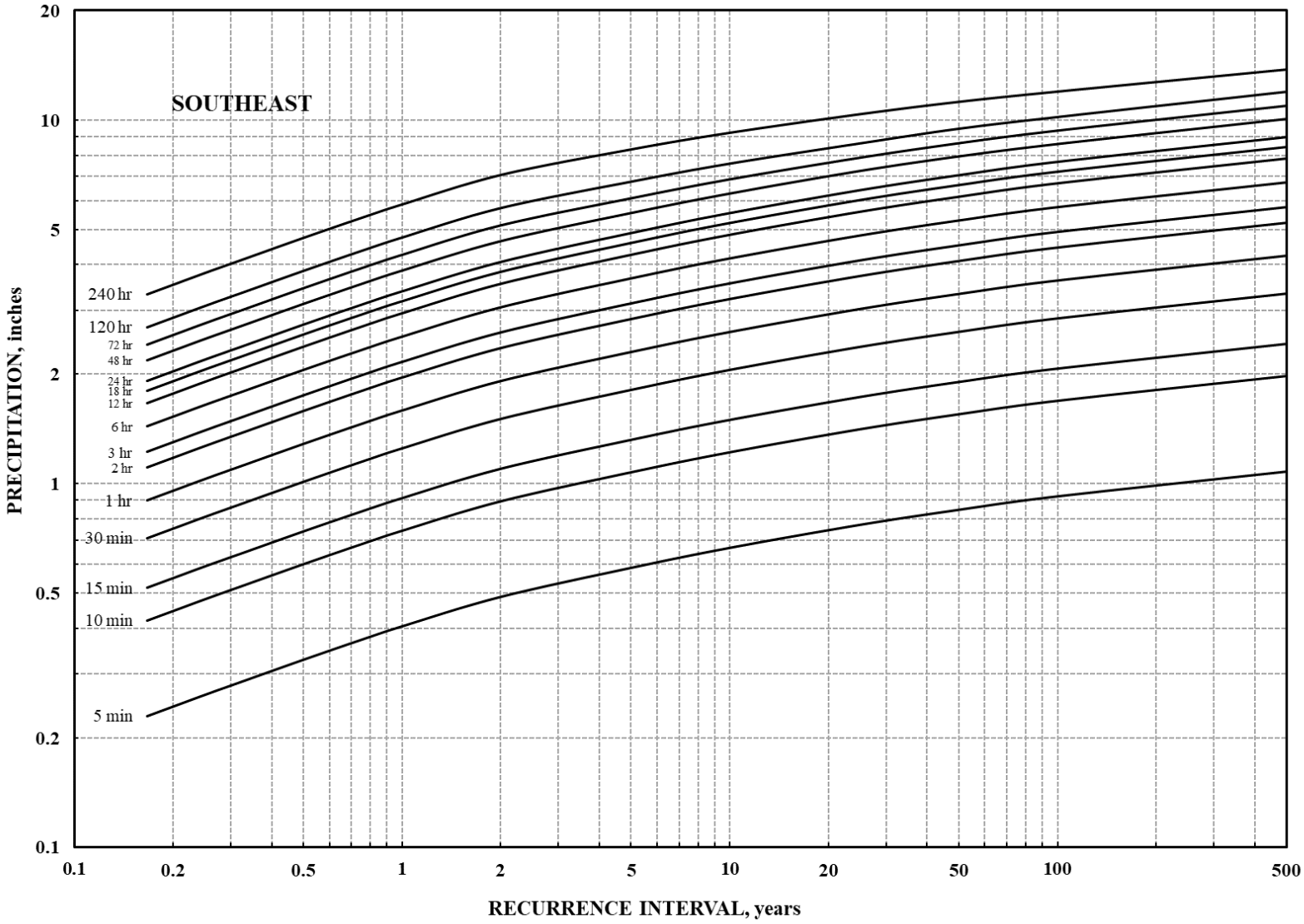

Figure 5.9. Precipitation frequency estimates for Section 9 (Southeast)

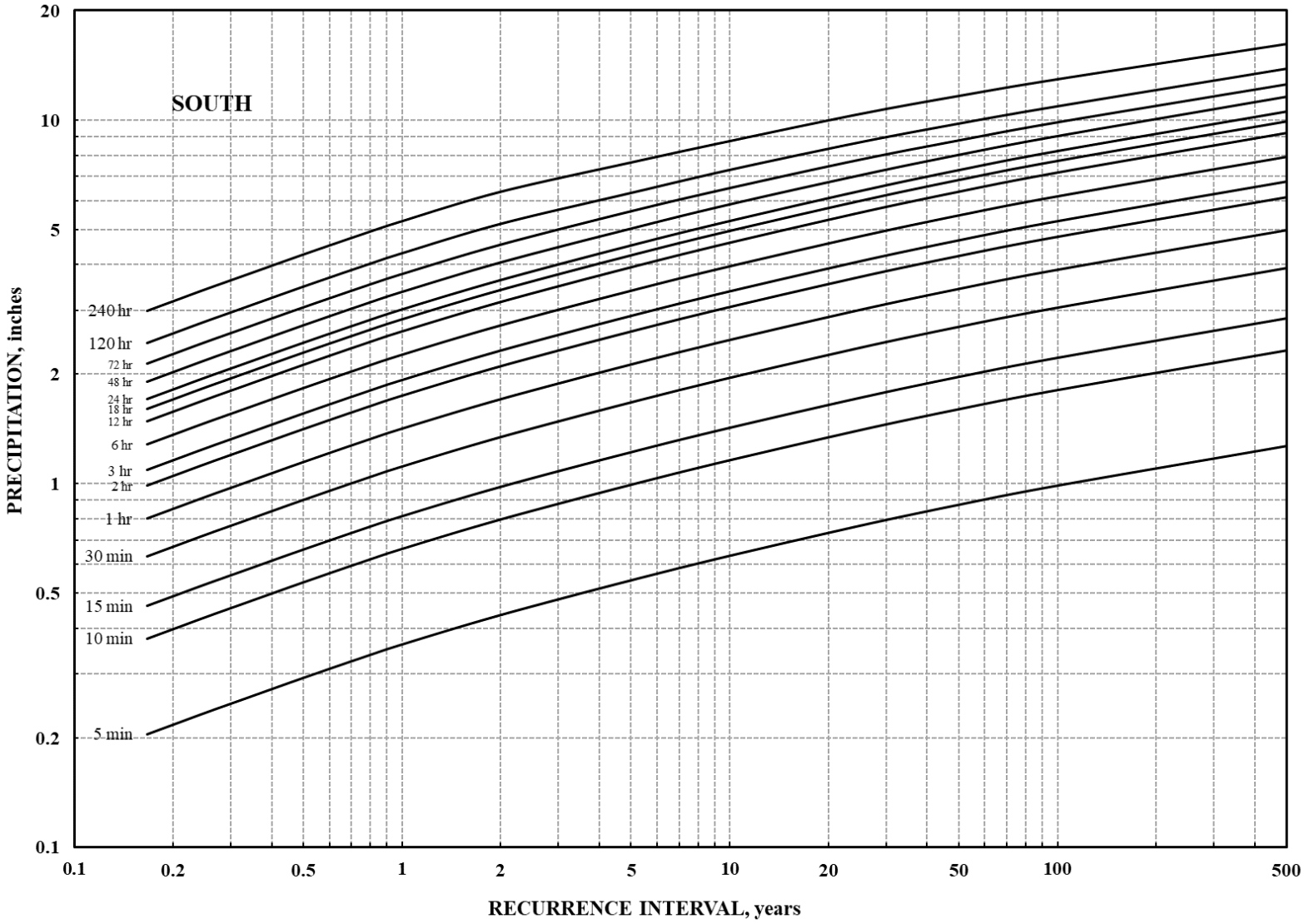

Figure 5.10. Precipitation frequency estimates for Section (South)

Appendices

Appendix 1. Daily precipitation stations used in this study

#	State	Section	Site Name	Station ID	Latitude	Longitude	Elevation	Start Date	End Date
1	IL	C	MOUNT STERLING	GHCND:USC00115935	39.9841	-90.7525	216.1	10/1/1942	4/16/2017
2	IL	C	BRADFORD 3 SSE	GHCND:USC00110868	41.146	-89.629	237.7	8/1/1980	2/23/2013
3	IL	C	CLINTON 1 SSW	GHCND:USC00111743	40.1375	-88.9675	210.3	1/1/1910	3/7/2017
4	IL	C	FARMER CITY 3 W	GHCND:USC00112993	40.2538	-88.7075	227.1	7/1/1948	5/20/2015
5	IL	C	AVON	GHCND:USC00110356	40.6632	-90.4447	193.5	11/1/1950	3/18/2017
6	IL	C	CANTON	GHCND:USC00111250	40.5379	-90.0421	195.1	10/1/1940	3/18/2017
7	IL	C	HAVANA	GHCND:USC00113940	40.303	-90.0647	141.1	3/1/1917	3/17/2017
8	IL	C	LINCOLN	GHCND:USC00115079	40.152	-89.3387	177.7	2/1/1906	3/20/2017
9	IL	C	MOUNT PULASKI	GHCND:USC00115927	40.0076	-89.2832	201.5	6/1/1893	3/21/2017
10	IL	C	DECATUR WTP	GHCND:USC00112193	39.8288	-88.9505	194.8	1/1/1893	3/20/2017
11	IL	C	LACON	GHCND:USC00114805	41.0187	-89.4153	139.6	11/1/1950	3/21/2017
12	IL	C	MASON CITY 4 SE	GHCND:USC00115413	40.1643	-89.6511	182.9	5/1/1937	10/4/2013
13	IL	C	BLOOMINGTON WATERWORKS	GHCND:USC00110761	40.4962	-88.9994	233.5	9/1/1949	3/20/2017
14	IL	C	CHENOA	GHCND:USC00111475	40.7394	-88.7109	216.4	6/1/1948	5/31/2015
15	IL	C	NORMAL 4 NE	GHCND:USC00110766	40.5493	-88.9501	240.8	1/1/1893	6/30/1977
16	IL	C	CHILLICOTHE	GHCND:USC00111627	40.9152	-89.5031	163.1	1/1/1941	4/2/2017
17	IL	C	PRINCEVILLE 2 W	GHCND:USC00117004	40.9274	-89.7563	228.6	1/1/1905	8/31/2013
18	IL	C	MONTICELLO RIVER	GHCND:USC00115792	40.0383	-88.5852	189	12/1/1964	10/5/2009
19	IL	C	RUSHVILLE 4 NE	GHCND:USC00117551	40.1347	-90.4791	203.9	1/1/1893	3/14/2017
20	IL	C	MACKINAW 1 N	GHCND:USC00115272	40.5515	-89.334	212.1	10/1/1940	4/2/2017
21	IL	C	MINONK	GHCND:USC00115712	40.9126	-89.034	228.6	10/1/1895	4/2/2017
22	IL	C	PEORIA INTERNATIONAL AIRPORT	GHCND:USW00014842	40.6675	-89.6839	198.1	5/4/1943	4/2/2017
23	IL	C	PEORIA	GHCND:USC00116701	40.7	-89.57	140.2	1/1/1940	1/31/1986
24	IL	C	TOULON	GHCND:USC00118630	41.09	-89.86	217	5/1/1942	4/1/2017
25	IL	E	CHAMPAIGN 3 S	GHCND:USC00118740	40.084	-88.2404	219.8	8/1/1902	4/18/2017
26	IL	E	GIBSON CITY	GHCND:USC00113413	40.47306	-88.3653	228.6	7/1/1935	3/31/2008
27	IL	E	PIPER CITY	GHCND:USC00116819	40.7569	-88.1827	204.2	11/1/1940	12/31/2012

Appendix 1. Daily precipitation stations used in this study (continued)

#	State	Section	Site Name	Station ID	Latitude	Longitude	Elevation	Start Date	End Date
28	IL	E	WATSEKA 2 NW	GHCND:USC00119021	40.7928	-87.7556	189	1/1/1893	3/18/2017
29	IL	E	STREATOR	GHCND:USC00118353	41.0908	-88.8158	185.9	4/8/1893	3/21/2017
30	IL	E	FAIRBURY WWTP	GHCND:USC00112923	40.7511	-88.4983	202.7	7/1/1948	3/20/2017
31	IL	E	PONTIAC	GHCND:USC00116910	40.8777	-88.6364	198.1	1/1/1903	3/18/2017
32	IL	E	DANVILLE SEWAGE PLANT	GHCND:USC00112145	40.1019	-87.5961	163.4	7/1/1948	4/2/2017
33	IL	E	HOOPESTON	GHCND:USC00114198	40.4664	-87.6851	216.4	6/1/1902	4/2/2017
34	IL	E	SIDELL 4 N	GHCND:USC00117952	39.9677	-87.8228	204.8	9/1/1913	4/2/2017
35	IL	E	RANTOUL	GHCND:USW00014806	40.313	-88.1598	230.1	1/1/1893	4/18/2017
36	IL	ESE	MOWEAQUA 2 S	GHCND:USC00115950	39.5879	-89.0159	190.5	8/22/1963	4/18/2017
37	IL	ESE	CASEY	GHCND:USC00111329	39.2975	-87.9746	189	1/1/1893	4/18/2017
38	IL	ESE	CHARLESTON	GHCND:USC00111436	39.4762	-88.1652	213.4	1/1/1896	4/18/2017
39	IL	ESE	MATTOON	GHCND:USC00115430	39.4726	-88.3545	213.7	1/1/1893	4/18/2017
40	IL	ESE	HUTSONVILLE	GHCND:USC00114317	39.1138	-87.6563	133.2	5/3/1946	4/2/2017
41	IL	ESE	PALESTINE	GHCND:USC00116558	39.0029	-87.6226	136.9	1/1/1893	3/5/2017
42	IL	ESE	GREENUP 3 SE	GHCND:USC00113683	39.2283	-88.1261	166.1	6/1/1942	8/31/2003
43	IL	ESE	TUSCOLA	GHCND:USC00118684	39.7946	-88.2909	199.6	3/1/1893	3/7/2017
44	IL	ESE	PARIS STP	GHCND:USC00116610	39.6185	-87.6672	197.8	4/1/1893	3/18/2017
45	IL	ESE	BEECHER CITY	GHCND:USC00110500	39.18122	-88.7827	185.3	9/1/1974	3/18/2017
46	IL	ESE	EFFINGHAM	GHCND:USC00112687	39.1181	-88.6244	190.5	1/1/1893	3/18/2017
47	IL	ESE	RAMSEY	GHCND:USC00117126	39.1483	-89.1022	182.9	2/1/1974	3/18/2017
48	IL	ESE	VANDALIA	GHCND:USC00118781	38.958	-89.0952	152.4	10/1/1899	3/17/2017
49	IL	ESE	WINDSOR	GHCND:USC00119354	39.4459	-88.5962	210.3	1/1/1904	4/2/2017
50	IL	ESE	MARSHALL	GHCND:USC00115380	39.39	-87.7	195.1	11/27/1939	11/30/2004
51	IL	NE	KANKAKEE METRO WWTP	GHCND:USC00114603	41.138	-87.8855	195.1	7/1/1948	3/21/2017
52	IL	NE	PERU	GHCND:USC00116753	41.3503	-89.1072	189	8/9/1963	12/27/2011
53	IL	NE	BARRINGTON 3 SW	GHCND:USC00110442	42.1153	-88.1639	266.7	11/1/1962	3/14/2017
54	IL	NE	CHICAGO BOTANICAL GARDEN	GHCND:USC00111497	42.1398	-87.7854	192	10/1/1981	3/14/2017

Appendix 1. Daily precipitation stations used in this study (continued)

55	IL	NE	CHICAGO MIDWAY AIRPORT 3 SW	GHCND:USC00111577	41.7372	-87.7775	189	2/29/1928	3/13/2017
56	IL	NE	PARK FOREST	GHCND:USC00116616	41.4947	-87.6802	216.4	6/1/1952	3/14/2017
57	IL	NE	DEKALB	GHCND:USC00112223	41.9342	-88.7756	266.1	3/1/1966	3/7/2017
58	IL	NE	WHEATON 3 SE	GHCND:USC00119221	41.8127	-88.0727	207.3	5/1/1895	12/6/2011
59	IL	NE	CHANNAHON DRESDEN ISLAND	GHCND:USC00111420	41.3978	-88.2819	153.9	6/1/1943	3/11/2013
60	IL	NE	MORRIS 1 NW	GHCND:USC00115825	41.3708	-88.4336	159.7	12/1/1911	3/21/2017
61	IL	NE	AURORA	GHCND:USC00110338	41.7805	-88.3091	201.2	1/1/1893	3/21/2017
62	IL	NE	ELGIN	GHCND:USC00112736	42.0628	-88.2861	232.6	12/1/1897	3/21/2017
63	IL	NE	MARSEILLES LOCK	GHCND:USC00115372	41.3286	-88.7533	149.4	1/1/1941	3/21/2017
64	IL	NE	OTTAWA 5 SW	GHCND:USC00116526	41.3283	-88.9106	160	5/1/1892	3/21/2017
65	IL	NE	ANTIOCH	GHCND:USC00110203	42.4811	-88.0994	228.6	7/1/1901	6/19/2010
66	IL	NE	WAUKEGAN	GHCND:USC00119029	42.34917	-87.8828	213.4	1/1/1923	7/31/2002
67	IL	NE	MARENGO	GHCND:USC00115326	42.2637	-88.6079	248.4	1/1/1893	3/13/2017
68	IL	NE	MCHENRY WG STRATTON LOCK&DAM	GHCND:USC00115493	42.3091	-88.2533	224.3	7/1/1948	3/20/2017
69	IL	NE	JOLIET BRANDON RD DM	GHCND:USC00114530	41.5033	-88.1027	165.5	6/1/1943	4/2/2017
70	IL	NE	PEOTONE	GHCND:USC00116725	41.3269	-87.7858	219.5	11/1/1940	2/28/2017
71	IL	NE	CHICAGO OHARE INT. AIRPORT	GHCND:USW00094846	41.995	-87.9336	201.8	11/1/1958	3/12/2017
72	IL	NE	CHICAGO UNIVERSITY	GHCND:USW00014892	41.78333	-87.6	181.1	1/1/1926	10/31/1994
73	IL	NW	TISKILWA 2 SE	GHCND:USC00118604	41.26667	-89.4667	195.1	5/1/1895	9/30/1990
74	IL	NW	WALNUT	GHCND:USC00118916	41.5603	-89.6024	204.5	1/1/1893	4/16/2017
75	IL	NW	MOUNT CARROLL	GHCND:USC00115901	42.098	-89.9841	195.1	4/20/1895	4/18/2017
76	IL	NW	GALVA	GHCND:USC00113335	41.1738	-90.0351	246.9	1/1/1893	1/31/2017
77	IL	NW	GENESEO	GHCND:USC00113384	41.4511	-90.1487	194.8	1/1/1895	3/20/2017
78	IL	NW	KEWANEE 1 E	GHCND:USC00114710	41.2429	-89.8997	237.7	8/1/1939	3/21/2017
79	IL	NW	GALENA	GHCND:USC00113312	42.3995	-90.386	229.5	8/1/1895	3/21/2017
80	IL	NW	STOCKTON 3 NNE	GHCND:USC00118293	42.3996	-89.9902	295.7	11/1/1943	3/20/2017
81	IL	NW	DIXON 1 W	GHCND:USC00112348	41.835	-89.5136	201.2	1/1/1893	3/21/2017

Appendix 1. Daily precipitation stations used in this study (continued)

82	IL	NW	PAW PAW 2 S	GHCND:USC00116661	41.6652	-88.978	271	9/1/1912	3/21/2017
83	IL	NW	ALEDO	GHCND:USC00110072	41.1977	-90.7447	222.5	1/1/1901	3/21/2017
84	IL	NW	KEITHSBURG	GHCND:USC00114655	41.09944	-90.9394	167.6	3/1/1896	9/30/2009
85	IL	NW	NEW BOSTON DAM 17	GHCND:USC00116080	41.1924	-91.0579	167	1/1/1938	3/21/2017
86	IL	NW	ROCHELLE	GHCND:USC00117354	41.9116	-89.0708	236.2	10/1/1978	3/21/2017
87	IL	NW	HENNEPIN POWER PLANT	GHCND:USC00114013	41.26472	-89.3381	140.2	8/1/1962	6/30/2009
88	IL	NW	ILLINOIS CITY DAM 16	GHCND:USC00114355	41.4255	-91.0094	167.6	6/1/1943	4/1/2017
89	IL	NW	FREEPORT WWP	GHCND:USC00113262	42.2972	-89.6038	228.6	6/1/1948	4/2/2017
90	IL	NW	FULTON DAM	GHCND:USC00113290	41.8978	-90.1545	180.4	1/1/1938	4/1/2017
91	IL	NW	MORRISON	GHCND:USC00115833	41.804	-89.9744	183.8	5/1/1895	4/2/2017
92	IL	NW	MOLINE QUAD CITY INT. AIRPORT	GHCND:USW00014923	41.46528	-90.5233	180.4	5/24/1943	4/2/2017
93	IL	NW	ROCKFORD GREATER RCKFRD AIRPORT	GHCND:USW00094822	42.1927	-89.093	222.5	1/1/1951	4/2/2017
94	IL	NW	PRINCETON	GHCND:USC00116998	41.37	-89.45	212.4	12/1/1987	4/18/2017
95	IL	NW	ROCK ISLAND LOCK AND DAM 15	GHCND:USC00117391	41.52	-90.56	173.1	2/1/1866	4/2/2017
96	IL	S	HARRISBURG	GHCND:USC00113879	37.7408	-88.5244	111.3	3/1/1898	8/20/2013
97	IL	S	SHAWNEETOWN OLD TOWN	GHCND:USC00117859	37.6977	-88.1336	106.7	1/6/1892	3/21/2017
98	IL	S	ROSICLARE 5 NW	GHCND:USC00117487	37.4747	-88.4122	121.9	2/1/1968	3/21/2017
99	IL	S	CARBONDALE SEWAGE PLANT	GHCND:USC00111265	37.7308	-89.1658	118.9	1/1/1894	3/21/2017
100	IL	S	GRAND TOWER 2 N	GHCND:USC00113595	37.6591	-89.5102	116.7	10/1/1940	9/30/2009
101	IL	S	BROOKPORT DAM 52	GHCND:USC00110993	37.1275	-88.653	100.6	11/1/1928	3/21/2017
102	IL	S	DIXON SPRINGS AGR CE	GHCND:USC00112353	37.4388	-88.6678	160.6	9/22/1967	3/14/2017
103	IL	S	ANNA 2 NNE	GHCND:USC00110187	37.4813	-89.2344	195.1	5/7/1895	12/2/2013
104	IL	S	MARION 4 NNE	GHCND:USC00115342	37.77483	-88.8982	145.4	5/1/1942	7/31/1998
105	IL	S	SMITHLAND LOCK AND DAM, KY US	GHCND:USC00118020	37.1644	-88.4311	108.8	12/1/1980	4/2/2017
106	IL	S	CAIRO 3 N	GHCND:USW00093809	37.0422	-89.1855	95.4	1/1/1908	12/4/2013
107	IL	S	GOLCONDA RIVER	GHCND:USC00113522	37.38	-88.49	107.9	1/1/1893	9/30/1980
108	IL	SE	CLAY CITY 6 SSE	GHCND:USC00111700	38.6058	-88.3117	140.2	6/1/1977	4/18/2017

Appendix 1. Daily precipitation stations used in this study (continued)

109	IL	SE	FLORA 5 NW	GHCND:USC00113109	38.7103	-88.5758	152.4	1/1/1893	11/30/2009
110	IL	SE	CENTRALIA	GHCND:USC00111386	38.5547	-89.1297	140.2	11/1/1899	4/18/2017
111	IL	SE	ALBION	GHCND:USC00110055	38.3777	-88.0569	161.5	12/1/1893	4/30/2006
112	IL	SE	BENTON	GHCND:USC00110608	38.0336	-88.9202	135.6	6/1/1948	2/28/2009
113	IL	SE	PLUMFIELD	GHCND:USC00116874	37.9116	-89.0091	123.4	10/1/1974	3/17/2017
114	IL	SE	MCLEANSBORO	GHCND:USC00115515	38.08444	-88.5425	135.9	1/1/1893	7/31/2002
115	IL	SE	DIX	GHCND:USC00112344	38.4627	-88.9433	183.5	3/1/1972	7/31/2008
116	IL	SE	MOUNT VERNON 3 NE	GHCND:USC00115943	38.3483	-88.8533	149.4	5/1/1895	3/21/2017
117	IL	SE	LAWRENCEVILLE 2 WSW	GHCND:USC00114957	38.7239	-87.7196	137.5	10/1/1962	3/21/2017
118	IL	SE	SALEM	GHCND:USC00117636	38.6452	-88.9461	167.6	7/1/1915	3/21/2017
119	IL	SE	OLNEY 2 S	GHCND:USC00116446	38.7003	-88.0816	139.9	1/1/1893	4/2/2017
120	IL	SE	MOUNT CARMEL	GHCND:USC00115888	38.4105	-87.7577	131.1	7/1/1891	9/30/2011
121	IL	SE	FAIRFIELD RADIO WFIW	GHCND:USC00112931	38.3805	-88.3263	131.1	7/7/1895	3/1/2017
122	IL	SE	CARMI 6 NW	GHCND:USC00111296	38.14972	-88.2244	118.9	5/22/1911	12/31/2000
123	IL	SE	WAYNE CITY 1 N	GHCND:USC00119040	38.35	-88.58	134.1	8/23/1946	4/26/2016
124	IL	SW	GREENVILLE	GHCND:USC00113693	38.8665	-89.4051	164.9	1/1/1983	4/17/2017
125	IL	SW	CARLYLE RESERVOIR	GHCND:USC00111290	38.6308	-89.3658	152.7	8/1/1962	4/18/2017
126	IL	SW	ALTON MELVIN PRICE	GHCND:USC00110137	38.8663	-90.1463	132.6	12/2/1892	3/21/2017
127	IL	SW	EDWARDSVILLE 2 W	GHCND:USC00112679	38.80972	-90.0028	152.4	2/1/1893	3/21/2017
128	IL	SW	HIGHLAND	GHCND:USC00114089	38.75833	-89.6556	160	10/1/1977	3/20/2017
129	IL	SW	WATERLOO	GHCND:USC00119002	38.36639	-90.1619	201.5	11/1/1911	7/2/2014
130	IL	SW	DU QUOIN 4 SE	GHCND:USC00112483	37.9877	-89.193	128	1/1/1893	3/23/2017
131	IL	SW	CHESTER	GHCND:USC00111491	37.9022	-89.8308	130.5	3/1/1905	4/2/2017
132	IL	SW	KASKASKIA RIV NAV LO	GHCND:USC00114629	37.9842	-89.9492	115.8	4/1/1974	4/2/2017
133	IL	SW	PRAIRIE DU ROCHER	GHCND:USC00116973	38.08861	-90.1619	123.1	10/16/1948	1/31/2017
134	IL	SW	RED BUD 5 SE	GHCND:USC00117157	38.1852	-89.9283	131.1	8/1/1947	4/2/2017
135	IL	SW	SPARTA 1 W	GHCND:USC00118147	38.11667	-89.7167	163.1	1/1/1893	1/26/2015

Appendix 1. Daily precipitation stations used in this study (continued)

136	IL	SW	CAHOKIA	GHCND:USC00111160	38.56694	-90.1942	121.9	5/1/1969	5/31/2012
137	IL	SW	NASHVILLE 1 E	GHCND:USC00116011	38.343	-89.3586	156.4	8/1/1895	4/2/2017
138	IL	SW	BELLEVILLE SIU RSRCH	GHCND:USW00013802	38.5199	-89.8466	137.2	6/1/1948	4/2/2017
139	IL	SW	PINCKNEYVILLE 2 N	GHCND:USC00116779	38.1	-89.38	131.1	3/1/1972	3/31/2017
140	IL	W	GOLDEN	GHCND:USC00113530	40.10639	-91.0222	218.8	5/1/1913	2/14/2011
141	IL	W	PAYSON	GHCND:USC00116670	39.8208	-91.2436	232.9	6/1/1948	12/31/2010
142	IL	W	QUINCY DAM 21	GHCND:USC00117077	39.9058	-91.4281	147.2	5/1/1937	4/18/2017
143	IL	W	BENTLEY	GHCND:USC00110598	40.3444	-91.1124	198.1	6/1/1948	3/21/2017
144	IL	W	LA HARPE	GHCND:USC00114823	40.5838	-90.9686	210.3	4/1/1895	3/20/2017
145	IL	W	GLADSTONE DAM 18	GHCND:USC00113455	40.8821	-91.0234	164	1/1/1938	3/21/2017
146	IL	W	GALESBURG	GHCND:USC00113320	40.9464	-90.3856	232	1/15/1895	3/21/2017
147	IL	W	MACOMB	GHCND:USC00115280	40.4786	-90.6698	185.9	8/1/1902	3/21/2017
148	IL	W	MONMOUTH	GHCND:USC00115768	40.9443	-90.6381	219.5	2/1/1893	3/31/2017
149	IL	W	QUINCY REGIONAL AIRPORT	GHCND:USW00093989	39.93694	-91.1919	234.4	6/1/1948	4/18/2017
150	IL	WSW	BEARDSTOWN	GHCND:USC00110492	40.0165	-90.4277	136.2	1/1/1896	8/31/2014
151	IL	WSW	VIRGINIA	GHCND:USC00118870	39.9495	-90.2084	185.9	6/14/1963	4/18/2017
152	IL	WSW	KINCAID	GHCND:USC00114739	39.5894	-89.4556	176.8	4/1/1973	4/18/2017
153	IL	WSW	MORRISONVILLE	GHCND:USC00115841	39.4157	-89.4615	192	7/1/1948	10/28/2015
154	IL	WSW	PANA	GHCND:USC00116579	39.3686	-89.0866	198.1	1/1/1893	4/18/2017
155	IL	WSW	GREENFIELD	GHCND:USC00113666	39.3425	-90.2058	167	7/1/1948	4/7/2017
156	IL	WSW	WHITE HALL 1 E	GHCND:USC00119241	39.4411	-90.379	176.8	1/1/1893	4/20/2017
157	IL	WSW	GRAFTON	GHCND:USC00113572	38.9681	-90.4289	135	4/1/1894	3/21/2017
158	IL	WSW	JERSEYVILLE 2 SW	GHCND:USC00114489	39.1025	-90.343	192	8/10/1940	3/21/2017
159	IL	WSW	CARLINVILLE	GHCND:USC00111280	39.2883	-89.8702	189.3	1/1/1893	7/31/2014
160	IL	WSW	MEDORA	GHCND:USC00115539	39.1563	-90.1391	185	6/1/1942	3/20/2017
161	IL	WSW	MOUNT OLIVE 1 E	GHCND:USC00115917	39.0719	-89.7008	210.3	10/1/1940	3/21/2017
162	IL	WSW	VIRDEN	GHCND:USC00118860	39.50611	-89.7689	205.7	4/1/1941	9/14/2011

Appendix 1. Daily precipitation stations used in this study (continued)

163	IL	WSW	HILLSBORO	GHCND:USC00114108	39.16111	-89.4919	192	4/1/1895	3/14/2017
164	IL	WSW	JACKSONVILLE 2 E	GHCND:USC00114442	39.7346	-90.1979	185.9	5/21/1895	3/19/2017
165	IL	WSW	GRIGGSVILLE	GHCND:USC00113717	39.7377	-90.7086	191.4	1/1/1893	4/15/2015
166	IL	WSW	SPRINGFIELD A. LINCOLN CAP. AIRPRT	GHCND:USW00093822	39.8447	-89.6839	181.1	1/1/1901	4/2/2017
167	IL	WSW	TAYLORVILLE 2 SW	GHCND:USC00118491	39.53	-89.31	191.4	7/1/1941	1/10/2017
168	IL	WSW	BLUFFS	GHCND:USC00110781	39.75	-90.53	164.6	6/1/1940	10/31/1986
169	IN	S	MT VERNON	GHCND:USC00126001	37.9286	-87.8956	108.8	10/1/1888	10/31/2017
170	KY	S	PADUCAH	GHCND:USW00003816	37.0683	-88.7719	119.5	8/1/1949	10/31/2017
171	MO	S	JACKSON	GHCND:USC00234226	37.3781	-89.6678	134.1	1/1/1893	4/30/2017
172	MO	S	CAPE GIRARDEAU MUNI AP	GHCND:USW00003935	37.2253	-89.5706	102.4	6/1/1960	4/30/2017
173	MO	SW	ST LOUIS LAMBERT INTL AP	GHCND:USW00013994	38.7525	-90.3736	161.8	4/1/1938	4/30/2017
174	MO	W	CANTON L&D 20	GHCND:USC00231275	40.1433	-91.5158	149.4	1/1/1893	4/30/2017
175	IA	W	BURLINGTON 2S	GHCND:USC00131060	40.7747	-91.1164	210.3	12/1/1964	4/30/2017
176	IA	W	DONNELLSON	GHCND:USC00132299	40.6458	-91.5639	214.9	1/1/1938	4/30/2017

Appendix 2. Hourly precipitation stations used in this study (HPD)

#	State	Section	Site Name	Station ID	Latitude	Longitude	Elevation	Start Date	End Date
1	IL	C	DOWNS 2 NE	COOP:112417	40.43333	-88.8667	242	7/1/1948	5/1/1987
2	IL	C	EDELSTEIN	COOP:112642	40.93333	-89.6333	244	12/1/1950	3/1/1984
3	IL	C	FARMER CITY 3 W	COOP:112993	40.2538	-88.7075	227	7/1/1948	1/1/2003
4	IL	C	MARIETTA	COOP:115334	40.501	-90.3915	195	7/1/1948	8/1/2011
5	IL	C	MAROA	COOP:115364	40.03639	-88.9542	220	7/1/1948	1/1/1984
6	IL	C	MASON CITY 4 SE	COOP:115413	40.1643	-89.6511	183	7/1/1948	11/1/2011
7	IL	C	PEORIA INTERNATIONAL AIRPORT	COOP:116711	40.6675	-89.6839	198	7/1/1948	12/30/2013
8	IL	C	WASHINGTON 2 W	COOP:118990	40.6994	-89.4477	230	7/1/1948	9/1/2001
9	IL	E	DANVILLE	COOP:112140	40.1391	-87.6479	169	5/1/1951	12/22/2013
10	IL	E	FAIRBURY WWTP	COOP:112923	40.7511	-88.4983	203	7/1/1948	12/30/2013
11	IL	E	HOOPESTON	COOP:114198	40.4664	-87.6851	216	7/1/1948	12/22/2013
12	IL	E	PIPER CITY	COOP:116819	40.7569	-88.1827	204	2/1/1949	3/1/2013
13	IL	E	RANTOUL	COOP:117150	40.313	-88.1598	230	7/1/1948	12/22/2013
14	IL	E	CHAMPAIGN 3 S	COOP:118740	40.084	-88.2404	220	1/1/1959	12/21/2013
15	IL	ESE	EFFINGHAM	COOP:112687	39.1181	-88.6244	190	7/1/1948	12/21/2013
16	IL	ESE	HUTSONVILLE	COOP:114317	39.1138	-87.6563	133	7/1/1957	12/22/2013
17	IL	ESE	NEWTON 6 SSE	COOP:116159	38.91361	-88.1183	155	7/1/1948	9/1/2003
18	IL	ESE	PARIS 1 N	COOP:116605	39.63333	-87.7	222	7/1/1948	11/1/1992
19	IL	ESE	SHELBYVILLE DAM	COOP:117876	39.4079	-88.7739	200	7/1/1970	12/22/2013
20	IL	ESE	SULLIVAN 3 S	COOP:118389	39.5608	-88.6066	196	7/1/1948	12/21/2013
21	IL	ESE	VANDALIA	COOP:118781	38.958	-89.0952	152	7/1/1948	12/21/2013
22	IL	NE	WENONA	COOP:119090	41.06667	-89.0667	210	7/1/1948	9/1/1990
23	IL	NE	CHICAGO OHARE INTERNATIONAL AIRPORT	COOP:111549	41.995	-87.9336	202	6/1/1962	1/1/2014
24	IL	NE	CHICAGO UNIVERSITY	COOP:111572	41.78333	-87.6	181	7/1/1948	2/1/1995
25	IL	NE	CHICAGO MIDWAY AIRPORT 3 SW	COOP:111577	41.7372	-87.7775	189	7/1/1948	1/1/2014
26	IL	NE	CRETE	COOP:112011	41.44919	-87.6221	216	7/1/1948	1/1/2014
27	IL	NE	KANKAKEE METRO WWTP	COOP:114603	41.138	-87.8855	195	7/1/1948	12/22/2013

Appendix 2. Hourly precipitation stations used in this study (HPD) (continued)

28	IL	NE	MCHENRY WG STRATTON LOCK AND DAM	COOP:115493	42.3091	-88.2533	224	7/1/1948	1/1/2014
29	IL	NW	BELVIDERE	COOP:110583	42.2551	-88.864	230	7/1/1948	1/1/2014
30	IL	NW	FREEPORT WWP	COOP:113262	42.2972	-89.6038	229	7/1/1948	1/1/2014
31	IL	NW	FULTON DAM	COOP:113290	41.8978	-90.1545	180	7/1/1948	12/29/2013
32	IL	NW	ILLINOIS CITY DAM 16	COOP:114355	41.4255	-91.0094	168	7/1/1948	12/22/2013
33	IL	NW	KEWANEE 1 E	COOP:114710	41.2429	-89.8997	238	5/1/1951	12/30/2013
34	IL	NW	LANARK	COOP:114879	42.0919	-89.8421	253	7/1/1948	12/31/2013
35	IL	NW	MOLINE QUAD CITY INTERNATIONAL AIRPORT	COOP:115751	41.46528	-90.5233	180	7/1/1948	12/30/2013
36	IL	NW	OREGON	COOP:116490	42.00544	-89.3279	207	11/1/1949	9/1/2002
37	IL	NW	PROPHETSTOWN	COOP:117014	41.6752	-89.9374	184	7/1/1948	12/30/2013
38	IL	NW	ROCKFORD GREATER ROCKFORD AIRPORT	COOP:117382	42.1927	-89.093	222	1/1/1951	1/1/2014
39	IL	NW	DAVENPORT LOCK AND DAM 15	COOP:132069	41.51667	-90.5667	173	8/1/1948	5/28/1984
40	IL	S	CAIRO 3 N	COOP:111166	37.0422	-89.1855	95	7/1/1948	1/1/2014
41	IL	S	DIXON SPRINGS AGR CE	COOP:112353	37.4388	-88.6678	161	9/1/1967	12/29/2013
42	IL	S	GOLCONDA RIVER	COOP:113522	37.37889	-88.4894	108	7/1/1948	10/1/1980
43	IL	S	MURPHYSBORO 2 SW	COOP:115983	37.7608	-89.3655	168	7/1/1948	12/21/2013
44	IL	SE	CISNE 2 S	COOP:111664	38.5047	-88.4094	138	7/1/1946	12/21/2013
45	IL	SE	MOUNT CARMEL 4 NW	COOP:115893	38.45	-87.7833	143	7/1/1948	12/1/1976
46	IL	SE	WEST SALEM	COOP:119193	38.525	-88.013	136	1/1/1971	1/1/2014
47	IL	SW	ASHLEY	COOP:110281	38.3306	-89.1769	162	11/1/1965	1/1/2014
48	IL	SW	BELLEVILLE SIU RSRCH	COOP:110510	38.5199	-89.8466	137	7/1/1948	12/21/2013
49	IL	SW	CARLYLE RESERVOIR	COOP:111290	38.6249	-89.363	153	7/1/1970	12/21/2013
50	IL	SW	COULTERVILLE 3 NW	COOP:111944	38.21667	-89.65	152	7/1/1948	5/28/1984
51	IL	SW	PRAIRIE DU ROCHER 3 WNW	COOP:116973	38.0886	-90.1619	123	7/1/1948	3/1/2007
52	IL	SW	SPARTA 1 W	COOP:118147	38.11667	-89.7167	163	1/1/1976	9/26/2010
53	IL	W	ALEXIS 1 SW	COOP:110082	41.0579	-90.5654	207	7/1/1948	12/30/2013
54	IL	W	AUGUSTA	COOP:110330	40.2333	-90.9471	207	7/1/1948	12/22/2013

Appendix 2. Hourly precipitation stations used in this study (HPD) (continued)

55	IL	W	QUINCY DAM 21	COOP:117077	39.9035	-91.4284	147	7/1/1948	12/22/2013
56	IL	W	YATES CITY	COOP:119816	40.7763	-90.0203	206	12/1/1950	12/26/2013
57	IL	WSW	CARLINVILLE 2	COOP:111284	39.288	-89.8699	189	9/1/1968	1/1/2014
58	IL	WSW	GREENFIELD	COOP:113666	39.3423	-90.2059	167	7/1/1948	12/21/2013
59	IL	WSW	JACKSONVILLE 2 E	COOP:114442	39.7346	-90.1979	186	4/1/1963	12/26/2013
60	IL	WSW	MORRISONVILLE	COOP:115841	39.4157	-89.4615	192	7/1/1948	12/26/2013
61	IL	WSW	NOKOMIS	COOP:116185	39.3052	-89.2827	207	1/1/1971	1/1/2014
62	IL	WSW	SPRINGFIELD ABRAHAM LINCOLN CAPITAL AIRPRT	COOP:118179	39.8447	-89.6839	181	7/1/1948	12/25/2013
63	IN	SE	JOHNSON EXPERIMENT F	COOP:124407	38.26667	-87.75	134	11/1/1949	4/1/1980
64	KY	S	FORDS FERRY DAM 5O	COOP:152961	37.46667	-88.1	110	8/1/1948	3/1/1984
65	KY	S	PADUCAH BARKLEY REGIONAL AIRPORT	COOP:156110	37.0563	-88.7744	126	8/1/1949	12/29/2013
66	KY	S	PADUCAH WALKER	COOP:156117	37.05	-88.55	104	8/1/1948	3/1/1996
67	MO	SW	ST LOUIS LAMBERT INTERNATIONAL AIRPORT	COOP:237455	38.7525	-90.3736	162	8/1/1948	12/23/2013
68	MO	WSW	CAP AU GRIS LOCK AND DAM 25	COOP:231283	39.003	-90.6886	137	8/1/1948	12/21/2013
69	MO	WSW	CLARKSVILLE LOCK AND DAM 24	COOP:231640	39.373	-90.9052	140	8/1/1948	12/25/2013
70	MO	WSW	HANNIBAL WATER WORKS	COOP:233601	39.7233	-91.3719	217	4/1/1950	12/26/2013
71	IA	NW	BELLEVUE L AND D 12	COOP:130608	42.2611	-90.4231	184	8/1/1948	12/31/2013
72	IA	NW	DUBUQUE REGIONAL AIRPORT	COOP:132367	42.39778	-90.7036	322	2/1/1951	12/31/2013
73	IA	W	BURLINGTON 2 S	COOP:131060	40.7747	-91.1165	210	12/1/1964	12/22/2013